https://ntrs.nasa.gov/search.jsp?R=19740020842 2020-03-23T05:38:51+00:00Z

NASA CONTRACTOR REPORT

NASA CR-2393

NASA CR-2393

TESTING AND EVALUATION OF SOLID LUBRICANTS FOR GAS BEARINGS

by P. R. Albrecht and W. H. Fischer

Prepared by
MECHANICAL TECHNOLOGY INCORPORATED
Latham, N.Y. 12110
for Lewis Research Center

NATIONAL AERONAUTICS AND SPACE ADMINISTRATION • WASHINGTON, D. C. • JUNE 1974

1. Report No.	2. Government Accession No.	3. Recipient's Catalog No.
NASA CR-2393		

4. Title and Subtitle	5. Report Date
TESTING AND EVALUATION OF SOLID LUBRICANTS FOR GAS BEARINGS	June 1974
	6. Performing Organization Code
7. Author(s)	8. Performing Organization Report No.
P. R. Albrecht and W. H. Fischer	MTI 73TR24
	10. Work Unit No.
9. Performing Organization Name and Address	
Mechanical Technology Incorporated 968 Albany-Shaker Road Latham, New York 12110	11. Contract or Grant No. NAS 3-16746
	13. Type of Report and Period Covered
12. Sponsoring Agency Name and Address	Contractor Report
National Aeronautics and Space Administration Washington, D. C. 20546	14. Sponsoring Agency Code

15. Supplementary Notes

Final Report. Project Manager, Thomas P. Hecker, Power Systems Division, NASA Lewis Research Center, Cleveland, Ohio

16. Abstract

This report describes the testing and results of testing solid film lubricants for gas lubricated bearing applications. The tests simulated operational hazards of tilting pad gas bearings. The presence of a low coefficient of friction and the endurance of the solid film lubricant were the criteria for judging superior performance. All solid lubricants tested were applied to a plasma sprayed chrome oxide surface. Molybdenum disulfide and graphite fluoride were the solid lubricants tested; other test parameters included the method of application of the solid lubricant and the surface finish of the plasma sprayed coating. In general, the application of a solid film lubricant was found to significantly improve the coefficient of friction of the rubbing surfaces.

17. Key Words (Suggested by Author(s))	18. Distribution Statement
Solid film lubricants; Gas bearings, elevated temperatures; Graphite fluoride; Molybdenum disulfide	Unclassified - unlimited CAT. 15

19. Security Classif. (of this report)	20. Security Classif. (of this page)	21. No. of Pages	22. Price*
Unclassified	Unclassified	140	$4.75

* For sale by the National Technical Information Service, Springfield, Virginia 22151

Page Intentionally Left Blank

TABLE OF CONTENTS

LIST OF FIGURES

LIST OF TABLES

1.0 SUMMARY

This report contains the descriptions of the test materials,* test methods and test results performed under NASA Contract No. NAS3-16746, "Testing and Evaluation of Solid Lubricants for Gas Bearings." Under this contract, forty-three (43) pad-sleeve pairs were fabricated, coated with plasma-sprayed chrome oxide with a nominal surface finish of either 0.254 or 0.762 μm (10 or 30 μin.) and lubricated with one of two solid lubricants, molybdenum disulfide (MoS_2) or graphite fluoride $(CF_x)n$. The MoS_2 was applied to the bearings by four methods: 1) burnishing, 2) sputtering, 3) polyimide bond and 4) metal matrix bond. The graphite fluoride, in the form of $(CF_{1.1})n$ was applied by two methods: 1) burnishing and 2) polyimide bond.

These test bearings were individually subjected to one of three tests, designed to simulate conditions that occur in operational use of gas bearings in turbomachinery.

The Start-Stop Test was designed to simulate the effects of start-up and shut-down of a typical turbomachinery shaft on the rubbing surfaces of the bearings.

The High-Speed Shock Test was designed to simulate the effects of momentary high loadings in producing millisecond contacts of the bearing surfaces.

The High-Speed, Long-Duration Rub Test was designed to simulate the effect of longer term loads upon the rubbing surfaces such as might be imposed by a seal rub or high g maneuvers.

Consideration of the frictional data from these tests and lubricant film thicknesses, led to the selection of sputtered MoS_2 on 0.254 μm (10 μin) finish chrome oxide for certification testing. Four such bearings were fabricated and subjected to an extended series of High-Speed, Long Duration Rub Tests to assess the reproducibility of bearing performance.

Based upon coefficients of friction and changes therein, graphite fluoride in polyimide or sputtered MoS_2 over the 0.254 μm (10 μin) surface finish chrome oxide performed best in the Start-Stop Test.

Sputtered MoS_2 again performed well in the High-Speed Shock Test but metal matrix bonded MoS_2 out performed the polyimide bonded graphite fluoride, with the 0.762 μm (30 μin) finish preferred.

---

*The mention of trade names and vendors is made for identification and as an aid to the reader and must not be construed as a recommendation on the part of either MTI or NASA.

In the High-Speed, Long-Duration Rub Test, the difference in results for the two surface finishes was not as great. Metal matrix bonded MoS_2 was the lubricant of choice for this test. This test gave the smallest differences between samples of all the tests.

Reproducibility in the Certification Test was not as good as hoped, although the coefficients of friction of the sputtered MoS_2 samples were quite low in three cases. The fourth sample was considered a failure since its coefficient of friction exceeded the preset limit of 0.2 when it had sustained only 42 of the planned 50 rubs.

Approximately 12 percent of the samples exhibited cracking of the chrome oxide layer. Only samples from the High-Speed Shock and High-Speed, Long-Duration Rub Tests were cracked. Cracking occurred on reference samples as well as lubricated samples. It is concluded that cracking is due to impactive wear and that cracking does not affect bearing performance.

Macro photographs were made before and after testing. Micro and electron photographs were taken after testing. The micro photos were less informative than the macro ones.

The High-Speed, Long-Duration Rub Test caused the most wear on both reference and lubricated samples while the Start-Stop Test wore the reference samples least and the High-Speed Shock Test wore the lubricated samples the least.

No evident correlation was found between coefficient of friction and wear, in either macro or micro photos.

On balance, sputtered MoS_2 over 0.254 μm (10 μin) surface finish chrome oxide appeared the best combination for immediate application, with metal matrix MoS_2 requiring additional investigation before it can be employed.

Polyimide bonded graphite fluoride had the lowest coefficient of friction after the Start-Stop Test, was average after the High-Speed, Long-Duration Rub Test and was marginal after the High Speed Shock Test. Since graphite fluoride will withstand higher temperatures in air than will MoS_2, this formulation must be seriously considered for air bearings operating up to 600 - 700°F.

In general, it can be said that any of the solid lubricants tested helped reduce the friction. The sputtered film of MoS_2 and the metal matrix bonded MoS_2 showed the largest reduction in friction in most cases and seem to hold the most promise for the necessary endurance. Polyimide bonded carbon graphite should be considered for high temperature air applications.

2.0 INTRODUCTION

The NASA Lewis Research Center is currently engaged in upgrading the closed Brayton cycle power system. As part of this program, there is a need for simplifying the gas lubricated bearing system to improve the reliability of the turbomachinery. A major step in this simplification is to eliminate the hydrostatic jacking now required. This goal can be accomplished by developing bearings with low start-up friction coefficients that will not degrade when subjected to start-stop situations and occasional high-speed rubbing.

The purpose of the effort was to determine if the goal could be met using solid film lubricants in conjunction with a ceramic coated substrate. Plasma-sprayed chrome oxide on AISI 4340 was used as a base to test the effectiveness of MoS_2 and graphite fluoride coated via various bonding procedures.

Tests were conducted on existing experimental facilities that simulate the actual bearings involved. To simulate the hazards of operation of these bearings, three types of tests were conducted; low-speed (3400 rpm) start-stop tests, high-speed (38,000 rpm) shock impact tests and high-speed (36,000 rpm) long-duration rub tests. The substrate and plasma-sprayed chrome oxide surface of the samples were prepared so as to conform to the bearing surfaces presently used. In the Brayton cycle turbomachinery, the solid lubricants were then applied to this configuration.

MoS_2 was applied by four different methods; burnishing, sputtering, metal matrix bonding and polyimide bonding. Graphite fluoride was applied by two methods: burnishing and polyimide bonding.

By simulating operating conditions and the hazards that are likely to occur therein, the results of this testing are directly applicable to the bearings of the Brayton cycle power system and can be indirectly applied to many gas bearing applications.

3.0 MATERIALS

3.1 Sample Configuration

The test samples were manufactured to dimensions which duplicate those encountered in actual practice. AISI 4340 steel substrates were rough machined then heat treated to R_c 35 - R_c 42. After heat treating an arc plasma-sprayed coating of chrome oxide was applied and the specimens were finished to the dimensions shown in Figures 1 and 2. A total of 43 test pairs were manufactured. The chrome oxide surfaces of 22 of these test pairs were lapped to a nominal 0.254 μm (10 μin) surface finish, and the remaining 21 were lapped to a nominal 0.762 μm (30 μin) surface finish. Each test pair was coded for later identification. This code identifies the surface finish, solid lubricant, application method and the type of test for each sample. Table I shows the key to this code while Table II gives the distribution of surface finishes for each of the test types.

3.2 Solid Lubricants

Molybdenum disulfide has a successful history as a solid lubricant[1]. Consequently, any solid lubricant evaluation study could well incorporate MoS_2, as was done in the present study. The material used was Molykote Z from Dow Corning Corporation, Midland, Michigan. The average particle size is 4.3 μm with limits of 4 to 62 μm and of 98.7 percent minimum purity with the major impurity being carbon.

Methods of applying MoS_2 to a bearing surface influence its performance so that several application techniques were selected for study.

The simplest method is simply burnishing the MoS_2 onto the mating surfaces. This operation was performed at MTI.

Burnished films of MoS_2 often have rather short operating lives. Resin binders are commonly used to extend coating life. One of the bonded films used in this study was polyimide bonded MoS_2. This is a commercial coating which was supplied by Hohman Plating and Manufacturing, Incorporated, Dayton, Ohio and designated by their trade name Surf-Kote M-2036.

A second film, Surf-Kote M-1284, was selected based upon the supplier's recommendation. This film also contains MoS_2 as the solid lubricant but utilizes a so-called metal matrix bonding principal which extends the operating range of loads, surface speeds and temperatures.

Any organic film is limited by its decomposition temperature. A method of bonding MoS_2 to the bearing surface more firmly than by burnishing but which does not suffer from the temperature limitation of a resin would be desirable. Such a method seems to be available in sputtering.[2] Accordingly, MoS_2

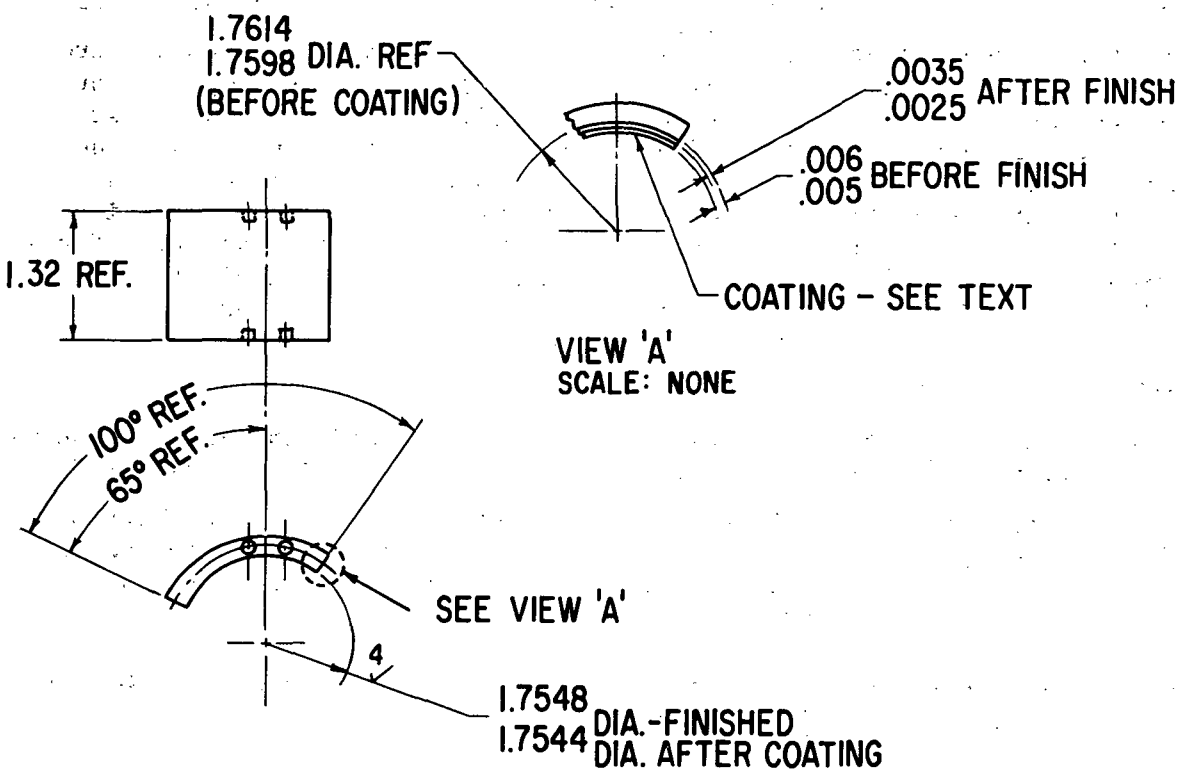

Fig. 1 Test Pad Dimensions

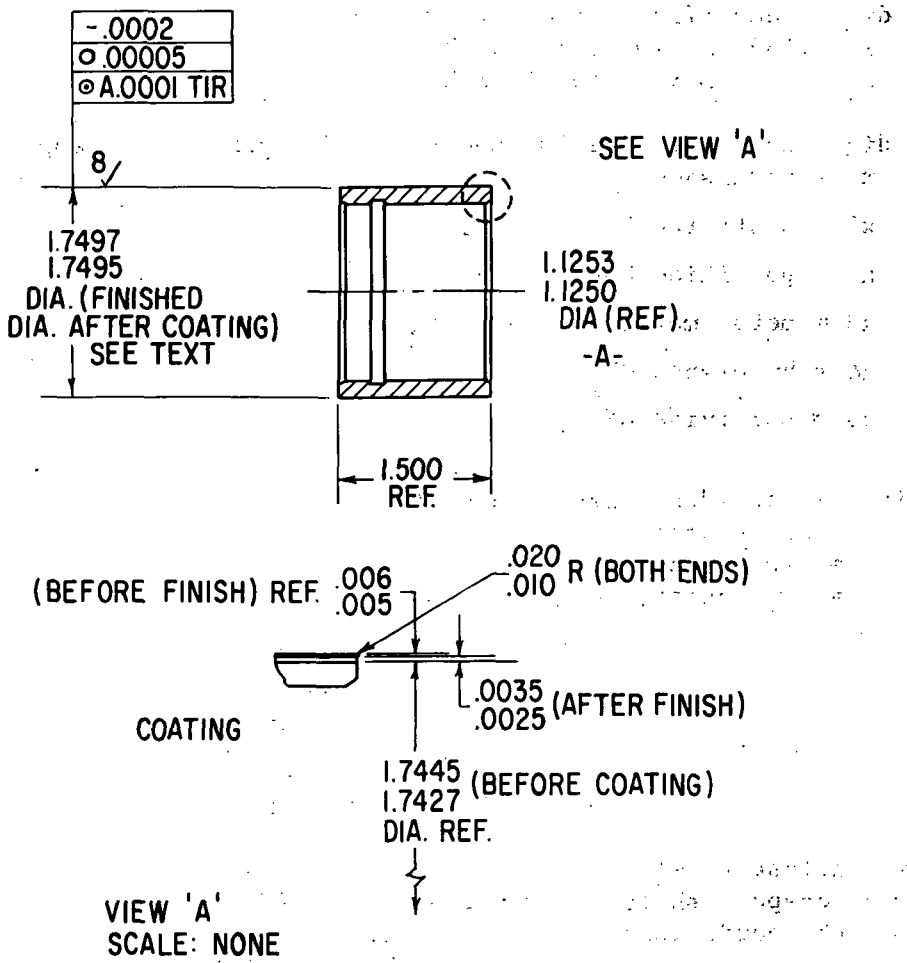

Fig. 2 Test Sleeve Dimensions

TABLE I

TEST SAMPLE CODE

1st digit identifies surface roughness.
- 1 = .254 μm (10 μin) finish
- 2 = .762 μm (30 μin) finish

2nd digit refers to coating and the technique used to apply it.
- x0 = burnished MoS_2
- x1 = sputtered MoS_2
- x2 = polyimide bonded MoS_2
- x3 = metal matrix bonded MoS_2
- x4 = burnished $CF_{1.1}$
- x5 = polyimide $CF_{1.1}$

Suffix letter identifies type of test.
- A = start-stop
- B = high-speed shock
- C = high-speed, long-duration rub

REFERENCE SPECIMENS

Plasma Sprayed Chrome Oxide

on 4340 Substrate Versus Itself

31 = start-stop reference
32 = high-speed shock reference
33 = high-speed, long-duration rub reference

CERTIFICATION TESTING

4x = certification test
x = 1,2,3,4 = test sequence number

TABLE II

NUMBER OF SAMPLES OF EACH SURFACE FINISH TESTED FOR EACH TEST TYPE

Test Type	Surface Finish, μm	
	0.254	0.762
Start-Stop Test	6	7
High-Speed Shock Test	6	7
High-Speed Rub Test	6	7
Certification Tests	4	0

Total Number of Samples Tested = 43

Number of 10 μin Surface Finish = 22

Number of 30 μin Surface Finish = 21

was sputtered onto the bearings.

Graphite fluoride is another material which has excellent potential as a high temperature solid lubricant. Under some sliding conditions, graphite fluoride coatings have a lower friction coefficient and longer wear life than MoS_2 coatings. Graphite Fluoride was obtained from Ozark-Mahoning Company, Tulsa, Oklahoma as Fluorographite $(CF_{1.1})_n$ and applied at MTI by burnishing.

Hohman Plating and Manufacturing Company furnished a polyimide bonded graphite fluoride film of the same formulation as that used by NASA[4].

3.3 Solid Lubricant Bonding Methods

The bonding method used to affix the solid lubricant to the substrate (in this case, chrome oxide) has been shown to be at least as important to life as the solid lubricant itself. For this reason, several bonding methods were tested which ranged in complexity from a very simple burnishing technique to fairly sophisticated sputtering.

Graphite fluoride was applied by two methods: burnishing and bonding with polyimide varnish. Molybdenum disulfide was applied by four different methods including burnishing, metal matrix bonding, polyimide bonding and sputtering.

Burnishing was the least complex of all the methods tested to bond the solid lubricant to the substrate. The technique used was simply to pour some pure solid lubricant onto a piece of clean cheesecloth and rub the solid lubricant into the surface. This was expected to be the least successful, since it relied solely on Van der Waals' forces for adhesion to the surface. However, the simplicity and economy of this method made burnishing a worthwhile technique for evaluation in this program.

The polyimide, PI 4701, used for both graphite fluoride and MoS_2 was supplied by Dupont. The solid lubricants were mixed with this polyimide and sprayed onto the bearing surfaces.

The spraying procedure was different for the two lubricants with the MoS_2 being the simpler of the two. It was sprayed to an average thickness of 15.24 μm (0.0006 in). This was then air dried for 30 minutes, oven cured at 93.3°C (200°F) for one hour and at 287.8°C (550°F) for one hour.

The polyimide graphite fluoride samples were sprayed in the same manner reported by Fusaro and Sliney[4]. This method prescribes spraying on a thin coat, then baking at 100°C (212°F) for one hour. This procedure is repeated until a thickness of 15.24 μm (0.0006 in) is reached. At this point, the remainder of the curing procedure was accomplished. This procedure consists

of baking at 100°C (212°F) for one hour then an additional hour at 300°C (572°F).

The metal-matrix bonded lubricant uses MoS_2 as a base. The exact composition of this coating is proprietary, but it is know to contain, in addition to MoS_2, some natural graphite as well as other materials, and uses an A stage phenolic and a high molecular weight epoxy as binders. This material was sprayed on with an average thickness after coating of 10.16 μm (0.0004 in) and was then baked at 160.3°C (325°F) for one hour.

Sputtering is a relatively new method for solid lubricant application. Sputtering is performed in a vacuum chamber containing two closely spaced plates with a high electrical potential between them. A noble gas, usually argon, is introduced into the system and is ionized. The coating material, known as the target, is the cathode. The positively charged gas ions strike the target, causing some of the target material to break off, strike, and adhere to the anode substrate by virtue of their high thermal energy. This process has been called a "sort of 'atomic shrapnel' effect"[5].

The samples in this study were coated to a thickness of approximately 0.406 μm (0.000016 in) with pure MoS_2.

4.0 DESCRIPTION OF TESTS

4.1 Test Facilities

Figure 3 is a schematic of the interior of the test rig used for the testing and evaluation of solid lubricants for gas bearings. This is essentially the same rig described in Reference 6. Slight modifications have been made to this rig to accommodate the comparatively large number of samples which were to be tested and to enable the High-Speed, Long Duration Rub Test to be made with this apparatus.

Figure 4 is a layout drawing of the test rig used. This rig consists of a support shaft (1) mounted on two high-speed, preloaded, angular contact bearings (2). The test sleeve (3) is shrunk onto the support shaft and an end cap (4) further secures the test sleeve to the support shaft to insure that the test sleeve is attached rigidly. The ball bearings and rear portion of the support shaft are enclosed in a water-cooled housing (5). Lubrication for the ball bearings is provided by an air-oil-mist system, while double labyrinth seals (6) prevent the air-oil-mist from entering the test chamber.

The tilting pad bearing (7) is dead weight loaded against the test sleeve through the pivot ball (8) and pad holder (9). The pivot ball provides for self-alignment during operation of the bearing. The load is applied by adding dead weights on top of the vertical load arm (10).

For the low speed Start-Stop Tests, the test rig is set up with an electric drive motor as shown. For the high speed tests, the electric motor is removed and the shaft is driven by an air turbine (11). The shaft speed is measured through a magnetic pickup (12). Temperature was maintained throughout testing by two banks of quartz heaters which are automatically controlled to maintain a preset temperature.

4.2 Conditions of Testing

While the actual testing procedure was different for each type of test, the conditions of testing remained constant. All tests were run at 260°C (500°F) in an atmosphere of argon at 1.035×10^5 N/m^2 (15 psia). With the exception of the certification testing, the same lubricants, lubricant bonding methods and substrate surface finishes were examined during each test. Table III shows the code and parameters tested for each type of test.

The procedure for measuring breakaway friction was the same for all tests. This procedure involved measuring the torque required to rotate the support shaft. The support shaft had to be removed from the test rig to mount each new journal sleeve. This required resetting the ball bearing preload for each test. Since the inherent friction of the test rig had to be compensated for in the friction calculations and the inherent friction is a very strong function of preload, two force measurements were made whenever pos-

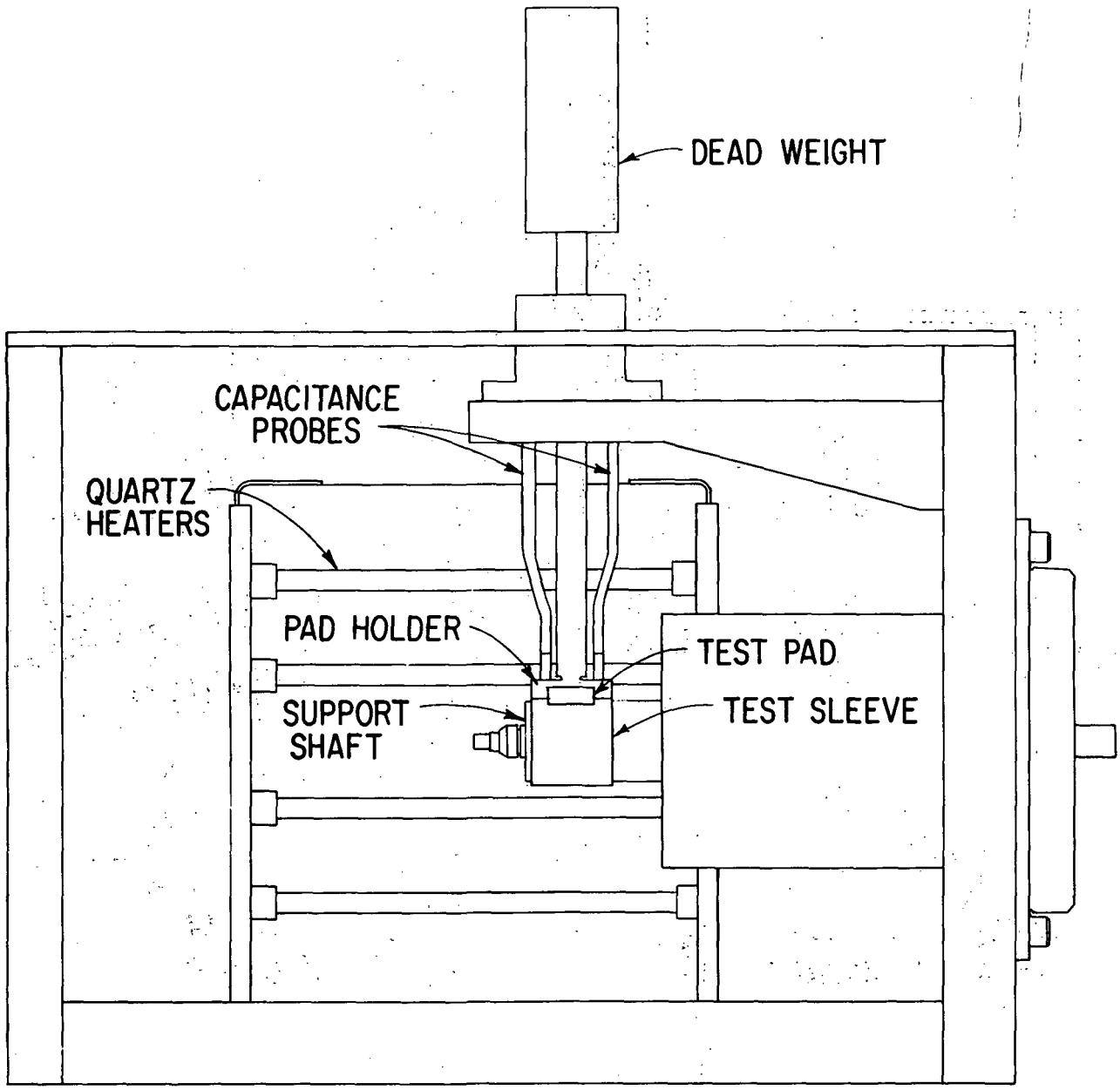

Fig. 3 High-Temperature Hydrodynamic Bearing Test Rig for Materials Evaluations

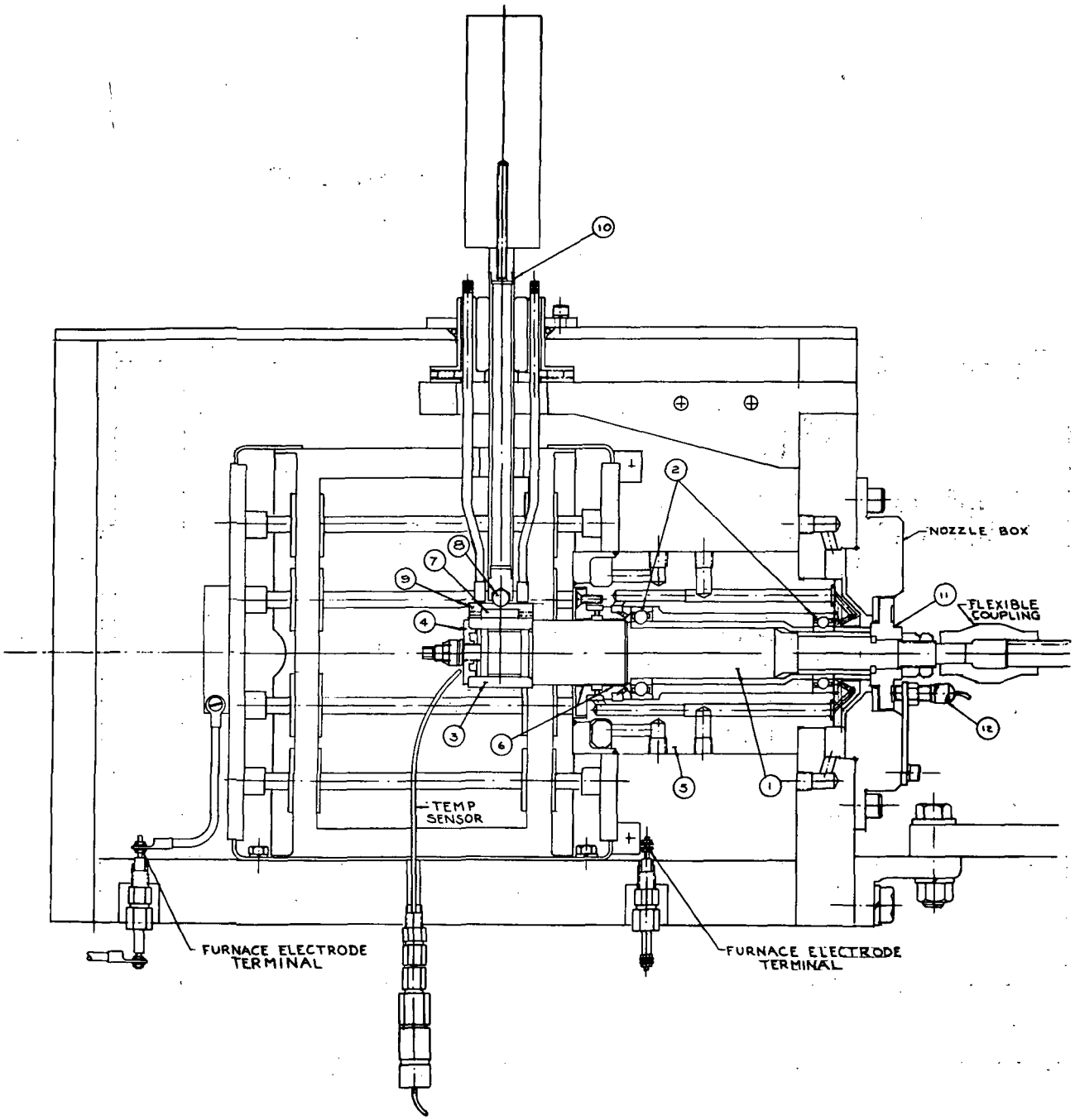

Fig. 4 Test Rig Layout

TABLE III

TEST SAMPLE PARAMETER

CONSTANT FOR EACH TYPE OF TEST

Sample Code	Surface Finish μm	(μin)	Solid Lubricant	Application Method
3x*	0.762	(30)	None	None
10	0.254	(10)	MoS_2	Burnished
11	0.254	(10)	MoS_2	Sputtered
12	0.254	(10)	MoS_2	Polyimide
13	0.254	(10)	MoS_2	Matrix
14	0.254	(10)	$CF_{1.1}$	Burnished
15	0.254	(10)	$CF_{1.1}$	Polyimide
20	0.762	(30)	MoS_2	Burnished
21	0.762	(30)	MoS_2	Sputtered
22	0.762	(30)	MoS_2	Polyimide
23	0.762	(30)	MoS_2	Matrix
24	0.762	(30)	$CF_{1.1}$	Burnished
25	0.762	(30)	$CF_{1.1}$	Polyimide

*3x is Unlubricated Reference Sample Where

x = 1 = Start-Stop Test

x = 2 = High-Speed Shock Test

x = 3 = High-Speed Rub Test

For Certification Testing

Sample Code	Surface Finish μm	(μin)	Solid Lubricant	Application Method
41	0.254	(10)	MoS_2	Sputtered
42	0.254	(10)	MoS_2	Sputtered
43	0.254	(10)	MoS_2	Sputtered
44	0.254	(10)	MoS_2	Sputtered

sible. One measurement was of the inherent resisting torque of the support shaft and ball bearings, the other was the total resisting torque of the loaded gas bearing without a gas film. The theory and a sample calculation of the coefficient of friction can be found in Appendix I. A discussion of the uncertainty associated with the coefficient of friction is contained in Appendix II.

Gas film thickness was monitored by two capacitance probes looking at the back of the pad holder (see Figure 5). Admittedly, this system does not enable one to make precise film thickness measurements. Its purpose, however, was only to enable one to determine if the pad had lifted off the shaft and the sensitivity of the system was more than adequate for this determination.

The load on the gas bearing was maintained at 2.76×10^4 N/m^2 (4 psi) projected area loading. This load was maintained as explained in Section 4.1.

.3 Tests

Three tests were used to simulate conditions that occur in normal operation of turbomachinery due to start-up and shut-down or that may occur in normal operation due to imposed loads of short or long duration.

4.3.1 Start-Stop Tests

The Start-Stop Tests were low speed tests, designed to simulate the effects of start-up and shut-down of the actual turbomachinery on the rubbing surfaces of the bearing.

The Start-Stop Tests consisted of 1000 starts and stops. A timing system was employed to control the electric motor drive which, in turn, accelerated the shaft to 3400 rpm. After five seconds at 3400 rpm, the timing system shut down the motor and the support shaft was allowed to coast to a complete stop. The coast down took approximately 10 seconds and the total shut down time was 15 seconds. In all cases, the development of a full fluid film between the pad and test sleeve occurred well within a half second of start-up.

4.3.2 High-Speed Shock Tests

In the operation of the actual turbomachinery, there is a high probability, due to momentary high loads, that rubs, milliseconds in duration, will occur. The High-Speed Shock Tests were designed to simulate just such conditions, so the effects of this hazard on the rubbing surfaces could be determined.

The High-Speed Shock Tests consisted of applying shock loads of predetermined magnitude to the bearing pad while the shaft was rotating at 38,000 rpm. The shock loads were applied at about 5 second intervals via a dead weighted pivot arm which was lifted to a fixed distance of 2.54 cm (1 in) before being dropped on the load rod of the test rig.

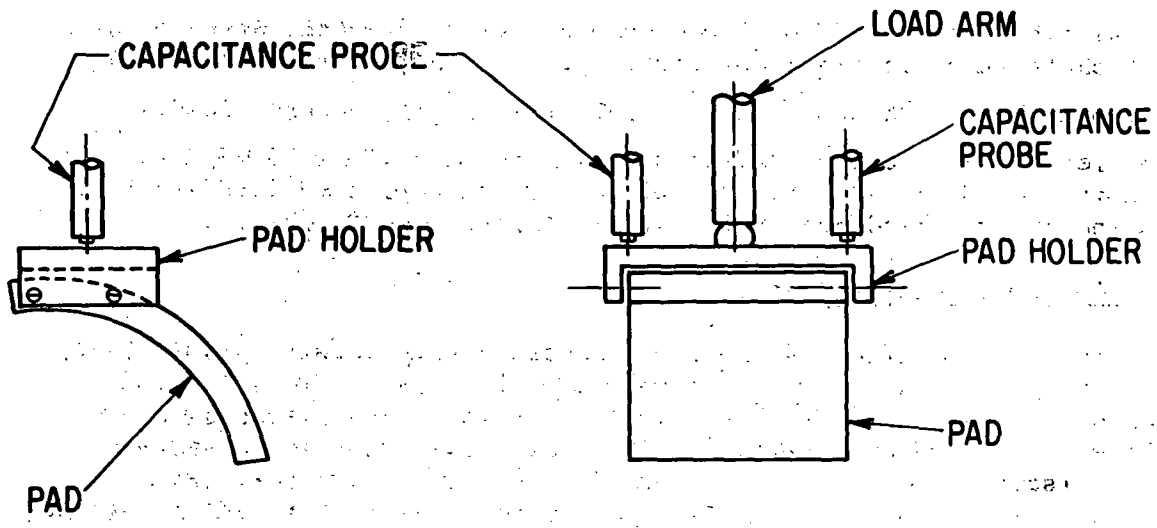

Fig. 5 Capacitance Probes Position

Figure 6 is a schematic of this test set-up, while Table IV shows the shock loading sequence and number of shocks at each load.

4.3.3 High-Speed, Long-Duration Rub Tests

The worst hazard which would be possible, from a bearing standpoint, is a long-duration, high-speed rub. While the probability of this type of situation arising is low, the possibility for catastrophic failure should the situation arise, is high. This type of rub could occur from a labyrinth seal or shroud rub or from unusually high maneuvering loads. These were the types of situations which were simulated in the High-Speed Rub Tests.

These tests consisted of 5 one second rubs at 5 second intervals with the shaft at an initial rotational speed of 36,000 rpm. A 9.55 kg (21 pound) or 7.245×10^4 N/m^2 (10.5 psi) projected area load was applied to the bearing pad in addition to the 2.76×10^4 N/m^2 (4 psi) running load. The load was applied through a pivoted load arm by a solenoid controlled pneumatic load cylinder (see Figure 7).

4.3.4 Certification Tests

The purpose of this testing was to determine test data repeatability. The test specimens were to incorporate the solid lubricant, bonding method and surface finish deemed to be optimum from preceding tests. While a detailed discussion of the results is presented in Section 5.0, some discussion is necessary at this point to justify the parameters which were chosen for further examination in the Certification Testing.

Table V gives the average coefficients of friction, after testing, for the various solid lubricants and bonding methods investigated. Column 1 identifies the bonding method and lubricant. Column 2 shows the average coefficient of friction for all the samples of that type. Columns 3 and 4 show the average coefficients of friction for the 0.254 and 0.762 μm (10 and 30 μin) surface finishes, respectively. This number is the average of one sample from each of the three kinds of tests. Examining column 2, it can be seen that the metal matrix bonded MoS_2 and the sputtered MoS_2 are the best lubricant choices. Comparing columns 3 and 4, it can be concluded that the 0.254 μm (10 μin) surface finish is superior for the sputtered film while there is no difference for the matrix film. The sputtered MoS_2 on 0.254 μm (10 μin) chrome oxide surface was chosen over the metal matrix bonded MoS_2 because of its thinness rather than a clear cut frictional advantage. It was postulated that the comparatively thick metal matrix might have a tendency to ball-up and cause a bearing failure. Since the test results show the sputtered film has virtually the same frictional coefficient as the metal matrix, the sputtered coating was chosen for further investigation.

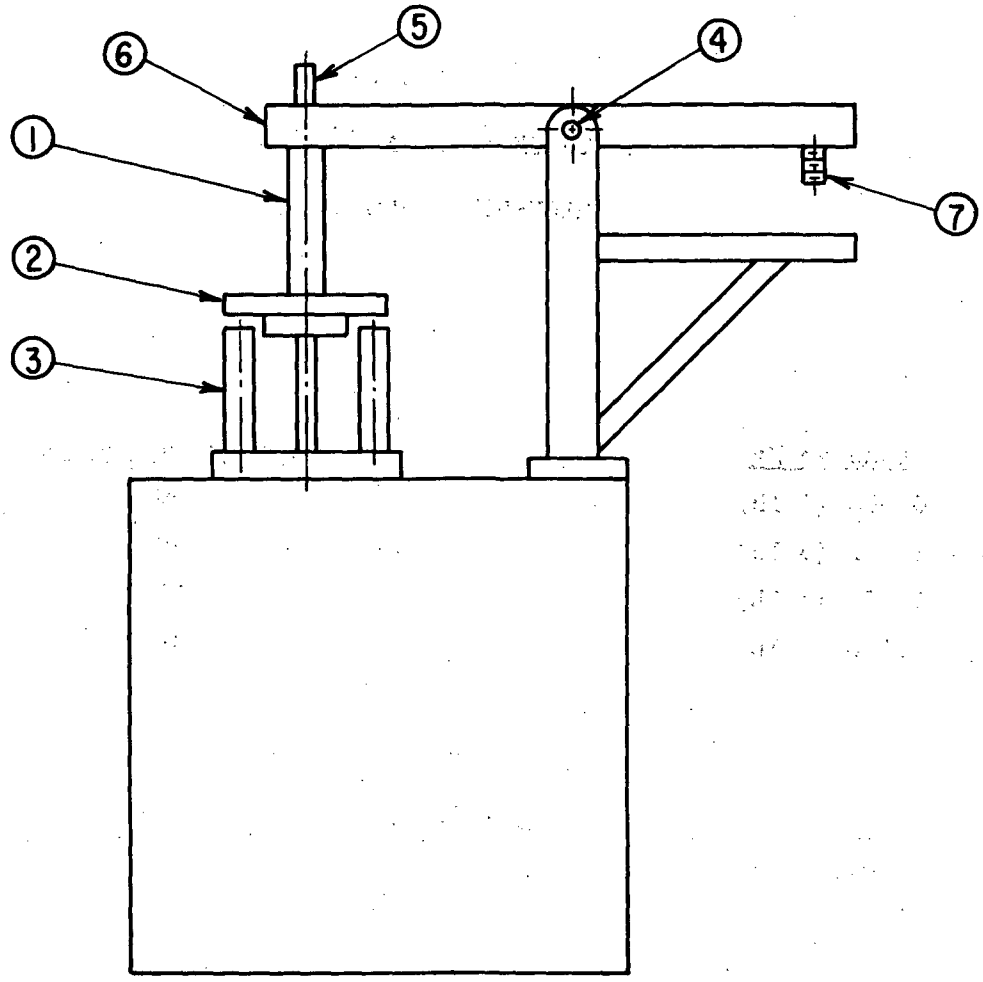

① LOAD ARM
② DEAD WEIGHT LOADING
③ CAPACITANCE PROBES
④ PIVOT
⑤ SHOCK LOAD HOLDER
⑥ SHOCK LOAD ARM
⑦ DISTANCE ADJUSTMENT

Fig. 6 High-Speed Shock Test Rig Schematic

TABLE IV

SHOCK LOADS APPLIED IN

HIGH-SPEED SHOCK TESTS

Load in Kg	Number of Shocks
0.394 (1 lb)	50
1.182 (3 lb)	20
1.970 (5 lb)	10
2.758 (7 lb)	10

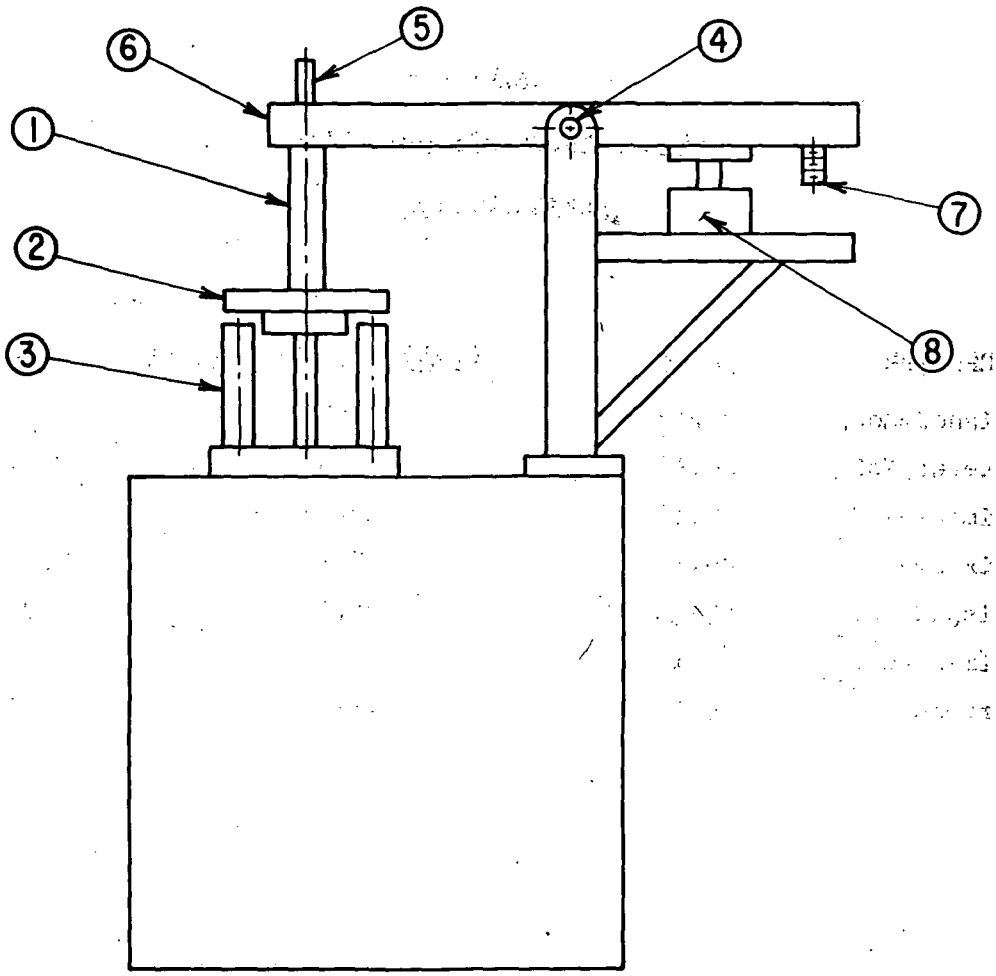

① LOAD ARM
② DEAD WEIGHT LOADING
③ CAPACITANCE PROBES
④ PIVOT
⑤ SHOCK LOAD HOLDER
⑥ SHOCK LOAD ARM
⑦ DISTANCE ADJUSTMENT
⑧ AIR CYLINDER

Fig. 7 High-Speed, Long-Duration Rub Test Schematic

TABLE V

AVERAGE COEFFICIENT OF FRICTION

AFTER TESTING

Specimen	Total	Surface Finish	
		0.254 μm (10 μin)	0.762 μm (30 μin)
Burnished MoS_2	0.22	0.19	0.25
Sputtered MoS_2	0.15	0.10	0.19
Polyimide MoS_2	0.17	0.15	0.20
Matrix MoS_2	0.11	0.11	0.11
Burnished $CF_{1.1}$	0.18	0.15	0.22
Polyimide $CF_{1.1}$	0.17	0.18	0.16
Reference	0.27	---	0.27

In summary, the choice of sputtered MoS_2 on 0.254 μm (10 μin) plasma sprayed chrome oxide was made for the following reasons:

- Low coefficient of friction
- Little change in coefficient of friction during High-Speed Shock Test
- Thin coating with high bond strength
- Low potential for debris generation

Certification testing used the same test set-up and procedure as for the High-Speed Rub Tests, the only difference being that 50 rather than 5 rubs were conducted. The interval between rubs was no greater than 15 seconds and no less than 5 seconds, except when breakaway friction measurements were being made. For this test, failure was defined as:

- A measured coefficient of friction of 0.2 or better
- Failure of the pad to lift off and develop a full gas film
- Damage to the chrome oxide surface.

5.0 TEST RESULTS

5.1 Review and Summary

The results show that all of the solid lubricants tested improved bearing contact performance compared to the uncoated chrome oxide surface.

The following conclusions are based on the data presented in Table VI and graphically in Figures 8 - 11:

1. All tests showed some improvement in coefficient of friction over the unlubricated reference.
2. The burnished samples, particularly MoS_2, generally did not retain the solid film lubricant throughout testing. The coefficient of friction was always higher after testing for burnished samples. Because of the low bond strength, the high wear rate and thin coating burnishing will probably prove most useful in applications such as component test rigs where a reduction in bearing friction is required, the number of surface rubs is limited and the coating must be applied in place by a technician who is not an expert in that field.
3. The 0.254 μm (10 μin.) surface finish samples generally have a reduced friction coefficient after testing. The inverse is true with the 0.762 μm (30 μin.) surface finish samples. The test results imply that, in general, a fine surface finish before solid lubricant application will result in lower friction for a longer period of time and less potential for debris generation, than will a coarse finish.
4. The sputtered samples show the least effects of rubbing (i.e., wear). This indicates a low wear rate, which is important for some gas bearing applications where it is critical to insure that bearing clearance dimensions remain constant from initial set-up through the life of the bearing.
5. Metal matrix bonded MoS_2 generally has the lowest coefficient of friction after testing, but highest before test. This result points strongly to the importance of run-in with this coating. In many situations this would not be necessary since even the starting friction was lower than the reference chrome oxide specimens.
6. Polyimide bonded graphite fluoride showed a slight frictional advantage over polyimide bonded MoS_2. This advantage is so marginal that the MoS_2 would probably be chosen for most applications on the basis of cost. However, the higher cost of graphite fluoride might be justified under circumstances where the operating temperature is high enough to decompose the MoS_2.
7. From a friction standpoint, the lubricants may be ranked from best

TABLE VI

AVERAGE COEFFICIENT OF FRICTION

SPECIMEN	Total Average		0.254 μm[1] Surface Finish		0.764 μm[1] Surface Finish		Start-Stop[2] Test		H.S. Shock[2] Test		H.S. Rub[2] Test	
	Before	After	Before	After	Before	After	Before	After	Before	After	Before	After
Burnished MoS_2	0.15	0.22	0.15	0.19	0.15	0.25	0.17	0.33	0.15	0.18	0.13	0.14
Sputtered MoS_2	0.15	0.15	0.19	0.10	0.11	0.19	0.18	0.17	0.14	0.08	0.12	0.19
Polyimide MoS_2	0.12	0.17	0.13	0.15	0.12	0.20	0.14	0.16	0.12	0.22	0.10	0.15
Matrix MoS_2	0.18	0.11	0.22	0.11	0.14	0.11	0.26	0.16	0.14	0.07	0.14	0.12
Burnished CF	0.15	0.19	0.16	0.15	0.14	0.22	0.16	0.18	0.16	0.21	0.12	0.16
Polyimide CF	0.11	0.17	0.11	0.18	0.10	0.16	0.10	0.12	0.09	0.22	0.13	0.18
Reference	0.21	0.27	-	-	0.21	0.27	0.26	0.31	0.24	0.28	0.14	0.21

[1] 0.254 & 0.764 μm columns are averages of the three test types

[2] Test type averages are the averages of both surface finishes

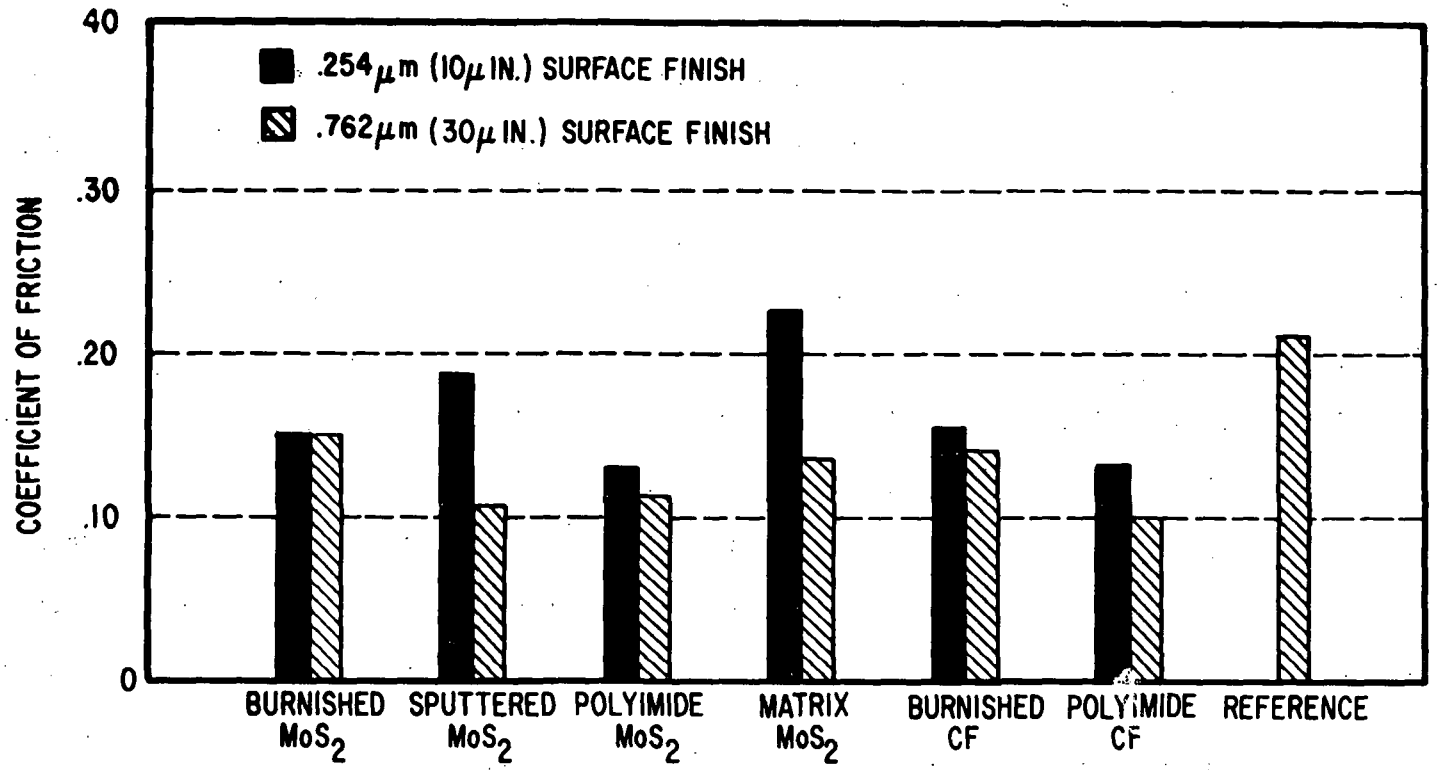

Fig. 8 Friction vs Surface Finish before Tests

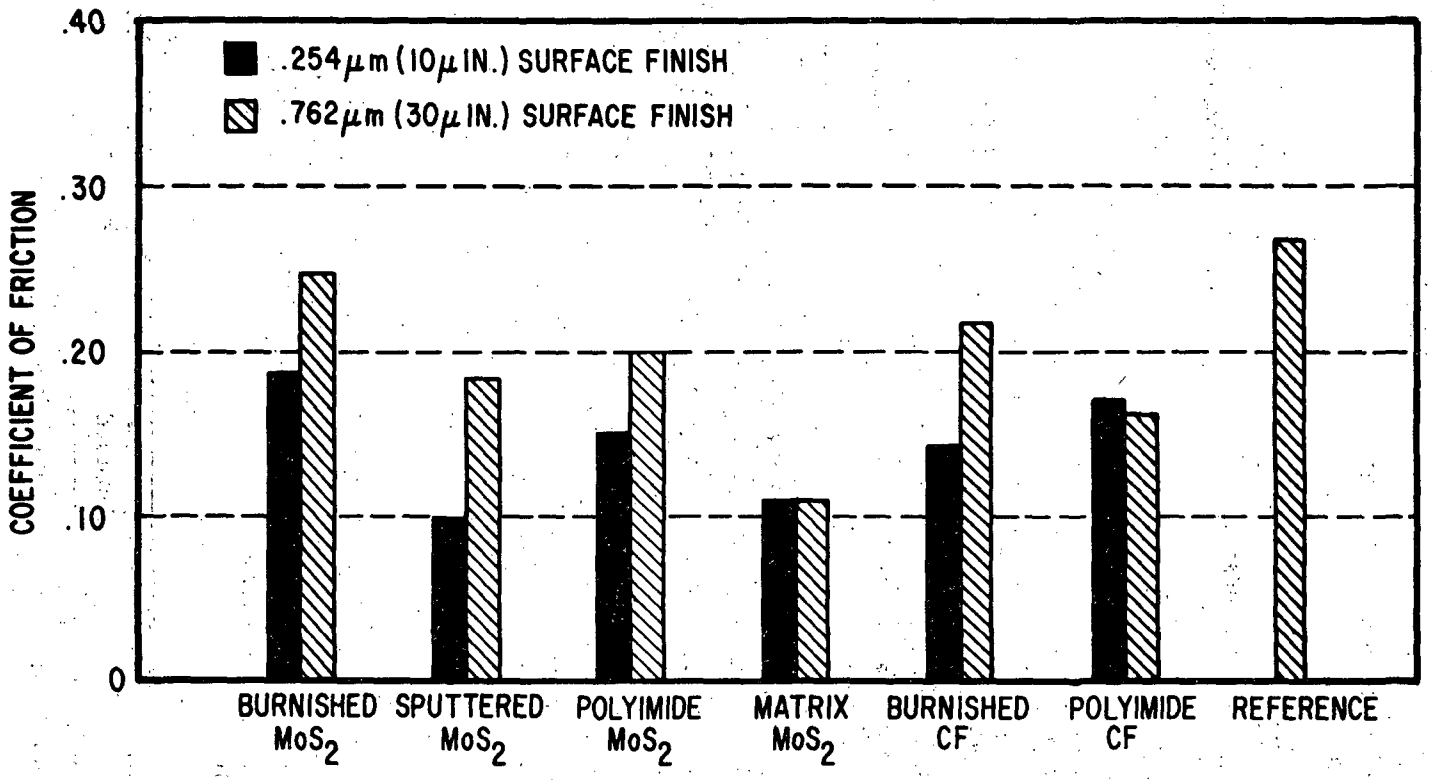

Fig. 9 Friction vs Surface Finish after Tests

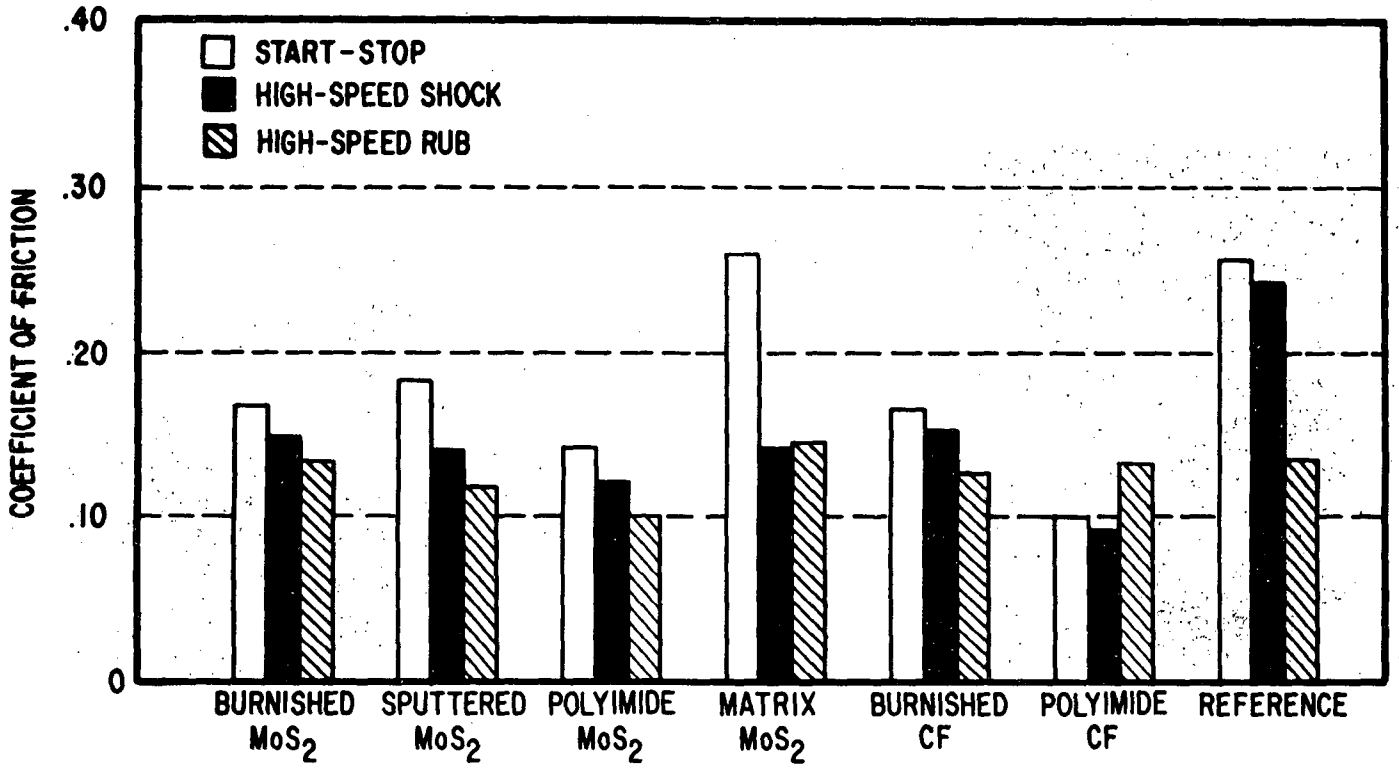

Fig. 10 Friction vs Test Type before Tests

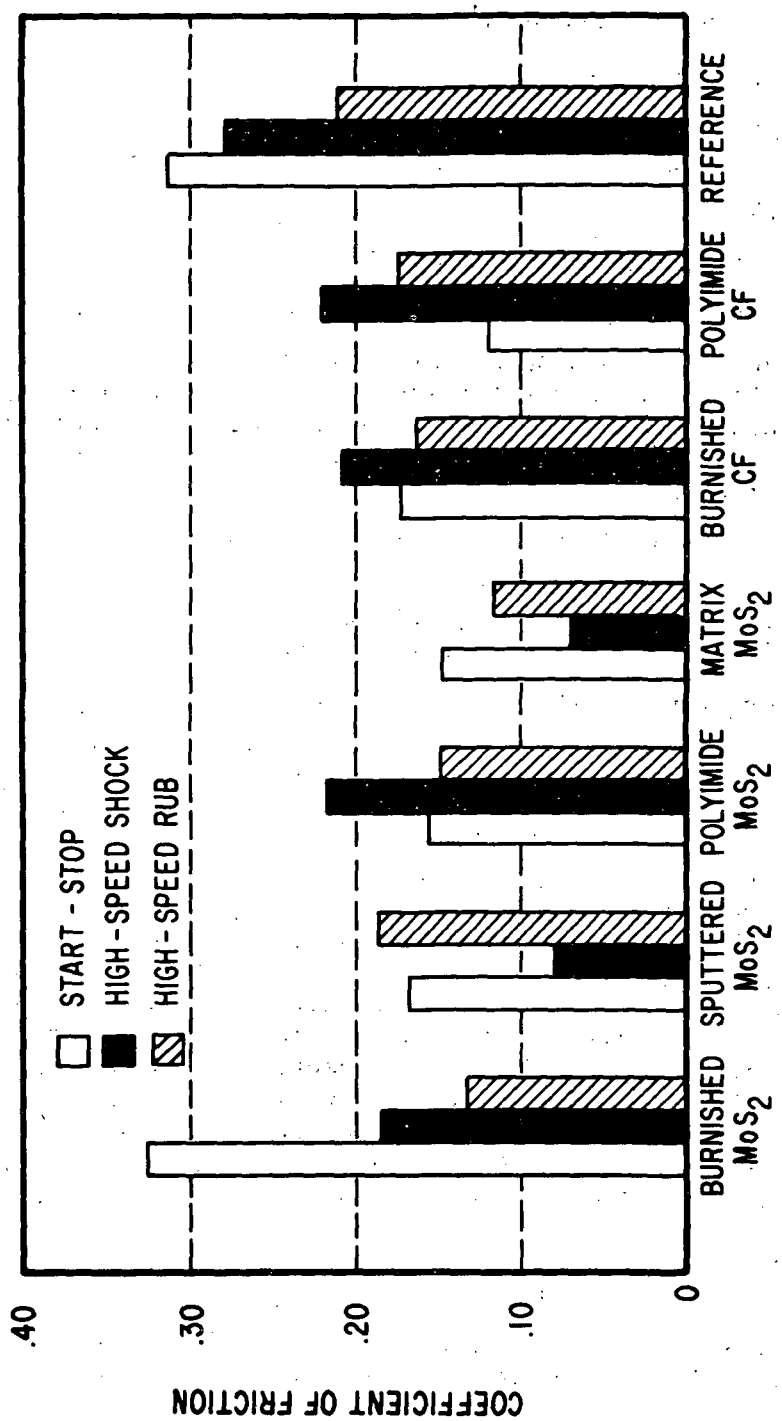

Fig. 11 Friction vs Test Type after Tests

to worst as follows:

a) Metal matrix bonded MoS_2

b) Sputtered MoS_2

c) Polyimide $CF_{1.1}$

d) Polyimide MoS_2

e) Burnished $CF_{1.1}$

f) Burnished MoS_2

8. In the Start-Stop Test, burnished MoS_2 exhibited a larger friction increase than did burnished graphite fluoride, but a smaller increase in the shock and rub tests. Therefore, if a burnished film was found to be necessary, the determination of which lubricant to use would depend on the type of hazard expected to be encountered most often.

9. Polyimide bonded films of either MoS_2 or graphite fluoride showed the most increase in the shock test although on balance there was little choice between the two lubricants; possibly the lower coefficient of friction of MoS_2 in the Start-Stop Test points to the choice of MoS_2 over graphite fluoride when polyimide bonded.

10. The coefficient of friction of the metal matrix bonded MoS_2 decreased in all tests, most in the Start-Stop Test and least in the Rub Test. The metal matrix MoS_2 shows promise as a gas bearing lubricant. It exhibits a low coefficient of friction and good endurance. There are several questions, however, which must be answered. Since the coating thickness is of the same order as a typical operating gas film thickness, careful measurements of the wear rate must be made to insure that clearances set at start up will not change significantly over life of the apparatus. With a thick coating, such as this, the potential for debris generation is high and this must be evaluated. It is not known if this material has a tendency to ball up and decrease the load carrying capacity of the bearings. Therefore while metal matrix bonded MoS_2 looks very promising as a lubricant some further testing is warranted.

11. Sputtered MoS_2 decreased in coefficient of friction in the Start-Stop and Shock Test but increased in the Rub Test. In spite of this increase, it is thought that sputtered MoS_2 is the best of the lubricants tested for immediate applications because the questions which arise in the metal matrix coating do not apply here because of the thin film.

5.2 Start-Stop Test Results

In the Start-Stop Test, a sleeve-pad pair were subjected to 1000 start-stop cycles. In each cycle, an electric motor brings the shaft up to 3600 rpm, holds it at the speed for 5 seconds and then shuts down, coasting to a stop. Coast-down time is approximately 10 seconds. After a 15 second delay, the cycle is repeated. The test data are summarized in Table VII.

Tallysurf measurements before the tests indicated that the MoS_2 polyimide films were significantly rougher than the chrome oxide substrates and the metal matrix films were somewhat rougher while the graphite fluoride polyimide films were comparable to the substrates in roughness. The burnished and sputtered films also showed little change from the substrate. Similar measurements after the tests indicated that the worn surfaces were smoother in nearly all cases. This indicates that no pronounced wear had taken place and that the bearings might be considered to be still in the "running-in" phase of their lives.

Considering the magnitudes of the various coefficients of friction after the Start-Stop Test, sputtered MoS_2 on 0.254 μm (10 μin) surface and graphite fluoride in polyimide on 0.762 μm (30 μin) surface have the lowest values. Considering the changes in the various coefficients of friction, the 0.762 μm (30 μin) surface finish generally exhibited larger increases or smaller decreases after testing.

It is apparent that the 0.254 μm (10 μin) surface finish is to be preferred, and that sputtered MoS_2 or graphite fluoride in polyimide are the solid film lubricants of choice based on the Start-Stop Test.

5.3 High-Speed Shock Test Results

In the High-Speed Shock Test, the shaft is rotated at 38,000 rpm by a turbine, with the pad riding on a gas film. The shock loads are applied manually at approximately 5 second intervals via dead-weight pivoted arm, which is lifted 2.54 cm (1 in) before being dropped onto the load rod of the test rig. The loading sequence and number of shocks at each load are given in Table IV. High-Speed Shock Test results are contained in Table VIII.

Surface finish measurements indicated that the MoS_2 in polyimide coatings were again much rougher than the substrate surface finishes, the metal matrix films somewhat rougher and all other films comparable in roughness to the substrates. Again, wear tended to smooth the surfaces.

The metal matrix bonded MoS_2 showed a greater decrease in coefficient of friction with the 0.254 μm (10 μin) than the 0.762 μm (30 μin) surface finish.

The sputtered MoS_2 decreased in friction on the 0.234 μm (10 μin) but

TABLE VII

START-STOP TEST DATA

Specimen	Lubricant	Method of Application	Surface Finish (μm) Before Pad	Surface Finish (μm) Before Sleeve	Surface Finish (μm) After Pad	Surface Finish (μm) After Sleeve	Frictional Force (kg) Before No Pad	Frictional Force (kg) Before Pad	Frictional Force (kg) After No Pad	Frictional Force (kg) After Pad	Coefficient of Friction Before	Coefficient of Friction After
31	-	-	0.65	0.71	0.30 & 0.51[1]	0.25	0.60	2.22	0.36	2.36	0.26	0.31
10A	MoS_2	Burnished	0.36	0.81	0.23	0.53	0.11	1.13	0.11	1.36	0.16	0.20
11A	MoS_2	Sputtered	0.51	0.23	0.30	0.25	0.36	1.81	0.14	0.60	0.23	0.07
12A	MoS_2	Polyimide	2.79	3.05	0.64 & 2.03[1]	0.64	0.54	1.50	0.27	1.25	0.15	0.15
13A	MoS_2	Matrix	1.32	0.51	0.89	0.56	0.77	2.95	0.64	1.54	0.34	0.14
14A	CF	Burnished	0.20	0.20	0.18	0.25	0.34	1.59	0.27	1.22	0.20	0.15
15A	CF	Polyimide	0.13	0.20	0.20	0.25	0.29	1.02	0.36	1.45	0.11	0.17
20A	MoS_2	Burnished	0.91	0.91	0.48 & 0.96[1]	0.66 & 0.96[1]	0.14	1.25	0.14	3.06	0.18	0.46
21A	MoS_2	Sputtered	0.58	0.58	0.38	0.51	0.27	1.13	0.34	2.04	0.14	0.27
22A	MoS_2	Polyimide	2.54	2.67	0.71 & 1.52[1]	1.22 & 1.52[1]	0.27	1.13	0.27	1.32	0.14	0.16
23A	MoS_2	Matrix	1.40	0.81	0.89	0.71	0.27	1.36	0.27	1.22	0.17	0.16
24A	CF	Burnished	0.64	0.71	0.38 & 1.27[1]	0.46	1.63[2]	1.29	2.09[2]	1.59	0.13	0.20
25A	CF	Polyimide	0.64	0.57	0.38	0.43	0.27	0.74	0.27	0.68	0.09	0.07

1 Numbers represent CLA readings in μin. in and out of wear scar respectively.

2 Inherent torque measured incorrectly. Coefficient of friction is based on average inherent torque of all tests.

TABLE VIII

HIGH-SPEED SHOCK TEST DATA

			Surface Finish (μm)				Frictional Force (kg)					
			Before		After		Before		After		Coefficient of Friction	
Specimen	Lubricant	Method of Application	Pad	Sleeve	Pad	Sleeve	No Pad	Pad	No Pad	Pad	Before	After
32	-	-	0.64	0.84	0.46	0.25	0.45	2.00	0.32	2.09	0.29	0.28
10B	MoS_2	Burnished	0.23	0.25	0.56	0.31	0.36	1.45	0.68	2.05	0.17	0.21
11B	MoS_2	Sputtered	0.31	0.31	0.20	0.20	0.34	1.59	0.23	0.68	0.20	0.06
12B	MoS_2	Polyimide	2.54	2.29	0.10 & 1.02[1]	0.23 & 0.86[1]	0.32	1.23	0.23	1.13	0.14	0.14
13B	MoS_2	Matrix	1.07	0.71	0.20	0.51	0.36	1.59	0.23	0.80	0.19	0.09
14B	CF	Burnished	0.20	0.20	0.15	0.15	0.54	1.36	0.45	1.45	0.13	0.16
15B	CF	Polyimide	0.43	0.25	0.38	0.31	0.23	0.68	0.19	1.73	0.07	0.23
20B	MoS_2	Burnished	0.81	0.69	0.51	0.43	2.27[2]	2.50	0.91[2]	1.59	0.13	0.16
21B	MoS_2	Sputtered	0.89	0.91	0.48 & 0.91	0.71	0.64	1.18	0.34	0.95	0.09	0.10
22B	MoS_2	Polyimide	2.67	3.05	0.97	0.89	0.32	1.08	0.41	2.28	0.10	0.29
23B	MoS_2	Matrix	0.89	0.97	0.41	0.25	0.54	1.13	0.45	0.84	0.09	0.05
24B	CF	Burnished	0.69	0.84	0.38	0.38	0.82	1.91	0.34	2.00	0.18	0.26
25B	CF	Polyimide	0.56	0.53	0.46	0.51	0.23	0.95	0.27	1.55	0.11	0.20

1 Numbers respectively represent CLA in μin. in and out of wear scar.

2 Inherent torque measured incorrectly. Coefficient of friction is based on average inherent torque of all tests.

slightly increased on the 0.762 μm (30 μin).

Turning to the absolute values of the coefficient of friction data from the shock test, the metal matrix bonded and sputtered MoS_2 solid lubricant films have the lowest values. Polyimide bonded MoS_2 on the 0.762 μm (30 μin) surface has a coefficient of friction larger than that of 0.762 (30 μin) surface finish reference.

The choice of surface finish based on the High-Speed Shock Test is again 0.254 μm (10 μin). Sputtered MoS_2 is again a good choice for the lubricant but metal matrix bonded MoS_2 performed better than did graphite fluoride in polyimide. Otherwise, the relative rankings are little changed.

5.4 High-Speed, Long-Duration Rub Test Results

In the High-Speed Rub Test, the shaft is driven by a turbine at 36,000 rpm. A load of 7.245×10^4 N/m^2 (10.5 psi) projected area is suddenly applied in addition to the 2.76×10^4 N/m^2 (4 psi) running load. This load is applied through a pivoted load arm by a solenoid controlled pneumatic load cylinder, maintained for one second, removed for 5 seconds and reapplied, and this is repeated 5 times. Table IX shows the data gathered in this test.

The only comment to be made about the surfaces of the High-Speed Rub Test specimens in addition to those applying to the previous test specimens is that the sputtered MoS_2 on the pads was rougher than usual. Even the rub test smoothed the surfaces.

The coefficients of friction measured before and after the High-Speed Rub Test differed less than those in the other tests and were more closely grouped in absolute values. That of the reference sample is lower than normal for chrome oxide which points to the possibility of contamination.

Metal matrix bonded MoS_2 showed decreases in coefficient of friction. There were no clear differences between the other coatings.

Surprisingly, the burnished MoS_2 on 0.762 μm (30 μin) surface and graphite fluoride on 0.254 μm (10 μin) surface, were nearly as low in friction as was the metal matrix.

Graphite fluoride in polyimide 0.762 μm (30 μin) surface finish equaled the reference sample in friction.

The 0.254 μm (10 μin) surface finish was better than the 0.762 μm (30 μin) while metal matrix bonded MoS_2 is the lubricant of choice for the High-Speed Rub Test. Sputtered MoS_2 and graphite fluoride in polyimide did not

TABLE IX

HIGH-SPEED, LONG-DURATION RUB TEST DATA

			Surface Finish (μm)				Frictional Force (kg)					
			Before		After		Before		After		Coefficient of Friction	
Specimen	Lubricant	Method of Application	Pad	Sleeve	Pad	Sleeve	No Pad	Pad	No Pad	Pad	Before	After
33	-	-	0.81	0.69	0.84	0.51	0.27	1.13	0.27	1.64	0.14	0.21
10C	MoS_2	Burnished	0.25	0.25	0.25	0.10	0.34	1.13	0.23	1.18	0.12	0.15
11C	MoS_2	Sputtered	0.25-0.99	0.20	0.25-1.02	0.31	0.32	1.18	0.27	1.41	0.14	0.18
12C	MoS_2	Polyimide	2.54	2.67	0.56 & 2.24[1]	1.57	0.32	0.95	0.23	1.23	0.10	0.16
13C	MoS_2	Matrix	1.55	0.81	0.51	0.69	0.45	1.36	0.41	1.13	0.14	0.11
14C	CF	Burnished	0.17	0.25	0.17	0.15	0.23	1.13	0.19	1.00	0.14	0.13
15C	CF	Polyimide	0.20	0.25	0.17	0.17	0.27	1.25	0.19	1.04	0.15	0.14
20C	MoS_2	Burnished	0.58	0.66	0.36 & 1.07[1]	0.48	0.27	1.18	0.19	0.95	0.14	0.12
21C	MoS_2	Sputtered	0.48-1.40	0.58	0.28 & 0.79[1]	0.31	0.34	1.00	0.34	1.59	0.10	0.20
22C	MoS_2	Polyimide	2.67	4.19	0.81 & 2.16[1]	0.71	0.27	0.95	0.23	1.13	0.11	0.14
23C	MoS_2	Matrix	1.73	1.02	0.43	0.31	0.23	1.18	0.19	0.95	0.15	0.12
24C	CF	Burnished	0.38	0.77	0.31	0.31	0.32	1.04	0.23	1.50	0.11	0.20
25C	CF	Polyimide	0.89	0.89	0.89	0.48	0.19	0.91	0.23	1.59	0.11	0.21

1 Numbers respectively represent CLA in μin. in and out of wear track.

perform nearly as well in this test as they had in previous tests.

5.5 Test Results Comparisons

Considering the simulation of actual gas bearing operation by the tests used in this study, the Start-Stop Test, in which graphite fluoride in polyimide did well, simulates a condition that will occur in operation, the High-Speed Shock Test simulates a less likely occurrence and the High-Speed, Long-Duration Rub Test simulates the least likely condition. On the other hand, the rub test imposes the most severe conditions on the bearing surfaces, while the shock test is probably the least severe as it was used here.

Referring back to the results of the various tests, it is evident that the 0.254 μm (10 μin) surface finish substrate is to be preferred over 0.762 μm (30 μin).

The choice of lubricant and method of application is not so clear-cut. In general, burnished films did not perform well and showed signs of rapid wear. Graphite fluoride in polyimide did well in the Start-Stop Test, although polyimide films in general did not perform exceptionally well throughout. Molybdenum disulfide, either sputtered or in the metal matrix binder, gave low coefficients of friction that changed little. Sputtered MoS_2 performed well in the Start-Stop and Shock Tests, while metal matrix bonded MoS_2 performed well in the Shock and Rub Tests.

The metal matrix film is about 40 times as thick as the sputtered deposit, which could affect the geometrical fit of curved bearing surfaces. Additionally, a thick film is more apt to produce large sized wear debris particles which may lodge in the narrow spacing of a gas bearing, causing damage and increasing frictional torque. These considerations point to the choice of sputtered MoS_2 solid lubricant films.

5.6 Certification Test Results

Based on the conclusions of the previous section, sputtered MoS_2 on 0.254 μm (10 μin) surface finish chrome oxide on AISI 4340 steel was selected for the Certification Test samples. The High-Speed, Long-Duration Rub Test was selected as the Certification Test method due to its severity. The Certification Test was made even more severe by increasing the number of rubs from 5 to 50.

Additional data was gathered by measuring the breakaway coefficient of friction at intervals throughout the Certification Tests.

Failure was defined as a coefficient of friction greater than 0.2 or failure of the pad to lift off the shaft sleeve or destruction of the chrome oxide layer. Neither of the last two failures occurred. One test sample did exceed the 0.2 coefficient of friction value, rising to 0.314 after 42 rubs. The other three samples easily survived all 50 rubs.

The test data are given in Table X and the average coefficients of friction are plotted in Figure 12, retaining the failed specimen data up to but not including the point of failure. Also given in Table X is the value for sample 11C from the first High-Speed, Long Duration Rub Test for comparison. The Certification Test samples have distinctly ower coefficients of friction. The reproducibility in the Certification Test was not as good as expected, the coefficients of friction after various numbers of shocks varying by nearly 50 percent. However, whether the individual sample data or the average data are examined, the same trend is evident: a running-in period during which coefficient of friction decreases followed by a rising coefficient of friction. Between the changes, a period of nearly constant coefficient of friction exists.

It is possibly significant that the surfaces of samples 42 and 44, particularly the pads, before testing, were rougher than those of samples 41 and 43 and that 42 and 44 had higher coefficients of friction than did 41 and 43. The sleeve of failed sample 42 was rougher than the other sleeves after testing although the pad was about the same. This again points out the necessity for smooth surfaces for low coefficients of friction.

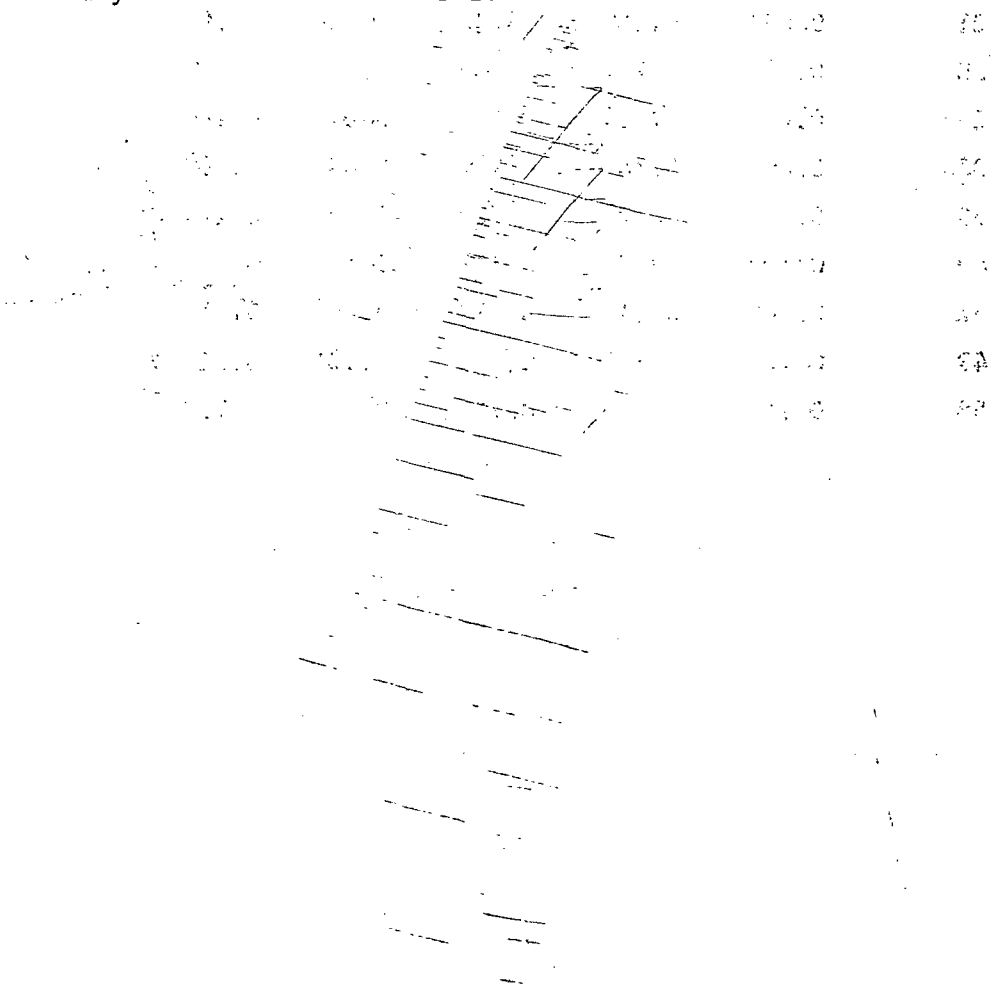

TABLE X

CERTIFICATION TEST DATA

Sample No.	41	42	43	44	$\bar{\mu}$	11C
Rub No.			Coefficient of Friction			
5	0.07	0.10	0.10	0.12	0.10	0.18
7	0.07	0.10	0.09	0.11	0.09	
12	0.08	0.12	0.07	0.10	0.09	
14	0.08	0.12	0.08	0.10	0.09	
19	0.08	0.14	0.08	0.10	0.10	
21	0.08	0.14	0.08	0.10	0.10	
26	0.08	0.15	0.09	0.10	0.10	
28	0.08	0.13	0.10	0.09	0.10	
33	0.09	0.14	0.10	0.08	0.10	
35	0.10	0.17	0.10	0.08	0.11	
40	0.10	0.17	0.10	0.10	0.12	
42	0.14	0.31	0.11	0.10	0.11	
47	0.14	-	0.12	0.10	0.12	
50	0.14	-	0.12	0.11	0.12	

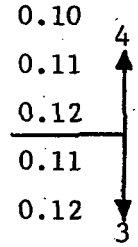

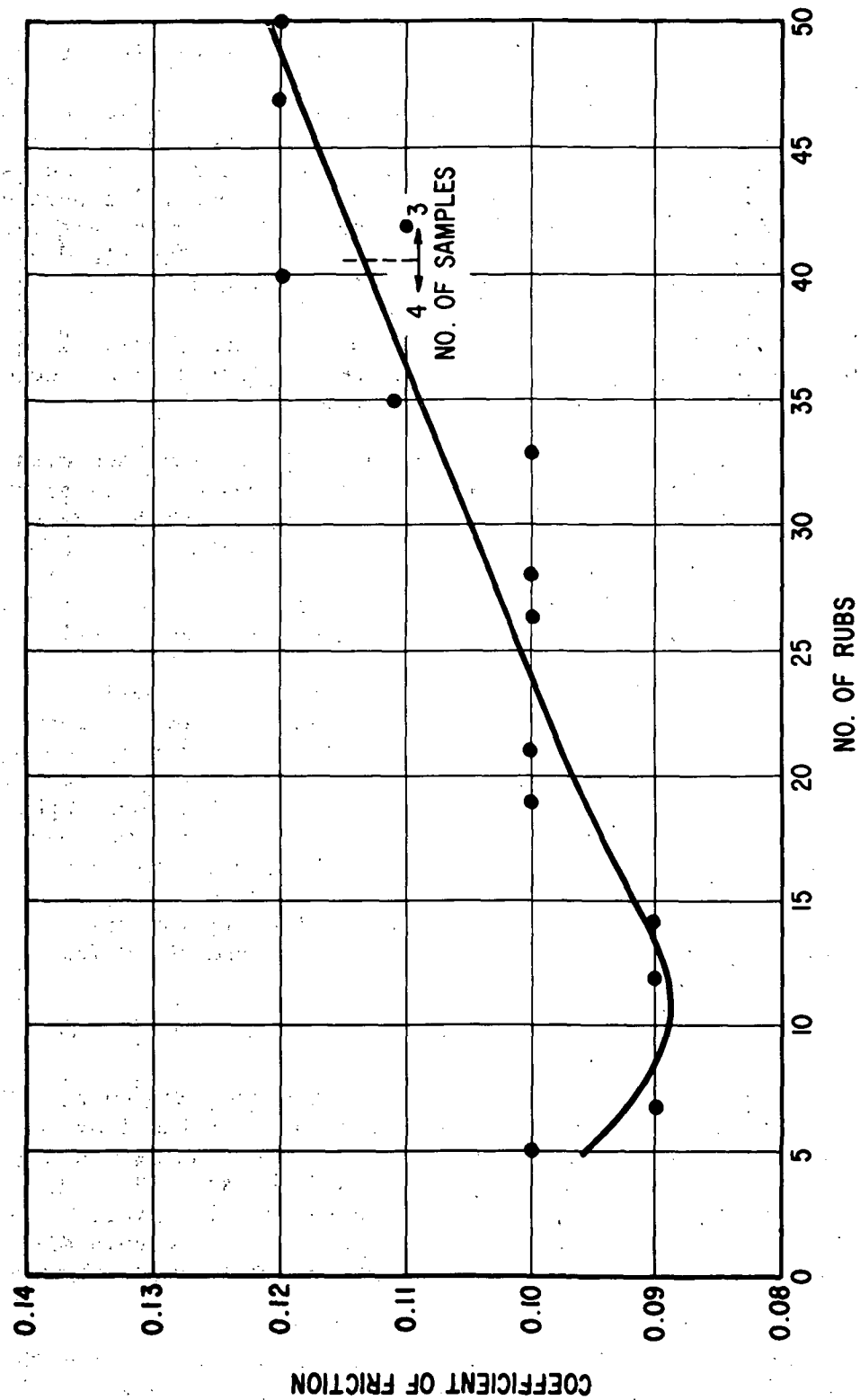

Fig. 12 Average Friction vs. Number of Rubs

6.0 PHOTOGRAPHIC STUDIES

Every pad and sleeve were photographed before and after testing at magnifications from 1X to 2.4X. Selected pictures are contained in the photographic atlas. The after test pad photos show the leading edge on the left. Wear is concentrated near the leading edge of the pads, but is spread more evenly over the sleeves, as is to be expected. In some pad photos, straight lines can be seen running across the pad (note particularly 23A (Plates 11 and 12) before and after testing). These marks are left by the Tallysurf stylus used to measure surface roughness. The sleeves were positioned so that the stylus marks were not in the field of view.

The macro photos were made with lens extension tubes on a Honeywell Pentax camera, using fluorescent illumination. The reflections of the fluorescent tubes can be plainly seen in the photos of the pads.

The micro photos of every pad and sleeve after testing were made with the same camera adapted to a Bausch and Lomb optical microscope used at 60X magnification. Illumination was by means of a standard incandescent opaque sample illuminator. The images in the micro photos arise from differences in reflectivity of the surfaces, since the illuminant is directed normal to the surface. Thus, bright areas in the photos are flatter areas on the surfaces and dark areas are inclined areas or holes.

All higher magnification photos are electron micrographs of selected pad samples made with a JEOL Scanning Electron Microscope. Energy dispersive electron analysis was used to delineate the arrangement of molybdenum disulfide on one surface. Additionally, a JEOL Electron Micro Probe was employed in an x-ray wave length dispersive mode to investigate the topography and surface composition of two other samples. The electron work was performed by Ernest F. Fullam, 900 Albany-Shaker Road, Latham, New York 12110.

To simplify discussion, the 0.254 μm (10 μin) surface finish will be referred to hereafter as the smoother surface finish and the 0.762 μm (30 μin) as the rougher surface finish.

6.1 Review and Summary

A screw-like pattern is visible on some of the reference and burnished sleeves after testing. This is probably an artefact arising from the hand method of diamond lapping used to produce the surface finishes on the chrome oxide. The burnished films may not be sufficiently thick to obscure the pattern, unlike the bonded films. The sputtered films, while also thin, are not as thin as the burnished films and are more evenly distributed than the burnished films, so that the sputtered films also obscure any similar artefact.

The Start-Stop Test affected the reference samples the least while the High-Speed, Long-Duration Rub Test caused the most visual wear marks.

The High Speed Shock Test caused the least wear on the lubricated samples and High-Speed, Long-Duration Rub Test the most. Wear is most apparent near the leading edge areas of the pads since the loads are applied near the leading edge while being spread over the entire sleeve area.

There was little or no correlation between wear and coefficient of friction, a common experience in friction and wear studies.

The most striking aspect of the micro photos was the incidence of cracking of the chrome oxide observed. The samples from the Start-Stop and Certification Tests did not show any cracking but both pads and sleeves from the High Speed Shock and High-Speed, Long-Duration Rub Test exhibited cracking of varying degrees. Approximately 12 percent of the samples were cracked. Both reference samples and lubricated samples were cracked. The cracking did not seem to affect the performance of the samples. This cracking will be discussed in more detail later in the report.

In general, the micro photos were not as informative as were the macro photos.

6.2 Start-Stop Test Photos

The screw-like pattern is more apparent on the burnished rougher finished sleeves (20A, 24A; Plates 8 and 13) than on the smoother (10A, 14A; Plates 2 and 6) due to the rougher finish showing through more strongly.

The graphite fluoride in polyimide samples (15A, 25A; Plates 7 and 14) show very little signs of wear while the molybdenum disulfide in polyimide (12A, 22A; Plates 4 and 10) have worn noticeably. The rougher surface finish seems to have accentuated wear.

The metal matrix bonded molybdenum disulfide (13A, 23A; Plates 5, 11 and 12) also showed considerable signs of wear, heavier on the rougher surface finish.

The tonal rendition of the surface and holes of sample 13A (Plate 69) are reversed on the electron micro photos from their appearance in the light micro photo (Plate 39). The metal matrix bonded molybdenum disulfide has an appearance of granularity not too different from that of the chrome oxide in the 1000X view.

A surface topographic view imaged by X-rays is given at 300X and the same field is shown imaged in a wave length dispersive mode (Plate 70) which shows that the surface is evenly coated with molybdenum disulfide except where pores or holes due to wear show the underlying dark chrome oxide.

The cross section of the metal matrix coating at 1000X in Plate 71 clearly shows its great thickness compared to the sputtered coating shown at 3,000X on sample 11A in Plate 67.

The sputtered molybdenum disulfide (11A, 21A; Plates 3 and 9) shows signs of wear on the smoother surface finish while the rougher finish has lost most of its lubricant and appears similar to the reference sample 31 in Plate 1.

The surface topographic view at 300 X and the same field imaged in a wave length dispersive mode (Plate 68) shows that the relief is rich in lubricant as indicated by the white areas caused by molybdenum disulfide.

Two somewhat tapered cross sections of this sample are shown in Plate 67, one at 500X showing that AISI 4340 steel, the porous chrome oxide (nominal thickness 63 μm (0.0025 in), the sputtered molybdenum disulfide and a brass facing block to prevent rounding of the edge of the specimen during polishing. Most of the pores in the chrome oxide are bright ringed in the photo due to electron build up on the corners. It might be thought that the sputtered coating is a similar artefact, but the coating is even more visible in the 3000X tapered cross section while the bright electron rings are less visible.

The micro photos of the burnished Start-Stop Test specimens show that graphite fluoride (14A, 24A; Plates 6 and 13) has a finer structure and wear pattern than does molybdenum disulfide (10A, 20A; Plates 2 and 8) and that the rougher surface finish (20A, 24A; Plates 8 and 13) wore more than the smoother (10A, 14A; Plates 2 and 6), in agreement with the findings from the macro photos.

The polyimide surfaces appear smoother than the burnished surfaces, with graphite fluoride (15A, 25A; Plates 7 and 14) smoother than molybdenum disulfide (12A, 22A; Plates 4 and 10), in agreement with the macro photos but the micro photos do not allow a firm conclusion as to the wear relative to surface finish, unlike the macro photos.

The tool marks visible on the sputtered molybdenum disulfide (11A, 21A; Plates 3 and 9) micro photos, however, are probably real since this film is so thin. Here too, the micro photos do not look like the macro photos.

6.3 High-Speed Shock Test Photos

This test does not seem to cause as much wear on the lubricated samples as does the Start-Stop Test.

A suggestion of the screw-like pattern is seen again on sample 10B in Plate 15, a burnished molybdenum disulfide film on the smoother surface finish, although the rougher surface finish sample (20B; Plate 21) does not show the pattern.

All burnished samples (10B, 20B, 14B, 24B; Plates 15, 19 21, and 25) show heavier wear on the rougher surface finish than on the smoother. The passage of a crack across a hole in the 1000X electron micro photo of sample 10B shown in Plate 72 is particularly striking.

There is little difference in wear appearance of the polyimide films (12B, 15B, 22B, 25B; Plates 17, 20, 23, and 26). Sample 22B pad was unfortunately sectioned for electron microscope examination before it was photographed. A series of electron micro photos of this sample (Plates 74 and 75) show the crack system at various magnifications. The areas in the three circles on the 300X view are reproduced at 2000 and 3000X. The cracks enter the polyimide coating which indicates that they were formed after the coating was applied. Since the conditions experienced during application of the polyimide are much less severe than those experienced during application of the chrome oxide, the cracks probably were formed during testing.

A photo obtained by an electron backscatter technique (Plate 76) shows the presence of molybdenum disulfide in pores in the chrome oxide and as white streaks smeared into the wear marks.

The 1000X electron micro photo of sample 12B in Plate 73 shows a layer structure, while that of sample 25B in Plate 77 does not, in agreement with the fineness of graphite fluoride compared to molybdenum disulfide noted from the optical micro photos of the Start-Stop Test samples.

The metal matrix bonded molybdenum disulfide (13B, 23B; Plates 18 and 24) show heavy wear, more so on the smoother surface finish in this test.

Wear was slightly more severe on the rougher surface finish carrying sputtered molybdenum disulfide than on the smoother surface finish chrome oxide (11B, 21B; Plates 16 and 22). This wear appears as plowing of the MoS_2 coating.

Table XI is a compilation of the after test coefficients of friction and a listing of the samples showing cracking. Cracking of sample 24 pad was not visible on the 60X light micro photo but showed up on the 1000X electron photomicrograph only. The table tends to indicate, since no pattern occurs, that cracking is probably common to all chrome oxide coatings. Because of the history of chrome oxide as a successful coating and because there does not seem to be any correlation between cracking and wear or coefficient of friction, it seems likely at this time that these cracks are not harmful in operation.

Note the visible wear marks on reference sample 32 (Plate 66), particularly in the 1000X view, which are not interacting with the cracks.

The burnished molybdenum disulfide samples (10B, 20B; Plates 40 and 46) show little difference, either between themselves, or compared to the burnished graphite fluoride samples (14B, 24B; Plates 44 and 50).

Much the same comment may be made about the polyimide samples (12B, 22B, 15B, 25B; Plates 42, 45, 48, and 51), the metal matrix bonded molybdenum disulfide (13B, 23B; Plates 43 and 48) and the sputtered molybdenum disulfide samples (11B, 21B; Plates 41 and 47).

TABLE XI

CRACKED SAMPLES

Sample No.	Test Type: Start-Stop (A)	High-Speed Shock (B)	High-Speed, Long-Duration Rub (C)	Certification (5 Rubs/50 Rubs)	Cracked Sample
	Post Test Coefficient of Friction				
31	0.31	---	---	---	
32	---	0.28	---	---	Pad and sleeve
33	---	---	0.21	---	Sleeve
10	0.20	0.21	0.15	---	B pad (slight)
11	0.07	0.06	0.18	---	
12	0.15	0.14	0.16	---	
13	0.14	0.09	0.11	---	
14	0.15	0.16	0.13	---	C Sleeve (very slight)
15	0.17	0.23	0.14	---	C Sleeve (questionable) B Sleeve
20	0.46	0.16	0.12	---	B Sleeve
21	0.27	0.10	0.20	---	C Pad
22	0.16	0.29	0.14	---	B Pad
23	0.16	0.05	0.12	---	
24	0.20	0.26	0.20	---	C Pad (1000X only)
25	0.07	0.20	0.21	---	
41	---	---	---	0.07/0.14	
42	---	---	---	0.10/failed	
43	---	---	---	0.10/0.12	
44	---	---	---	0.12/0.11	

6.4 High-Speed, Long-Duration Rub Test Photos

No screw-like pattern can be discerned in the after test samples from this test, attesting to the severity of wear caused by the High-Speed, Long-Duration Rub Test which completely rearranges the surfaces. This test is the most severe of the three tests used in this work.

The burnished samples did not wear too badly in this test although the rougher surface finish samples (20C, 24C; Plates 33 and 37) wore more than the smoother (10C, 14C; Plates 27 and 31). Graphite fluoride (14C, 24C; Plates 31 and 37) wore less than molybdenum disulfide (10C, 20C; Plates 27 and 33).

The 1000 electron micro photo of sample 24C in Plate 78 shows cracks in the chrome oxide which were not visible in the 100X electron photos nor in the 60X light photos in Plate 62.

The polyimide samples wore very little with graphite fluoride (15C, 25C; Plates 32 and 38) wearing more than molybdenum disulfide (12C, 22C; Plates 29 and 35) and the rougher surface (22C, 25C; Plates 35 and 38) wearing more than the smoother surface finish (12C, 15C; Plates 29 and 32).

There is little difference in wear of the metal matrix bonded molybdenum disulfide (13C, 23C; Plates 30 and 36). One corner of the coating on the smoother surface finish pad was chipped but it is not known if this occurred during the test or in handling.

The sputtered molybdenum disulfide samples (11C, 21C; Plates 28 and 34) wore very badly in the High-Speed, Long-Duration Rub Test.

The micro photos of the burnished molybdenum disulfide samples (10C, 20C; Plates 52 and 58) and graphite fluoride samples (14C, 24C; Plates 56 and 62) bear out the slight wear noted from the macro photos.

The macro photo conclusions on the polyimide samples (12C, 15C, 22C, 25C; Plates 29, 32, 35, and 38) are borne out by the micro photos (Plates 54, 57, 60, and 63).

The micro photos of the metal matrix bonded molybdenum disulfide (13C, 23C; Plates 55 and 61) show more extensive wear on the rougher surface finish.

Again, the micro photos of the sputtered molybdenum disulfide samples (11C, 21C; Plates 53 and 59) indicate heavy wear, more so on the rougher surface finish.

6.5 Certification Test Photos

The certification test was an extension of the High-Speed, Long-Duration Rub Test in which 50 rather than 5 rubs were used. The lubricant was sputtered molybdenum disulfide on 0.254 μm (10 μin) surface finish chrome

oxide.

In comparison with sample 11C, the same composition subjected to only 5 rubs, more wear occurred due to the increased number of rubs.

The sample (42; Plate 64) that failed one of the test criteria (coefficient of friction greater than 0.2) does not appear significantly different from the other samples.

The reticulated pattern seen on pad 11C (Plate 53) is faintly present in pad 44 (Plate 65), predominantly in the leading edge area. Pad 44 was chipped on two corners during grinding before testing.

All pads show signs of wear on the corners which again points to the severity of this test and may indicate that the pads oscillate during lift off or while lifted. The sleeves show pronounced wear tracks near the edges due to the pad corners. Sample 11C (Plate 28) shows this to a lesser extent as to be expected from the fewer rubs it underwent.

The certification test micro photos show little differences between the samples, although sleeve 42 (Plate 64) from the failed sample has a pattern transverse to the wear lines whose significance is not known.

7.0 DISCUSSION

There are consistent increases in coefficients of friction of the reference samples of unlubricated chrome oxide in all tests. There are generally lower coefficients of friction of the lubricated samples, even when they increased in friction during a particular test, showing that any of the tested lubricants are an improvement. However, some lubricants are more of an improvement than others.

Burnished films, whether of molybdenum disulfide or graphite fluoride, performed less well than bonded or sputtered films. Graphite fluoride is marginally better than molybdenum disulfide when burnished.

Polyimide bonded films of molybdenum disulfide or graphite fluoride showed the most increase in coefficient of friction in the High-Speed Shock Test. Graphite fluoride showed a slight frictional advantage.

Metal matrix bonded molybdenum disulfide performed best of all the bonded films. Its coefficient of friction decreased in all tests, most in the Start-Stop Test and least in the High-Speed, Long-Duration Rub Test.

Only slightly behind the matrix formulation was the sputtered molybdenum disulfide, considering frictional behavior alone. Its extreme thinness compared to bonded films and its better wear properties compared to burnished films make it an item for serious consideration.

The smoother surface finish 0.254 μm (10 μin), chrome oxide gave better performance and wear than did the rougher 0.262 μm (30 μin) finish. This is particularly noticeable in the Start-Stop Test where, for sputtered molybdenum disulfide, the smoother surface finish is in the lowest coefficient of friction group while the rougher is in the highest. The only lubricated samples that had coefficients of friction larger than the reference samples after testing were all on the rougher surface finish.

There is no correlation between wear or evenness of wear and coefficient of friction, as can be seen by comparing the low friction samples 11A, 25A, 11B, and 23B with the high friction samples 20A, 21A, 15B, and 24B.

Burnished molybdenum disulfide in the Start-Stop Test showed increases in coefficient of friction, particularly on the rougher surface finish, which had a coefficient of friction greater than that of the unlubricated reference sample. In the High-Speed Shock Test, its coefficient of friction again increased while in the High-Speed, Long-Duration Rub Test, surprisingly, its coefficient of friction was similar to that of the best lubricant, metal matrix molybdenum disulfide, and the coefficient of friction of the rougher surface finish was less than that of the smoother. In all tests, the wear was greater on the rougher surface finish, with least wear evident in the High-Speed, Long-Duration Rub test, where its coefficient of friction was among the lowest. This is a rare example of friction and wear behaving alike.

Burnished graphite fluoride exhibited an increase in coefficient of friction for the rougher surface finish in the Start-Stop Test while the smoother surface finish decreased in coefficient of friction. In the High-Speed Shock Test, its coefficient of friction increased similarly to that of the reference sample for both surface finishes. Like burnished molybdenum disulfide, burnished graphite fluoride performed similarly to the metal matrix molybdenum disulfide in the High-Speed, Long-Duration Rub Test although its coefficient of friction was larger than that of the burnished molybdenum disulfide and larger on the rougher surface finish, unlike molybdenum disulfide. In all tests, wear was greater on the rougher surface finish but less than the wear of molybdenum disulfide, particularly in the High-Speed, Long-Duration Rub Test. Burnished graphite fluoride has a finer structure and finer wear pattern than burnished molybdenum disulfide despite its greater coefficient of friction. This is the more common case, friction and wear not behaving alike.

Polyimide bonded molybdenum disulfide increased in coefficient of friction during all tests, generally more so when on the rougher surface finish. In the High-Speed Shock Test, the rougher surface finish coefficient of friction exceeded that of the reference sample after testing. Wear was more pronounced on the rougher surface finish. The lubricant seems to be in pores in the chrome oxide, which probably act as reservoirs from which the molybdenum disulfide is transferred to the wear streaks.

Graphite fluoride in polyimide wore somewhat more than molybdenum disulfide in polyimide, particularly in the High-Speed, Long-Duration Rub Test although the coefficient of friction of the two lubricants are generally similar in magnitude and changes. In the High-Speed, Long-Duration Rub Test, the coefficient of friction of graphite fluoride in polyimide on the rougher surface finish was equal to that of the reference sample after testing.

Although the wear of the metal matrix molybdenum disulfide was fairly large, particularly on the rougher surface finish, its coefficient of friction was generally quite low. In the High-Speed Shock and the High-Speed, Long-Duration Rub tests, it was in the lowest coefficient of friction group while in the Start-Stop Test it was in the middle group. Despite its granular appearance at high magnification, the molybdenum disulfide is evenly distributed over the surface.

Sputtered molybdenum disulfide also has a low coefficient of friction, being in the lowest group in the High-Speed Shock Test, the smoother surface finish being in the lowest group in the Start-Stop Test, although the rougher surface finish was in the highest, and being high in the High-Speed, Long-Duration Rub Test. It had a low coefficient of friction in the certification test which was maintained in three of four cases throughout 50 rubs and through 42 rubs in the remaining case. It performs much better on the smoother surface finish, probably because its lamellar surface distribution is somewhat uneven compared with that of the metal matrix molybdenum disulfide.

Burnished films did not perform well and showed signs of rapid wear. Polyimide films did not perform exceptionally well throughout, although graphite fluoride in polyimide did well in the Start-Stop Test. Molybdenum disulfide, either sputtered or in the metal matrix binder, gave lower coefficients of friction that changed little during testing. Sputtered molybdenum disulfide performed well in the Start-Stop and High-Speed Shock Tests while metal matrix bonded molybdenum disulfide performed well in the High-Speed Shock and High-Speed, Long-Duration Rub Tests.

The surface roughness data show that all tests had a smoothing effect indicating that no serious wear had taken place and that the bearings might be considered to be still in the "running-in" phase of their lives. Although the surface of the metal matrix molybdenum disulfide is exceeded in roughness only by that of the polyimide surfaces, the metal matrix molybdenum disulfide has the lowest coefficient of friction. However, for any given lubricant formulation, the smoother surfaces generally exhibit the lower coefficients of friction. In the certification tests on sputtered molybdenum disulfide, the rougher surfaces had the larger coefficients of friction and one of them failed during the test.

8.0 CONCLUSIONS AND RECOMMENDATIONS

Based upon the data gathered in the three tests used in this study on six solid lubricant formulations, the best lubricant from a frictional standpoint is metal matrix bonded molybdenum disulfide. Sputtered molybdenum disulfide is a close second choice and one that clearly warrants immediate consideration. Due to its extreme thinness, the sputtered molybdenum disulfide would be a good choice for immediate application in an operating gas bearing. Because of its lower coefficient of friction, the metal matrix molybdenum disulfide should be investigated further to ascertain if its comparatively thick film will produce wear debris that is damaging to gas bearings. Graphite fluoride in polyimide should be considered for applications in high temperature air bearings.

Bonded films perform better than burnished films, although any film is better than unlubricated chrome oxide which acts only as a hard wear surface. Sputtered films, by virtue of their physical bond, also perform very well.

Smoothness of surface, in the 0.254 μm (10 μin) range or less, both of substrate and applied solid lubricant film, is clearly important to good lubricant performance.

Microscopic cracking of the substrate or lubricating film is not deleterious to good bearing or lubricant performance.

The lift off of the pad from the sleeve was monitored by capacitance probes working against the back side of the pad holder. The rocking of the pad prevented measurement of the gas film thickness. If the capacitance probes are remounted on the pad holder so as to work against the sleeve, it will be possible not only to monitor lift off but also to measure gas film thickness and duration of contact during rub and shock tests.

The friction measurements made in the present testing represent only breakaway friction and were made in a rather coarse manner. More accurate measurements that would be dynamic as well as static could be made by redesigning a portion of the present test rig or by using a different rig with flat rather than curved specimens.

The polyimide and matrix bonded solid lubricant films are roughly 15 μm (0.0006 in) thick which effectively increases the diameter of the sleeve and decreases the diameter of the pad simultaneously. This could cause the pad to pinch the sleeve resulting in erroneous friction and wear data. Redesign of the bearing components to allow for these thicknesses would be worthwhile.

The bond of the chrome oxide to the steel is known to decrease with increasing temperature, ultimately failing at temperatures over 537°C (1000°F). Monitoring the temperature of the oxide-steel interface on the pad with a thermocouple would give an indication of incipient bond failure as well as allow an independent measure of lubrication effectiveness through

the frictional temperature generated, the better lubricants generating smaller temperature rises.

A series of tests in an air atmosphere would be desirable for two reasons, to ascertain if the inert argon atmosphere has any advantages and to ascertain if the material's are suitable for operation in air or in an air bearing. This particularly applies to comparison of graphite fluoride in polyimide against any molybdenum disulfide solid film lubricant.

One of the most beneficial aspects of this program is its almost direct application to other areas of technology. For instance, to the application of sputtered molybdenum disulfide in foil bearings. Sputtered molybdenum disulfide is a very thin film with high bond strength, low coefficient of friction and long life which will cause little if any change in the characteristics of the foil.

Plasma spraying is a crude method of material deposition, requiring grinding and lapping after deposition. Direct sputtering of chrome oxide may yield a better surface. Because of the lower temperatures involved in sputtering, it may not be necessary to grind after coating. A sputtered chrome oxide coating, because of its thinness, should be less susceptible to thermal distortions of the substrate and provide better heat dissipation. A sputtered coating should have a greater bond strength than a plasma sprayed coating.

The combination of chrome oxide and molybdenum disulfide simultaneously sputtered onto a bearing component such as a foil should offer the advantage of high wear resistance while continuously exposing new lubricant at the new surface. It ought to be possible to begin by sputtering chrome oxide alone, then to decrease its sputtering rate to zero while simultaneously increasing the sputtering rate of the molybdenum disulfide. This would give a film with inverse gradients of chrome oxide and molybdenum sulfide from pure chrome oxide at the substrate to a thin layer of molybdenum disulfide at the surface. We would thus obtain a film of enhanced bond strengths due to the gradient structure coupled with optimum surface lubrication resulting from the molybdenum disulfide while still retaining the high wear resistance of the chrome oxide and continuous exposure of new lubricant from the chrome oxide.

9.0 REFERENCES

1. Bisson, E. E., et al, "Friction, Wear, and Surface Damage of Metals as Affected by Solid Surface Films," NASA Report No. 1254, 1956.

   Palmer, E.B., "Solid-Film Molybdenum Disulfide Lubricants," Materials in Design Engineering, August 1961, 122 - 126.

   Winer, W.O., "Molybdenum Disulfide as a Lubricant: A Review of the Fundamental Knowledge," Wear 10 (1967) 422 - 452.

2. Buckley, D.H. and Spalvins, T., "Use of Sputtering for Deposition of Solid Film Lubricants," Sputtering and Ion Plating, NASA SP-5111, National Aeronautics and Space Administration, Lewis Research Center, Cleveland, Ohio, 16 March 1972.

3. Fusaro, R.L. and H.E. Sliney, "Graphite-Fluoride $(CF_x)_n$ - A New Solid Lubricant," ASLE Trans. 13 (1970) 56 - 65.

4. Fusaro, R.L. and H.E. Sliney, "Graphite-Fluoride as a Solid Lubricant in a Polyimide Binder," NASA Technical Note TND-6714, National Aeronautics and Space Administration, Lewis Research Center, Cleveland, Ohio, March 1972.

5. Riegert, R.D., "Gun Sputtering - A New Technique," Res./Dev. 24#2 (1973) 64 - 65.

6. Murray, S.F., "Research and Development of High Temperature Gas Bearings," NASA Contractor Report CR-1477, National Aeronautics and Space Administration, Washington, D.C., December 1969.

APPENDIX I

CALCULATION OF COEFFICIENT OF FRICTION

Definition of Terms

T_S = torque required to start rotation

T_R = torque resisting rotation

T_B = torque resisting rotation of support shaft only

F_1 = force required to start rotation of support shaft only

F_2 = force required to start rotation of shaft with load on pad

μ = coefficient of friction

N = load on pad, 3.64 Kg (8 lb)

R_1 = radius of test sleeve, 2.22 cm (0.875 in.)

R_2 = radius of point of application of forces, 1.27 cm (0.5 in.)

The torque required to start rotation is equal to the resisting torque

$$T_S = T_R \qquad (I - 1)$$

$$T_S = F_2R_2 \qquad (I - 2)$$

$$T_R = \mu NR_1 + T_B$$

$$T_B = F_1R_2$$

$$T_R = \mu NR_1 + F_1R_2 \qquad (I - 3)$$

Substitute equation I - 2 and I - 3 into equation I - 1

$$F_2R_2 = \mu NR_1 + F_1R_2$$

$$F_2R_2 - F_1R_2 = \mu NR_1$$

$$(F_2 - F_1)\, R_2 = \mu NR_1$$

$$\text{Let } F_A = F_2 - F_1$$

$$F_AR_2 = \mu NR_1$$

$$\mu = \frac{F_A R_2}{N R_1} = \frac{(F_2 - F_1)\, R_2}{N R_1}$$

Sample calculation using data from sample 31 before testing where

$F_1 = 1.3$ lb

$F_2 = 4.9$ lb

$$\mu = \frac{0.5\ (4.9 - 1.3)}{8 \times 0.875}$$

$\mu = 0.257$

APPENDIX II

UNCERTAINTY IN COEFFICIENT OF FRICTION

DUE TO MEASUREMENT ERRORS

According to H. Schenck, Jr.: Theories of Engineering Experimentation, 2nd ed., McGraw-Hill, New York, 1968, pp. 57 - 59:

ω_a = uncertainty associated with the parameter identified by the subscript

Theory: If result R = f(x,y,z) where x,y and z are experimental parameters, the uncertainty of the result (ω_R) is equal to

$$\omega_R = \left\{ \left[\frac{\partial}{\partial x} f(x,y,z)\right]^2 \omega_x^2 + \left[\frac{\partial}{\partial y} f(x,y,z)\right]^2 \omega_y^2 + \ldots\ldots \right.$$

$$\left. \ldots\ldots + \left[\frac{\partial}{\partial z} f(x,y,z)\right]^2 \omega_z^2 \right\}^{1/2} \qquad \text{(II - 1)}$$

where ω_x, ω_y and ω_z are the uncertainty of x,y and z respectively.

This theory can be expanded to any number of parameters as long as there is a functional relationship connecting the parameters.

In the present case, the coefficient of friction can be expressed in terms of

F_a = force required to overcome the friction of the test bearing only

R_1 = radius of test bearing

R_2 = radius to point of application

N = load on pad

by the expression

$$\mu = \frac{F_a R_2}{N R_1}$$

but F_a is composed of two forces

$$F_a = F_2 - F_1$$

where F_2 = force required to cause rotation of shaft with load on pad

F_1 = force required to cause rotation of support shaft only.

The uncertainty of F_a from equation II - 1 is then

$$\omega_{F_a} = \left\{ \left[\frac{\partial}{\partial F_1} (F_1 - F_2) \right]^2 \omega_{F_1}^2 + \left[\frac{\partial}{\partial F_2} (F_1 - F_2) \right]^2 \omega_{F_2}^2 \right\}^{1/2} \qquad \text{(II - 2)}$$

Since F_1 and F_2 are measured with the same instrument

$$\omega_{F_1} = \omega_{F_2}$$

and equation II - 2 can be reduced to

$$\omega_{F_a} = \omega_{F_1} \left[F_1^2 + (-F_2)^2 \right]^{1/2} \qquad \text{(II - 3)}$$

The uncertainty of μ from equation I - 1 is

$$\omega_\mu = \left[\left(\frac{R_2}{NR_1}\right)^2 \omega_{F_a}^2 + \left(\frac{F_a}{NR_1}\right)^2 \omega_{R_2}^2 + \left(\frac{-F_a R_2}{N^2 R_1}\right) \omega_N^2 + \cdots\cdots \right.$$

$$\left. \cdots\cdots + \left(\frac{-F_a R_2}{F R_1^2}\right) \omega_{R_1}^2 \right]^{1/2} \qquad \text{(II - 4)}$$

In the present case, only F_1 and F_2 are test variables, thus making F_A variable also. All other parameters are constant.

R_1 = 2.22 cm (0.875 in.) $\qquad \omega_{R_1}$ = 0.00254 cm (0.001 in.)

R_2 = 1.27 cm (0.5 in.) $\qquad \omega_{R_2}$ = 0.127 cm (0.05 in.)

N = 3.64Kg (8 lb.) $\qquad \omega_N$ = 0 (same weight always used)

F_a = variable ω_{F_1} = 0.11Kg (0.25 lb.)

The uncertainties above are estimated from machining tolerances for ω_{R_1} and from scale intervals for ω_{R_2} and ω_{F_1}.

Sample calculation from sample 10A before testing, where

F_1 = 0.25 lb.

F_2 = 2.50 lb.

giving

$F_a = F_2 - F_1 = 2.25$ lb.

From equation II - 3

$$\omega_{F_a} = 0.25 \left[(0.25)^2 + (-2.5)^2\right]^{1/2}$$

$$= 0.25 \left[0.0625 + 6.25\right]^{1/2}$$

$$= 0.25 \left[6.3125\right]^{1/2}$$

$$= 0.25 \left[2.512\right]$$

$$\omega_{F_a} = 0.628 \text{ lb.}$$

Let

$$\alpha = \frac{R_2}{NR_1} = \frac{0.5}{8x0.875} = 7.14 \times 10^{-2}$$

$$\beta = \frac{F_a}{NR_1} = \frac{2.25}{8x0.875} = 3.21 \times 10^{-1} \qquad \text{(II - 5)}$$

$$\delta = \frac{F_a R_2}{N^2 R_1} = \frac{2.25x0.5}{64x0.875} = 2.01 \times 10^{-2}$$

$$\gamma = \frac{F_a R_2}{NR_1^{\,2}} = \frac{2.25x0.5}{8x0.766} = 1.84 \times 10^{-1}$$

Combining equation II - 4 and II - 5

$$\omega_\mu = \left[(\alpha\omega_{F_A})^2 + (\beta\omega_{R_2})^2 + (-\delta\omega_N)^2 + (-\gamma\omega_{R_1})^2\right]^{1/2}$$

$$= \left[(7.14\times10^{-2}\times6.28\times10^{-1})^2 + (3.21\times10^{-1}\times5\times10^{-2})^2 + (-2.01\times10^{-2}\times0)^2 + (-1.84\times10^{-1}\times10^{-3})^2\right]^{1/2}$$

$$= \left[(4.48\times10^{-2})^2 + (1.605\times10^{-2})^2 + (0)^2 + (-1.84\times10^{-4})^2\right]^{1/2}$$

$$= \left[2.01\times10^{-3} + 2.58\times10^{-4} + \cancel{3.39\times10^{-8}}\right]^{1/2}$$

negligible

$$= \left[2.27\times10^{-3}\right]^{1/2}$$

$$= 0.048$$

The equations were programmed for a computer and all samples were run. A representative value for the uncertainty in the coefficient of friction, ω_μ is 0.050. While this uncertainty is high, it is included only to temper the use of the coefficient of friction. All conclusions contained in this report which have been based on the coefficient of friction are considered valid because this uncertaintv was strongly considered at that time.

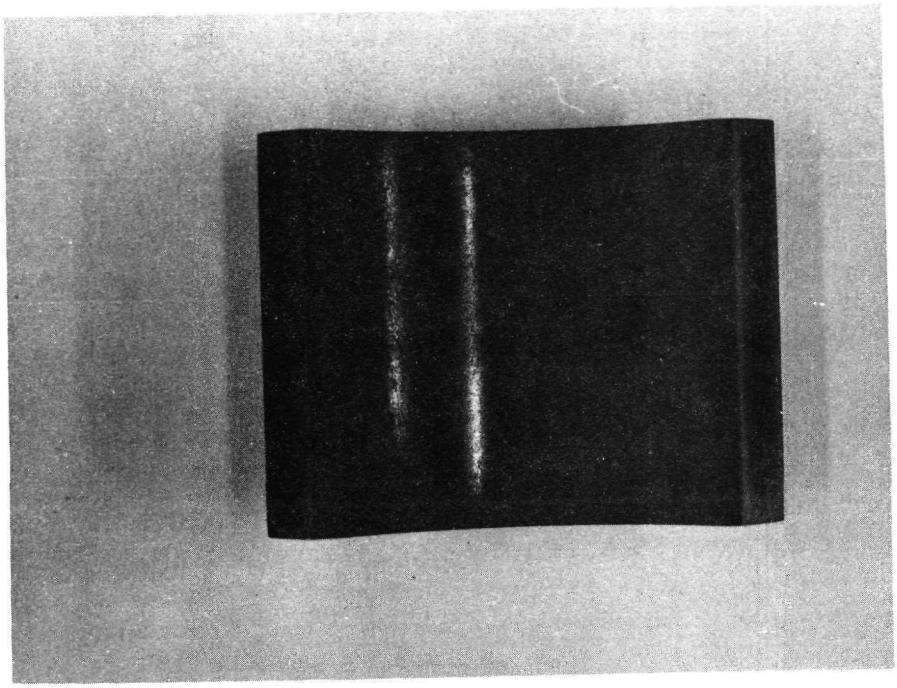

Pad After Testing

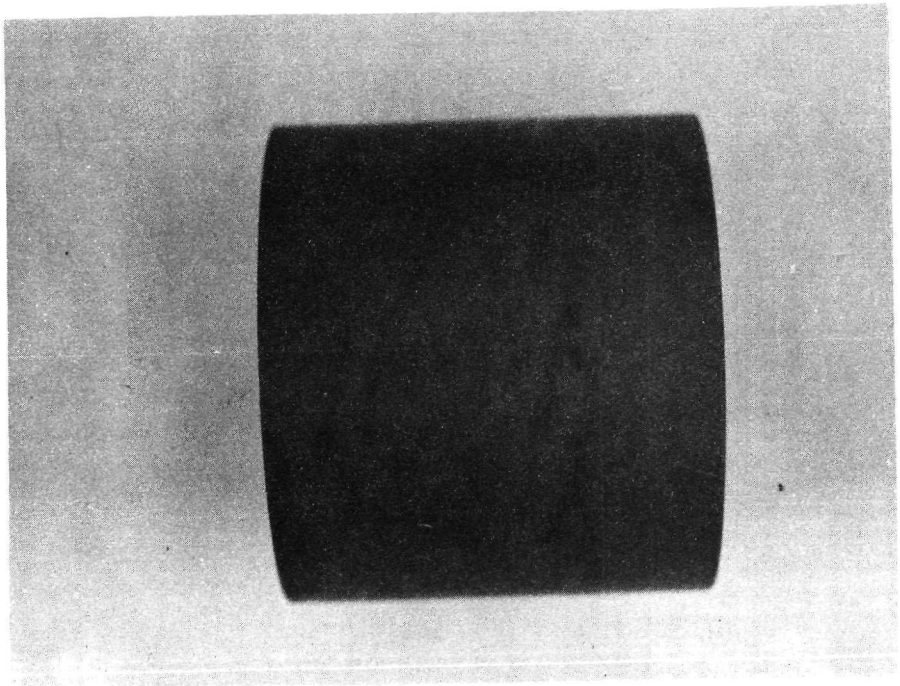

Sleeve After Testing

Plate 1 31 Reference

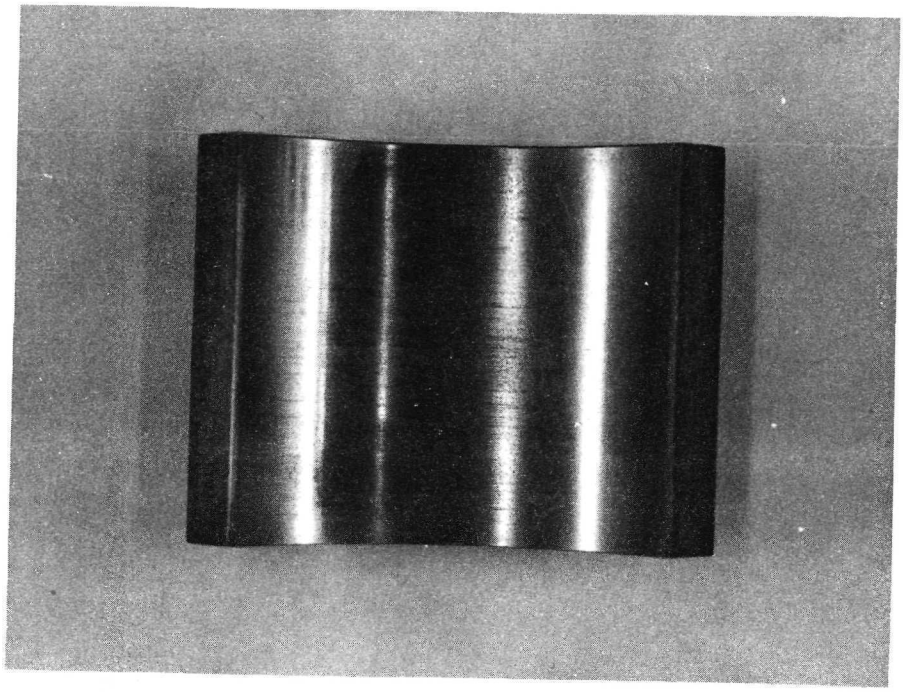

Pad After Testing

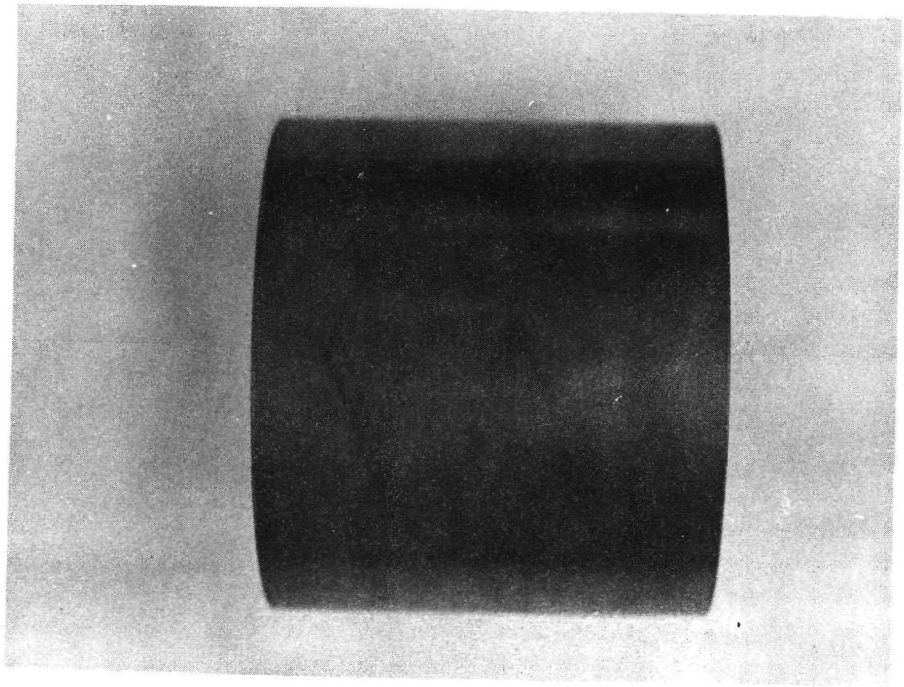

Sleeve After Testing

Plate 2 10A Burnished MoS_2

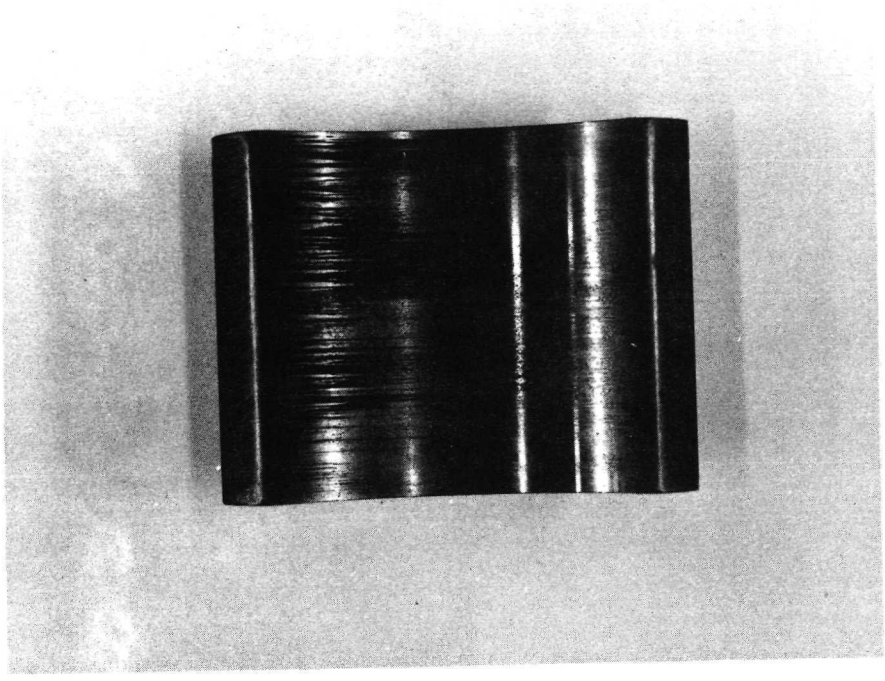

Pad After Testing

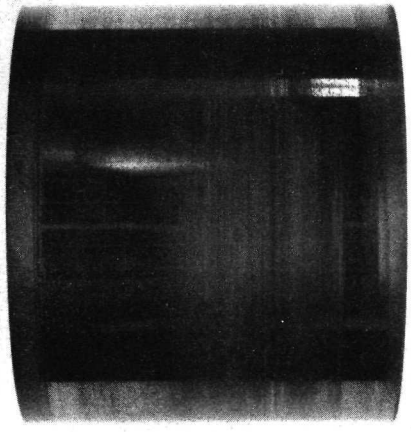

Sleeve After Testing

Plate 3 11A Sputtered MoS_2

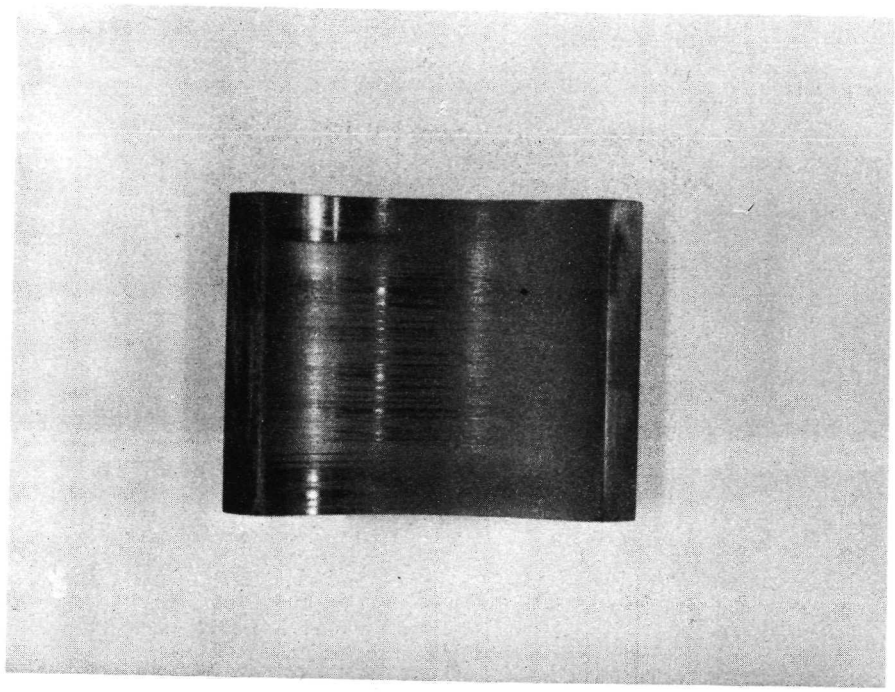

Pad After Testing

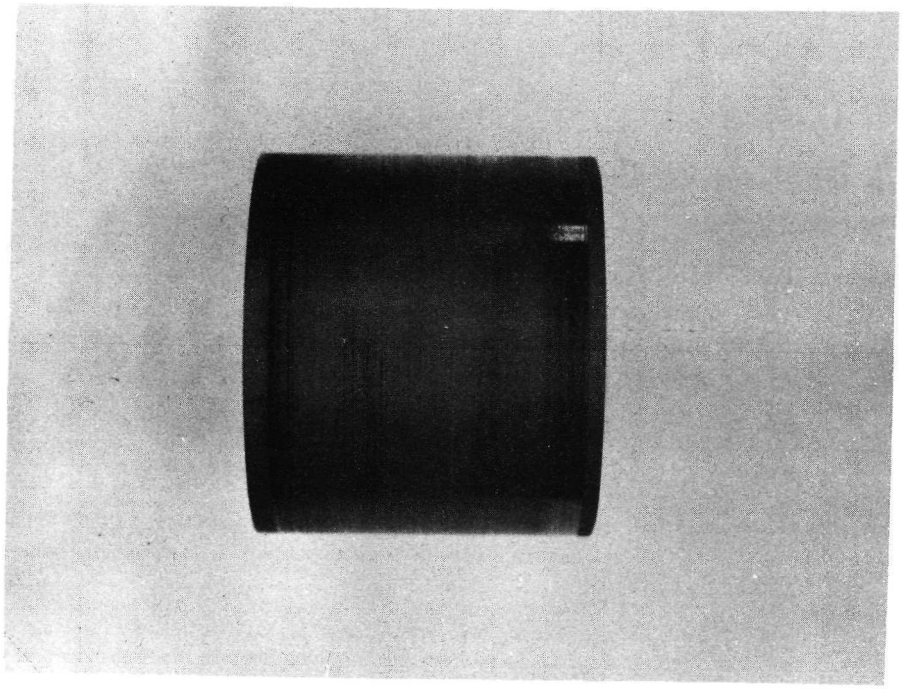

Sleeve After Testing

Plate 4 12A Polyimide MoS_2

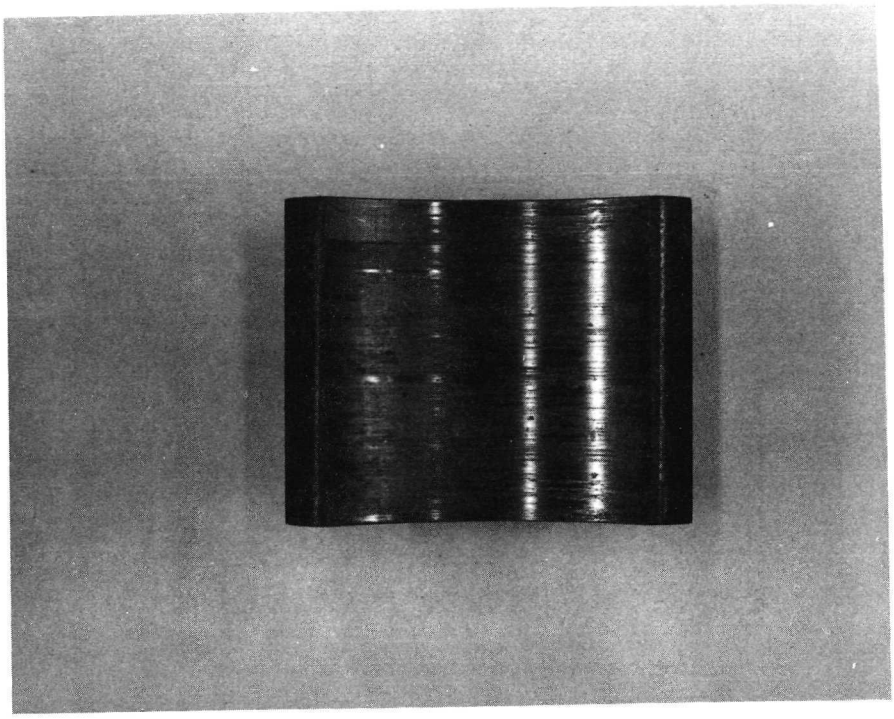

Pad After Testing

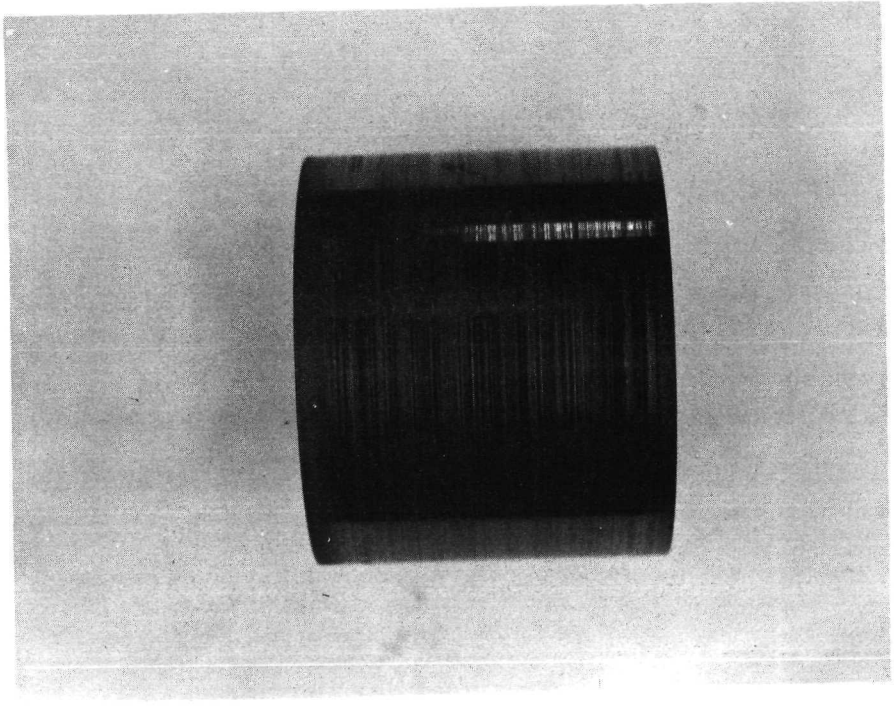

Sleeve After Testing

Plate 5 13A Metal Matrix MoS_2

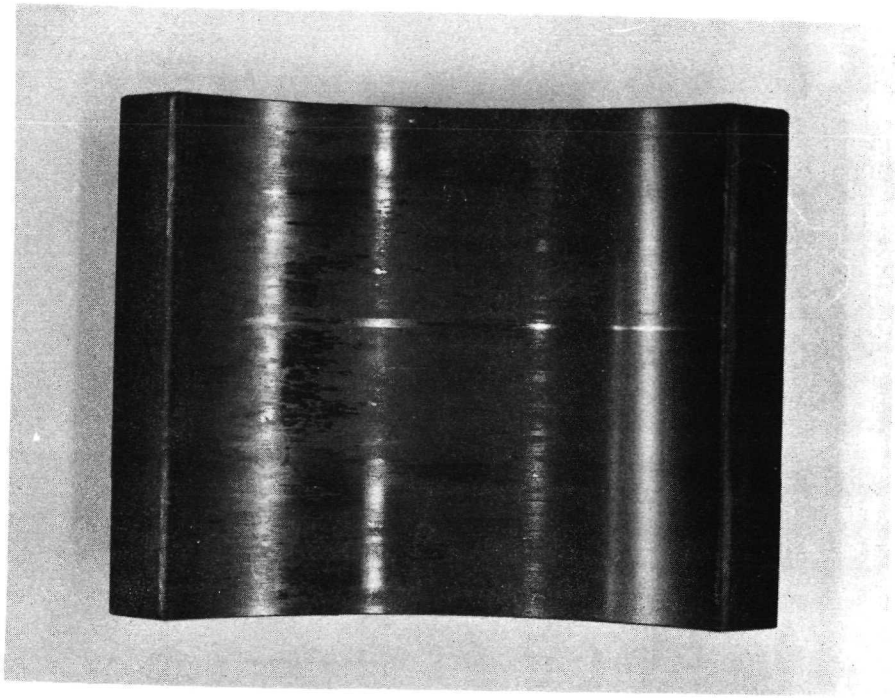

Pad After Testing

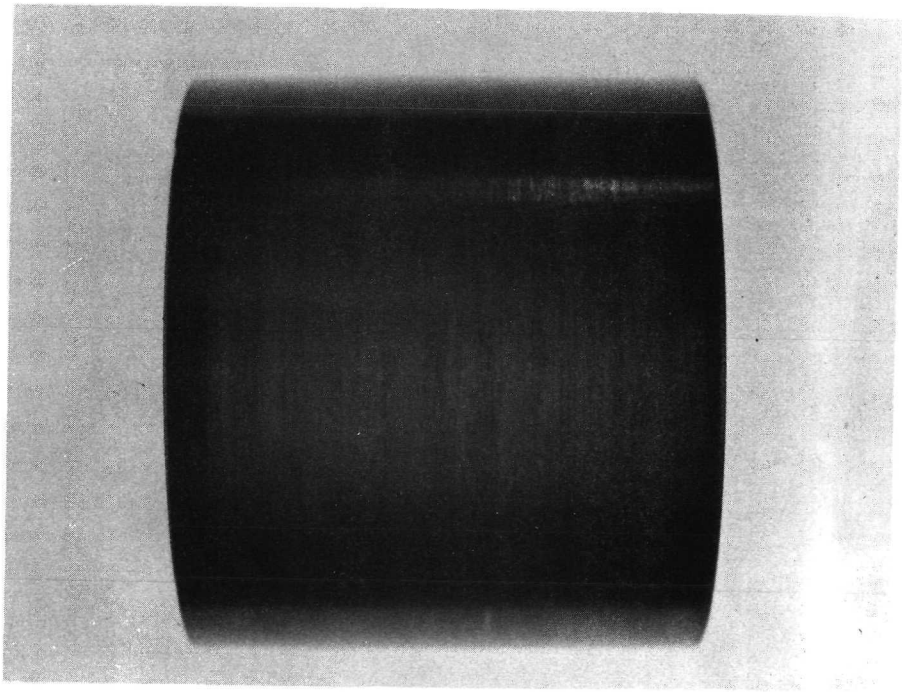

Sleeve After Testing

Plate 6 14A Burnished CF

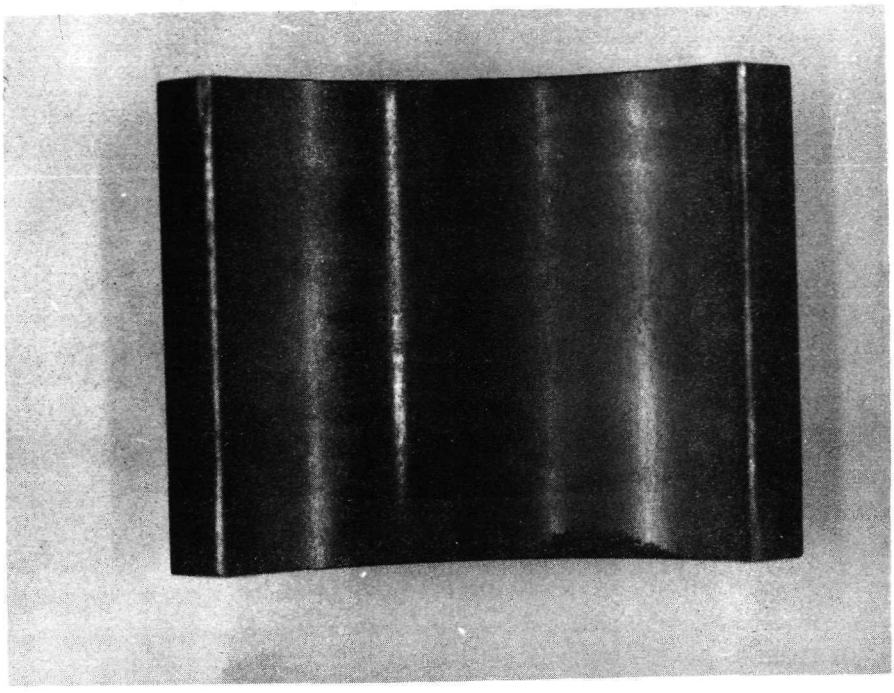

Pad After Testing

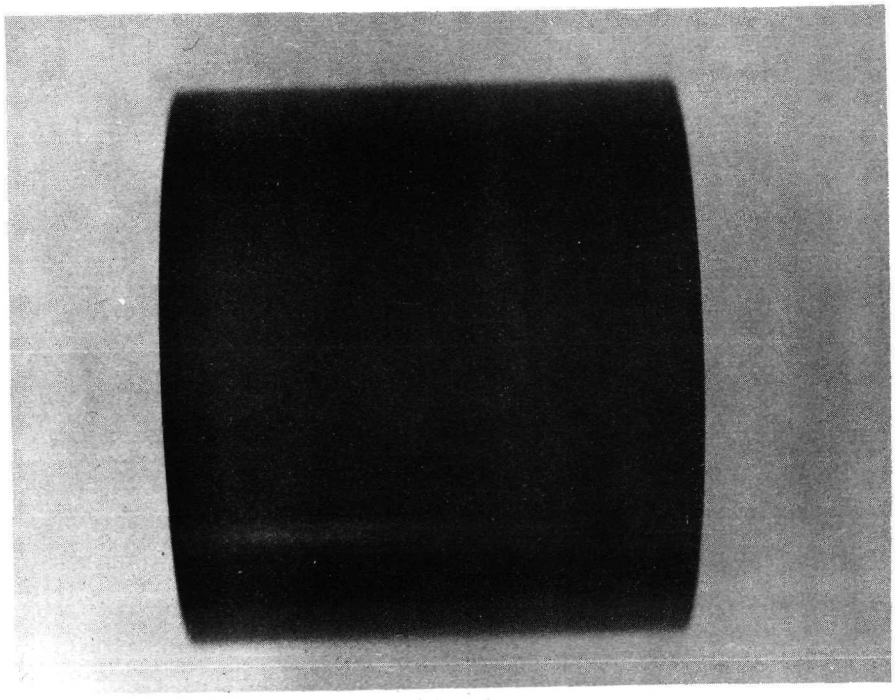

Sleeve After Testing

Plate 7 15A Polyimide CF

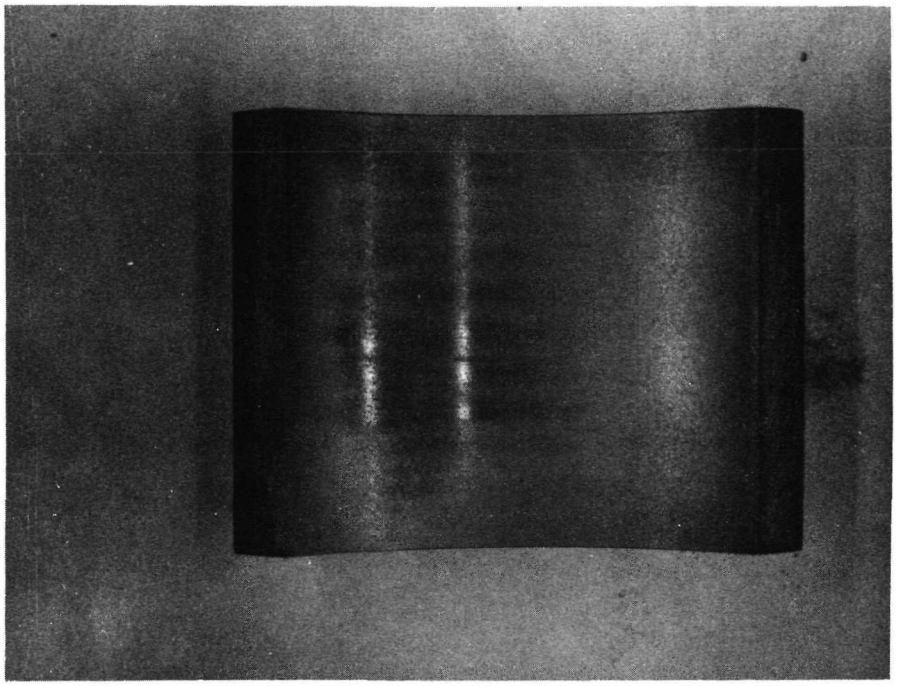

Pad After Testing

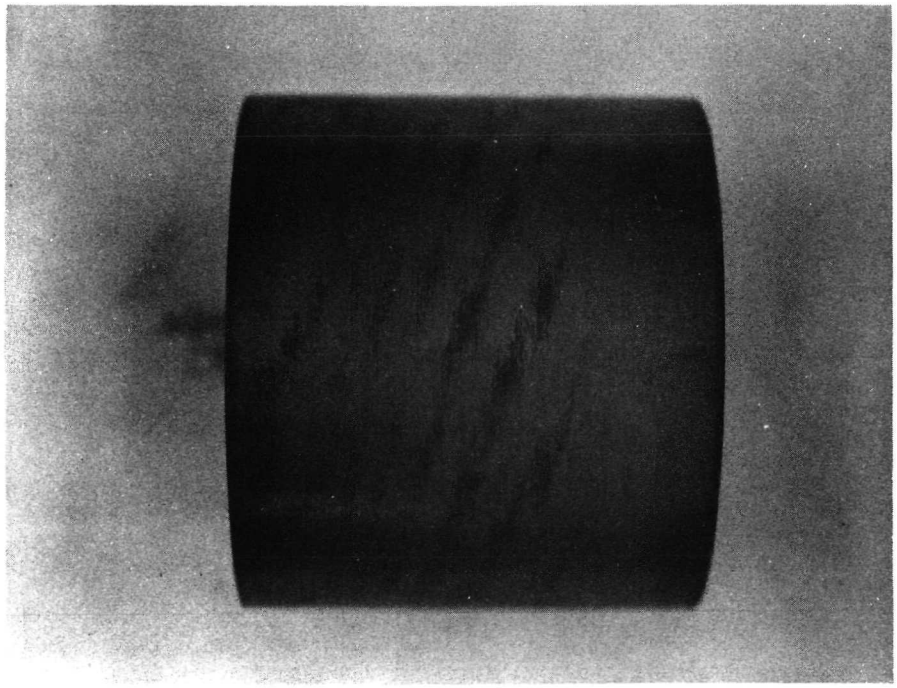

Sleeve After Testing

Plate 8 20A Burnished MoS_2

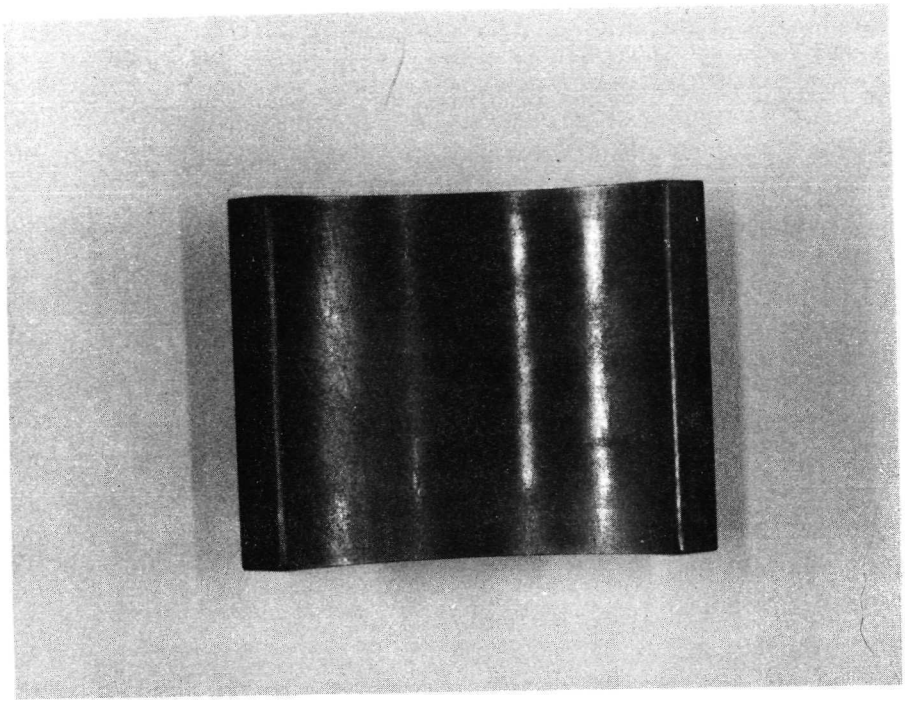

Pad After Testing

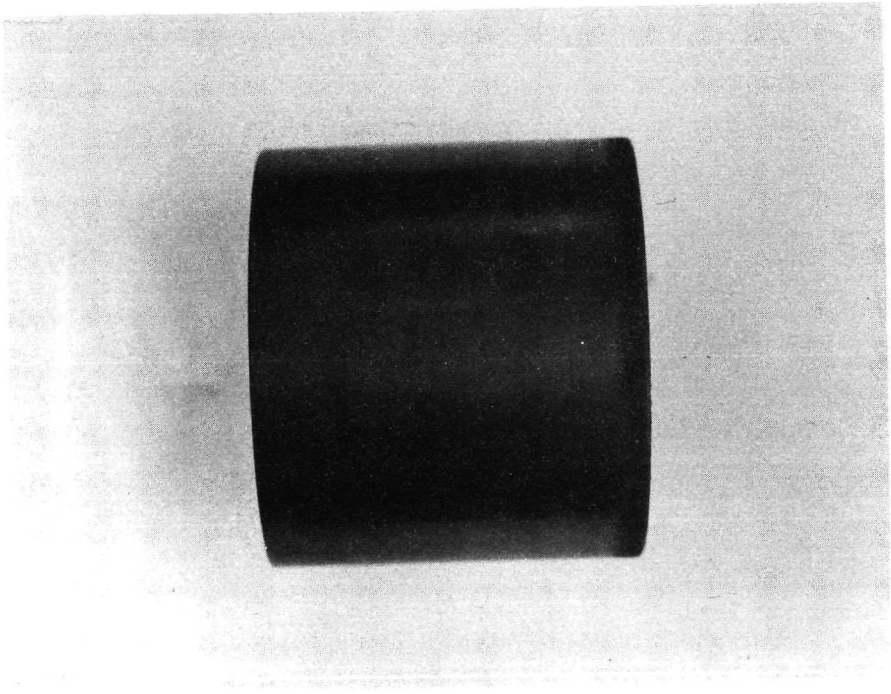

Sleeve After Testing

Plate 9 21A Sputtered MoS_2

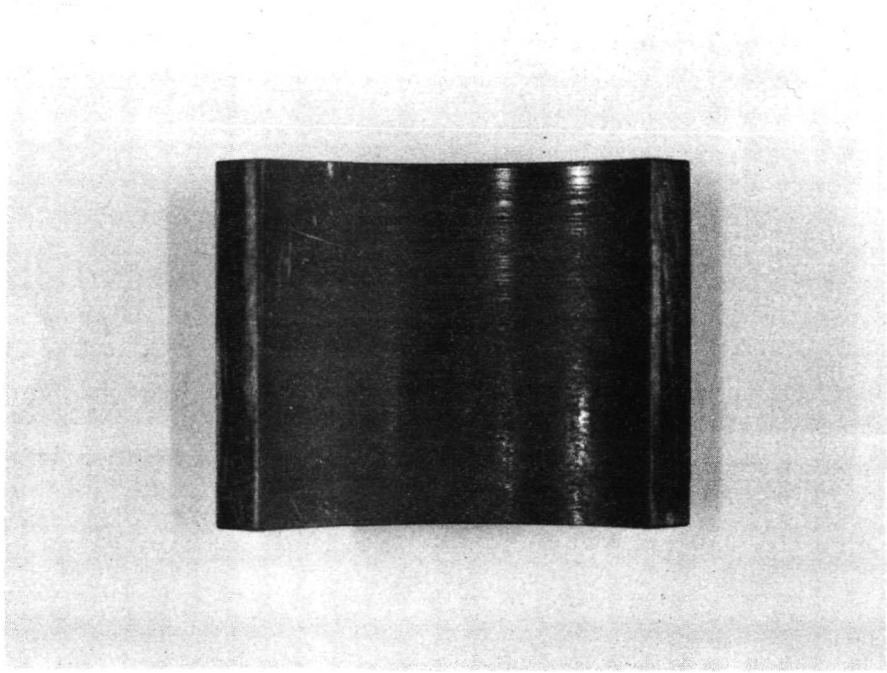

Pad After Testing

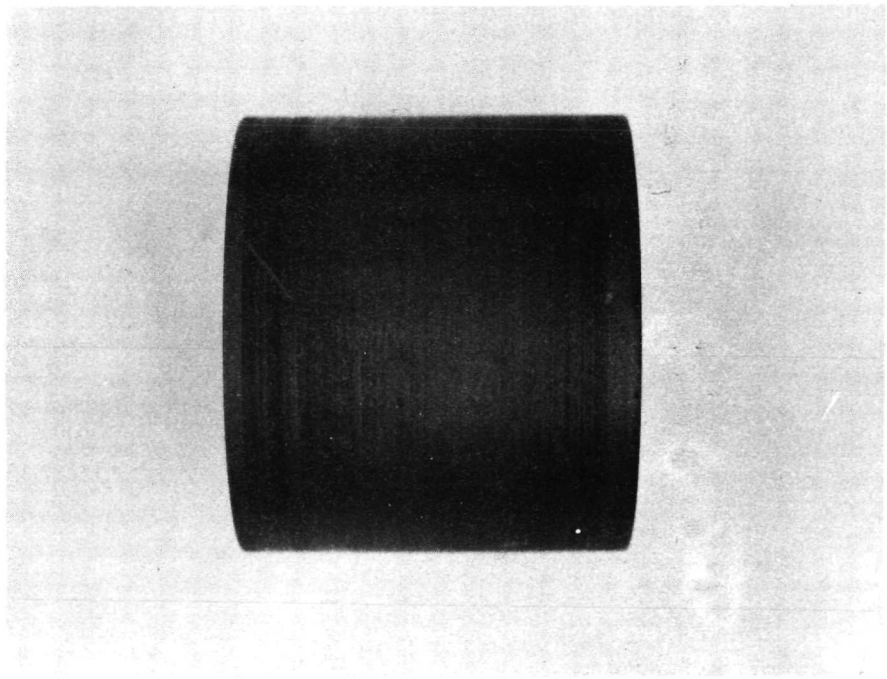

Sleeve After Testing

Plate 10 22A Polyimide MoS_2

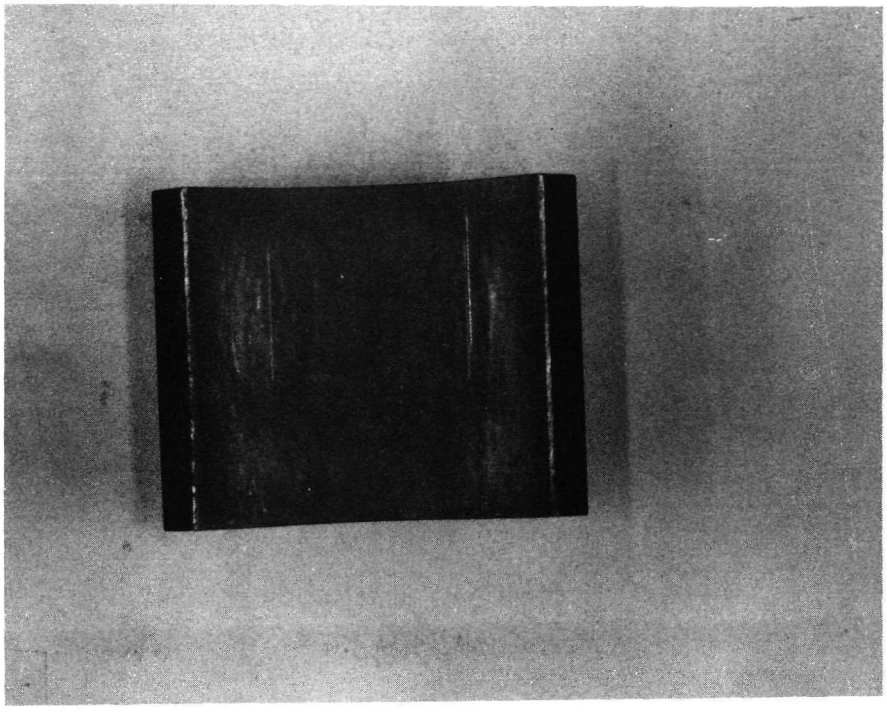

Pad Before Testing

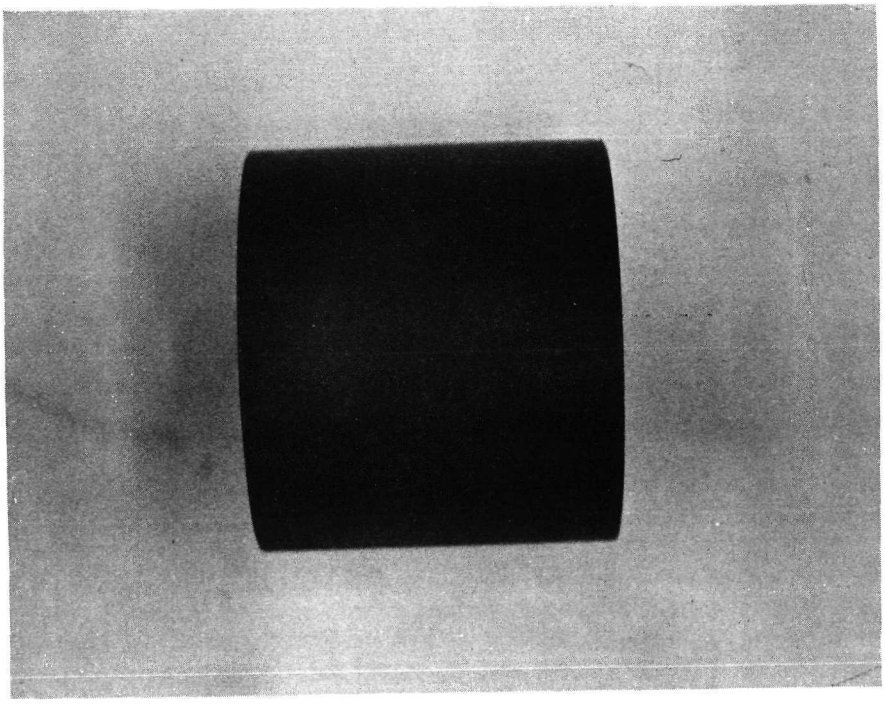

Sleeve Before Testing

Plate 11 23A Metal Matrix MoS_2

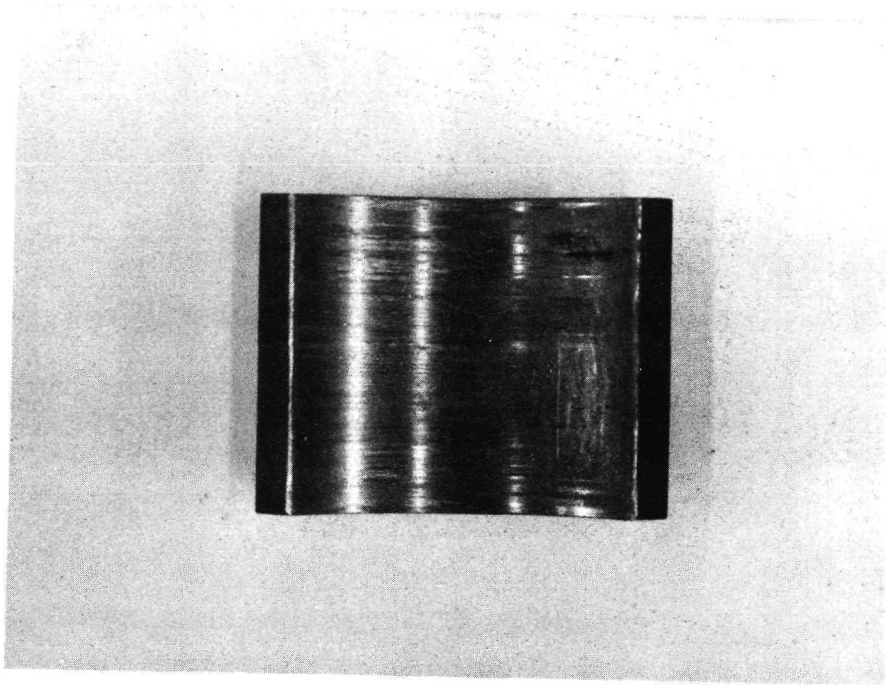

Pad After Testing

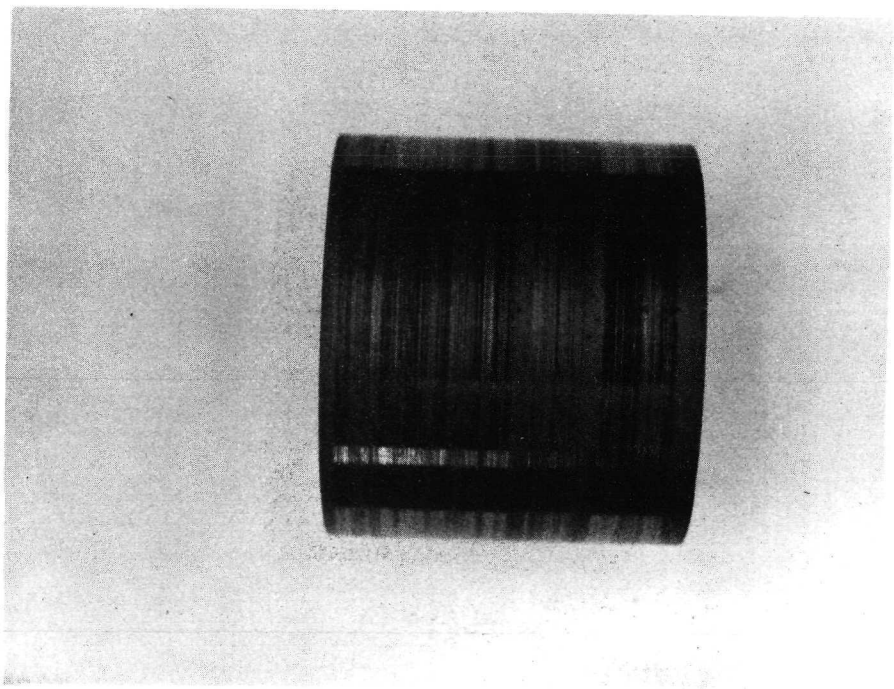

Sleeve After Testing

Plate 12 23A Metal Matrix MoS_2

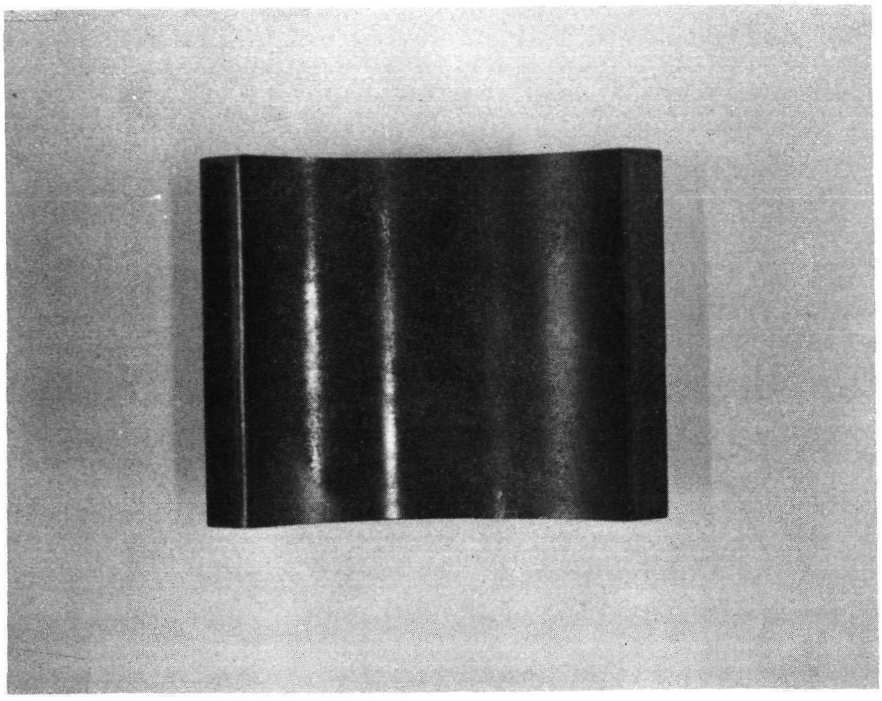

Pad After Testing

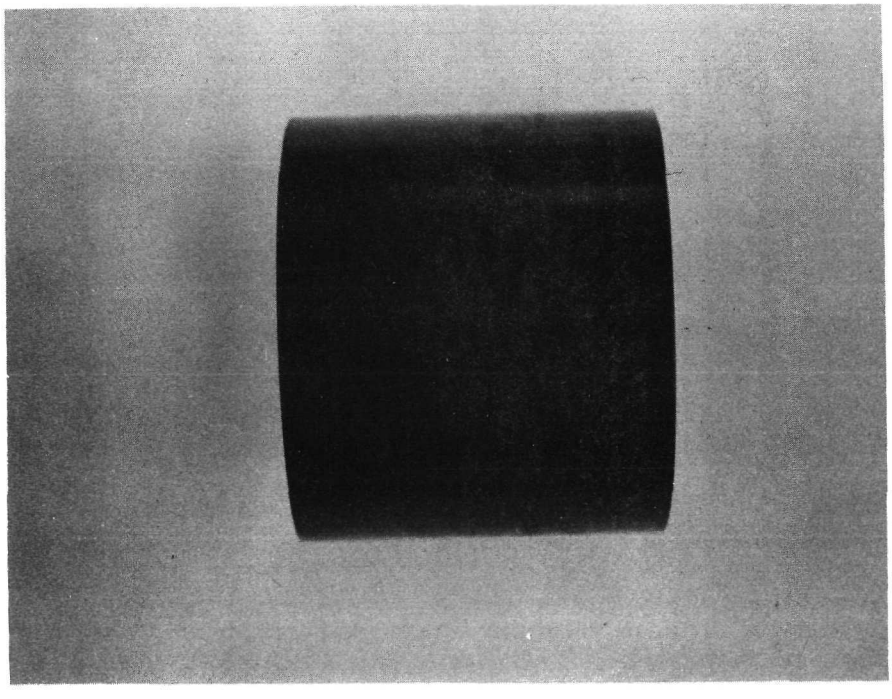

Sleeve After Testing

Plate 13 24A Burnished CF

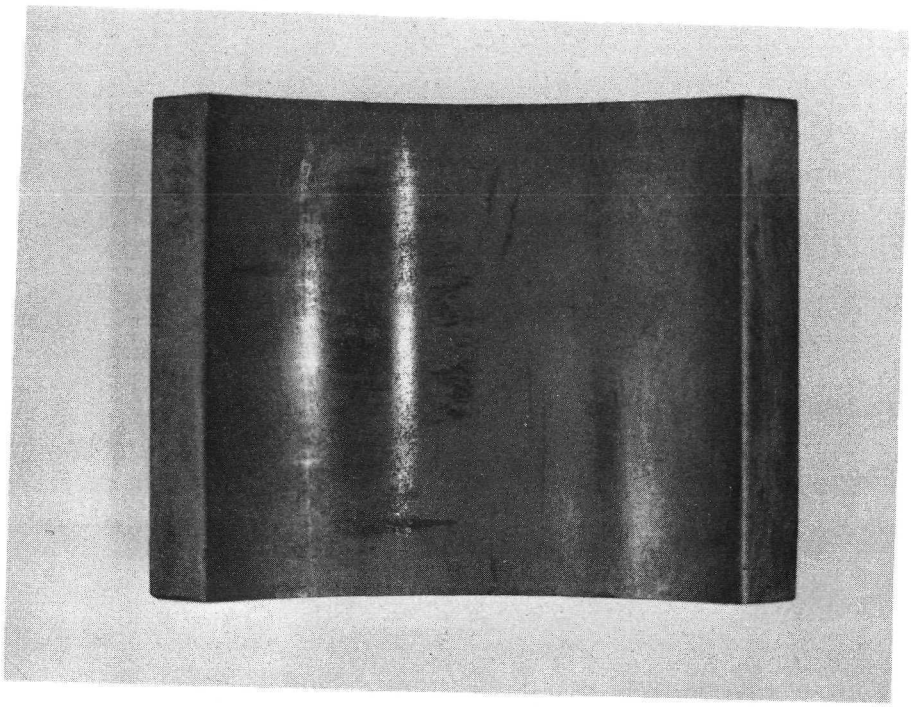

Pad After Testing

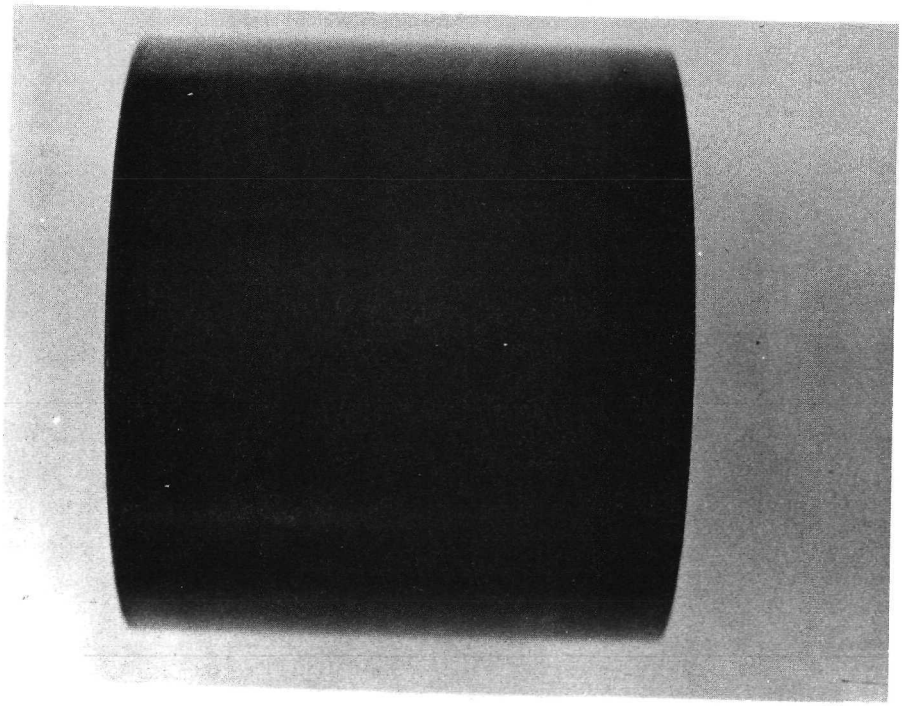

Sleeve After Testing

Plate 14 25A Polyimide CF

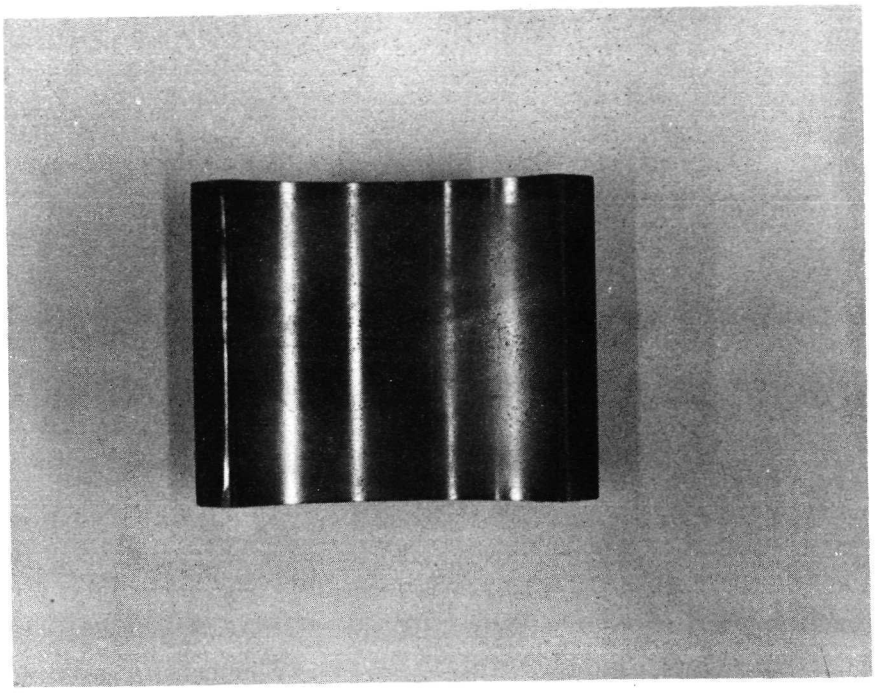

Pad After Testing

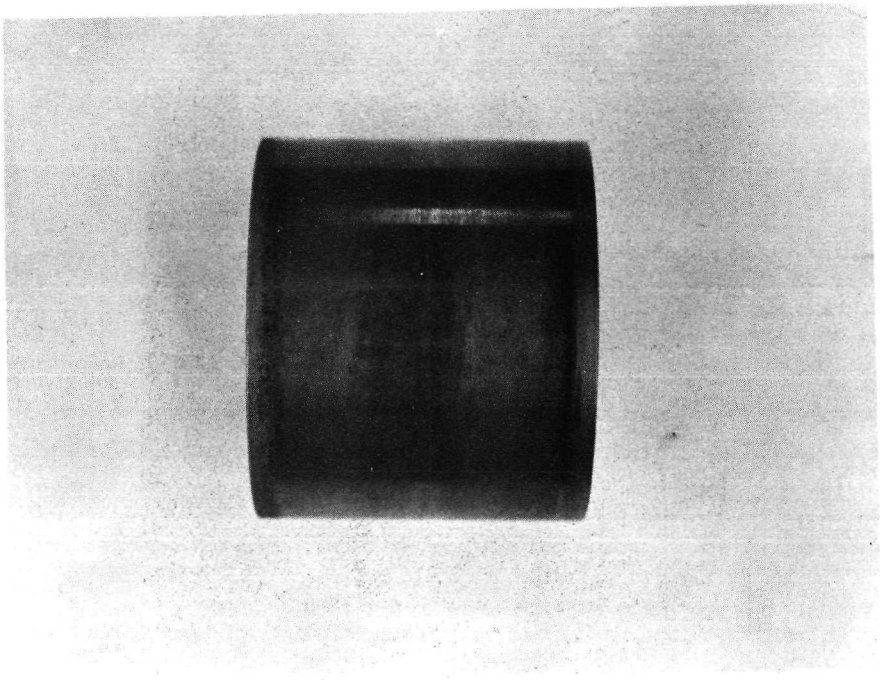

Sleeve After Testing

Plate 15 10B Burnished MoS_2

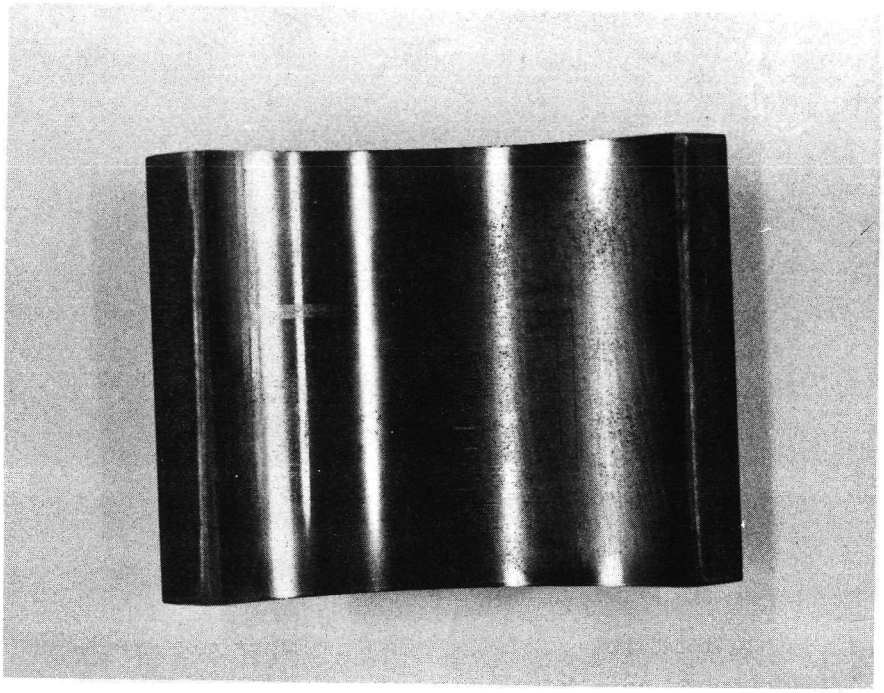

Pad After Testing

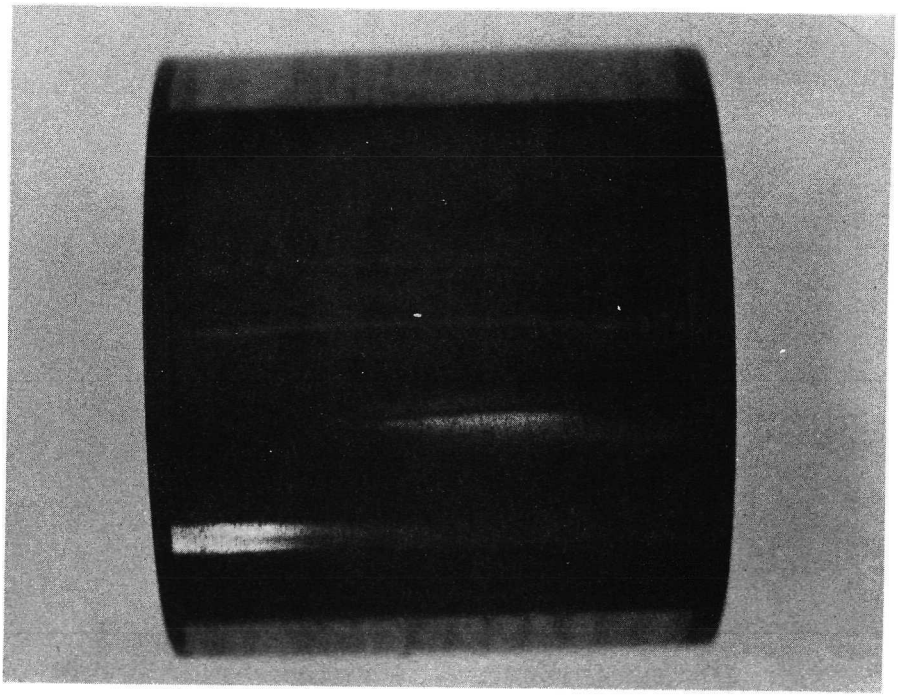

Sleeve After Testing

Plate 16 11B Sputtered MoS_2

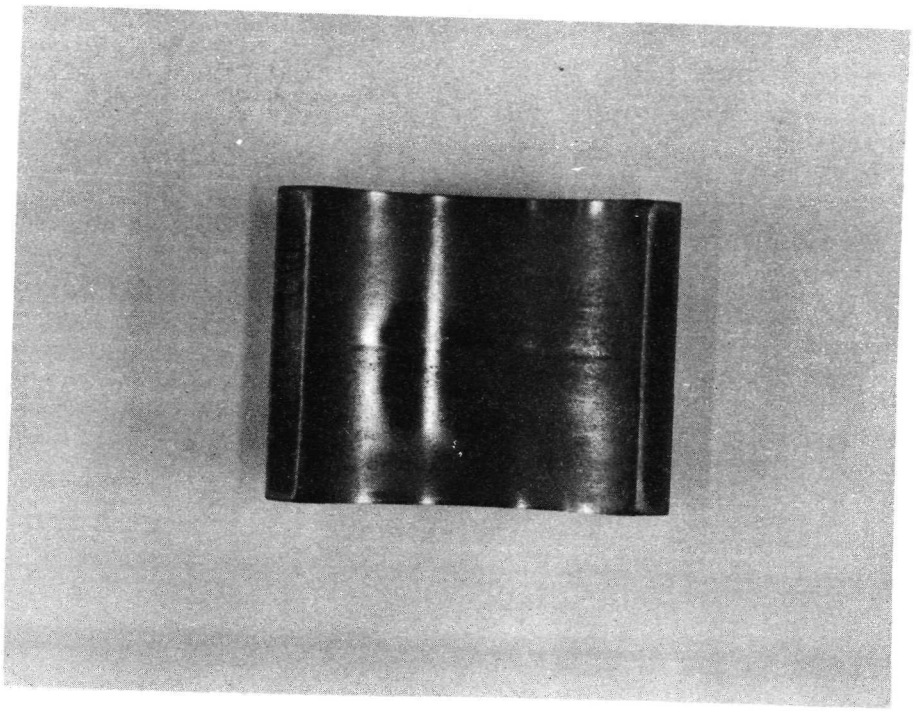

Pad After Testing

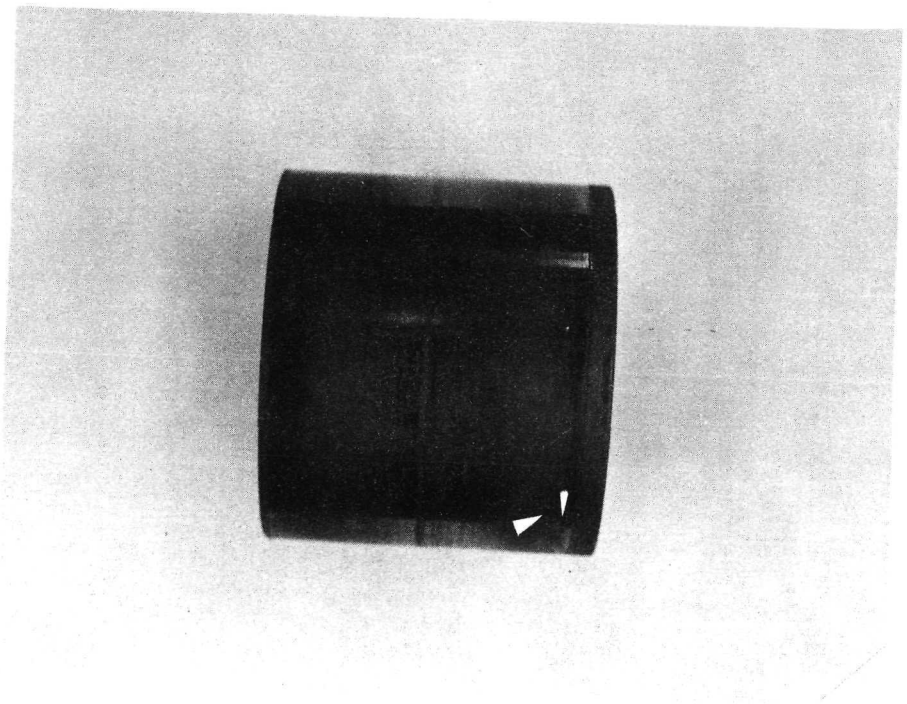

Sleeve After Testing

Plate 17 12B Polyimide MoS_2

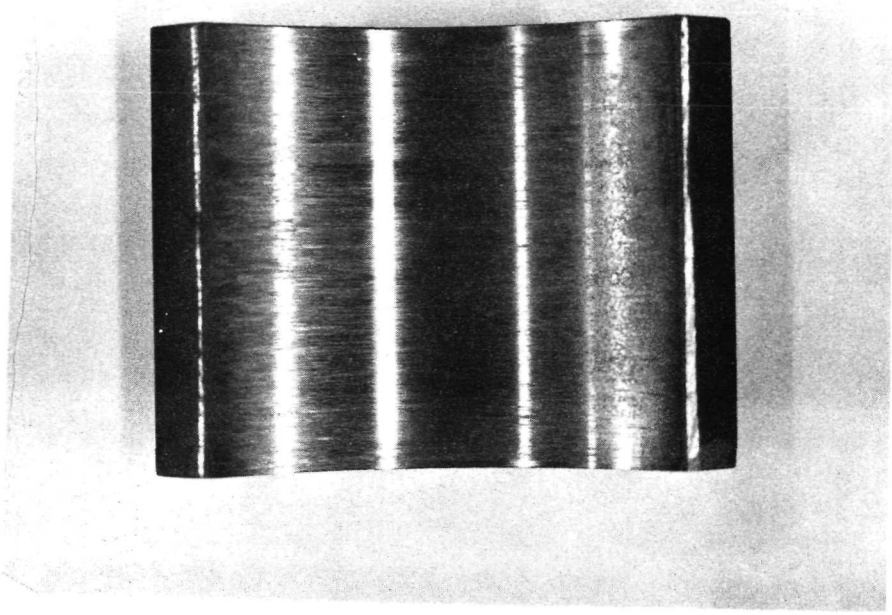

Pad After Testing

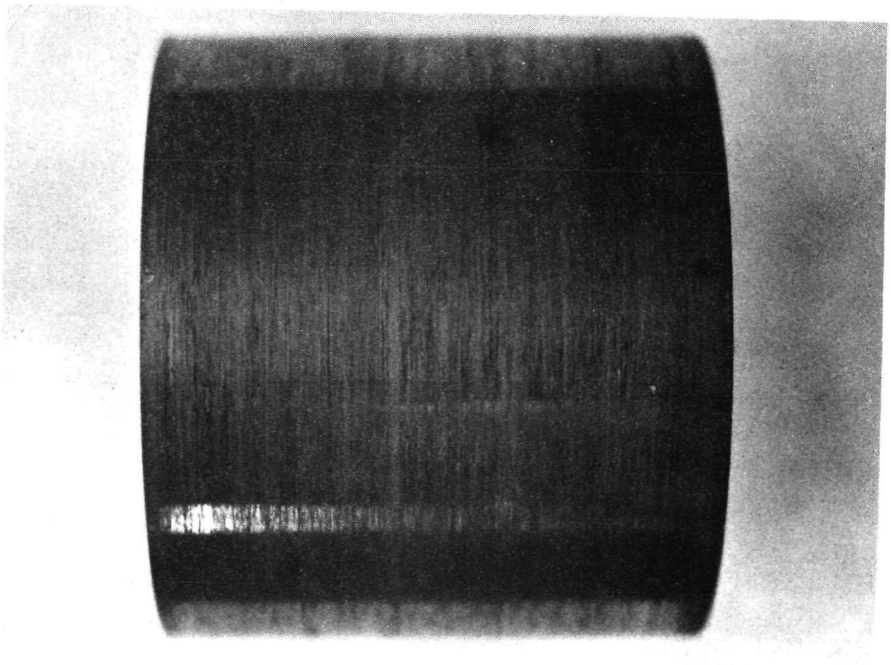

Sleeve After Testing

Plate 18 13B Metal Matrix MoS_2

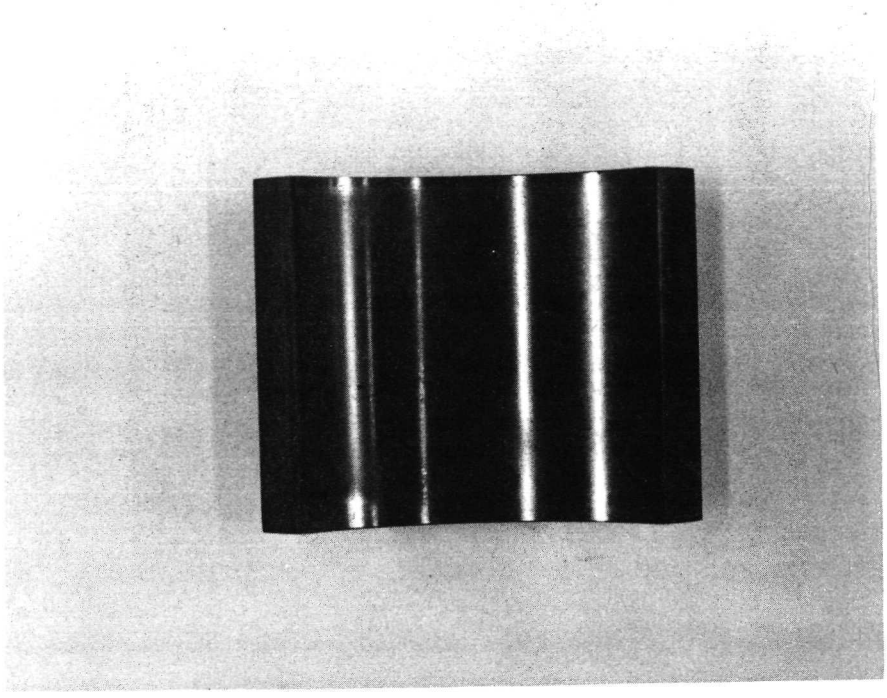

Pad After Testing

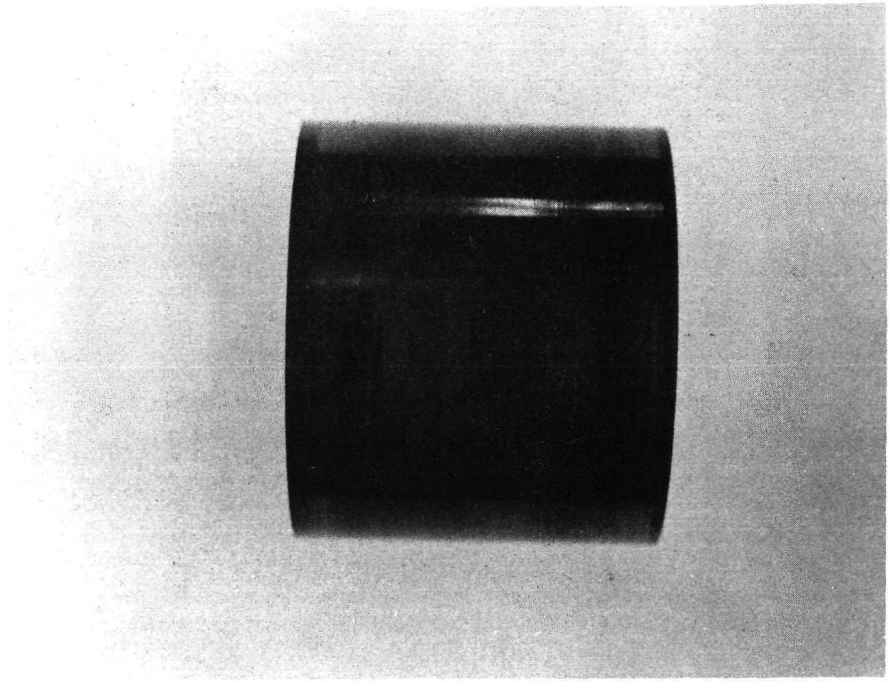

Sleeve After Testing

Plate 19 14B Burnished CF

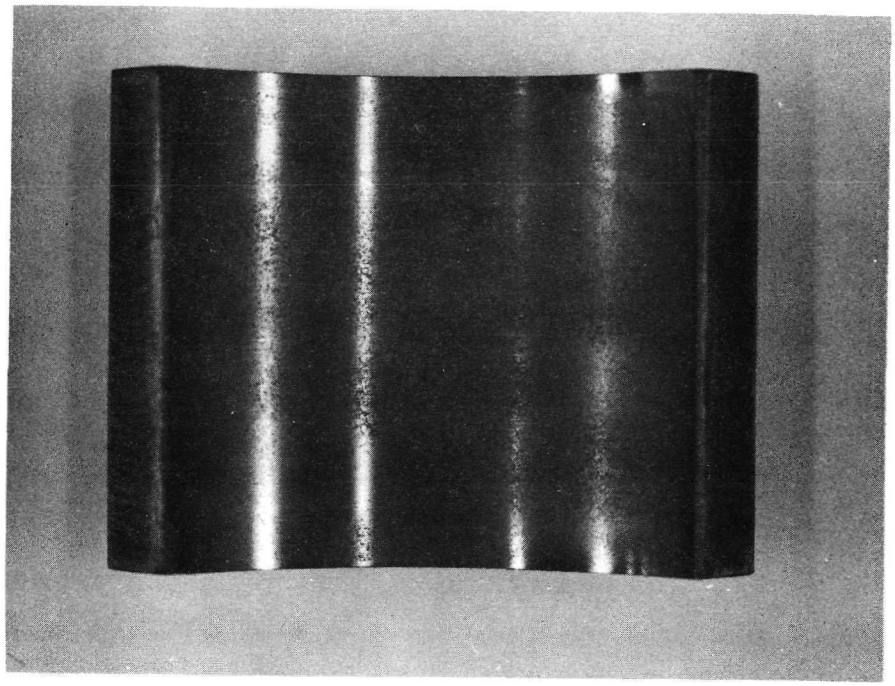

Pad After Testing

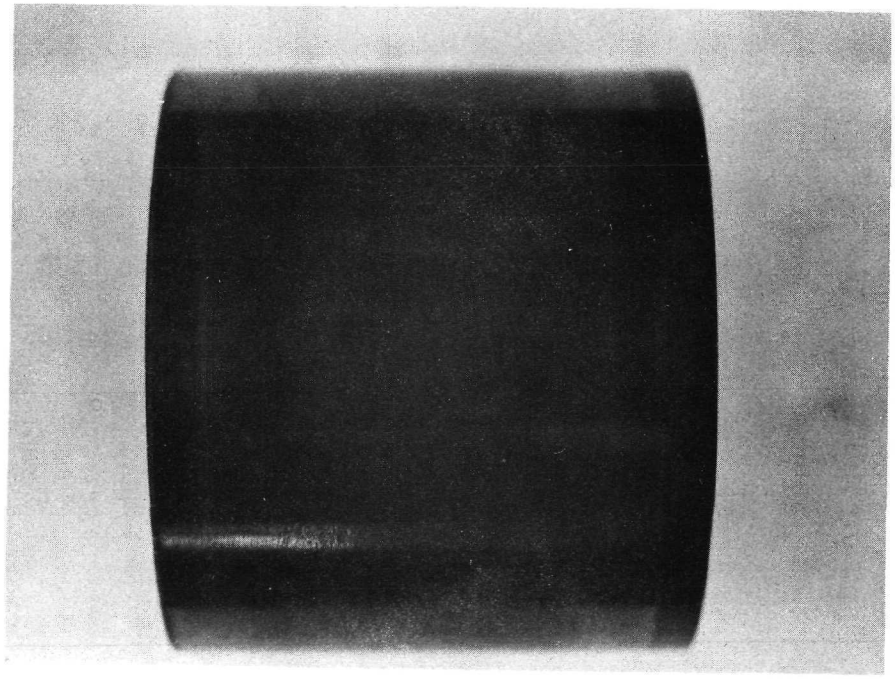

Sleeve After Testing

Plate 20 15B Polyimide CF

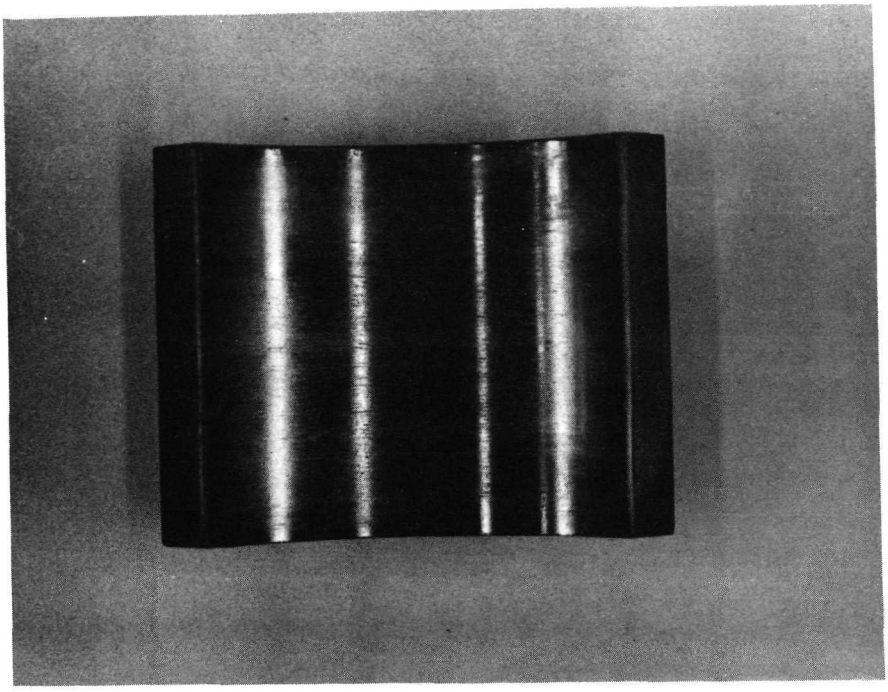

Pad After Testing

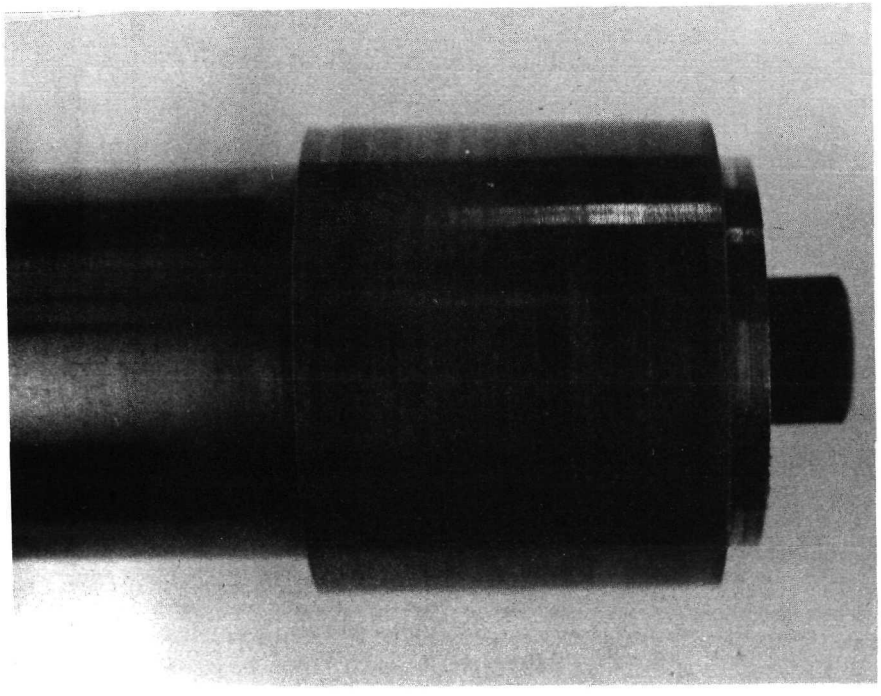

Sleeve After Testing

Plate 21 20B Burnished MoS_2

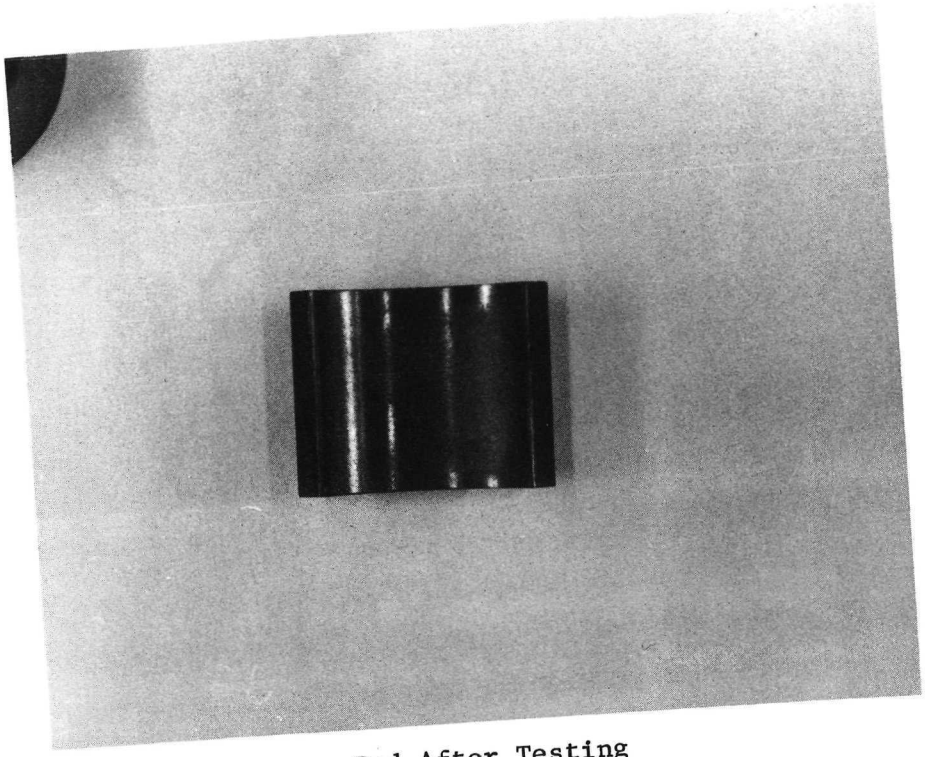

Pad After Testing

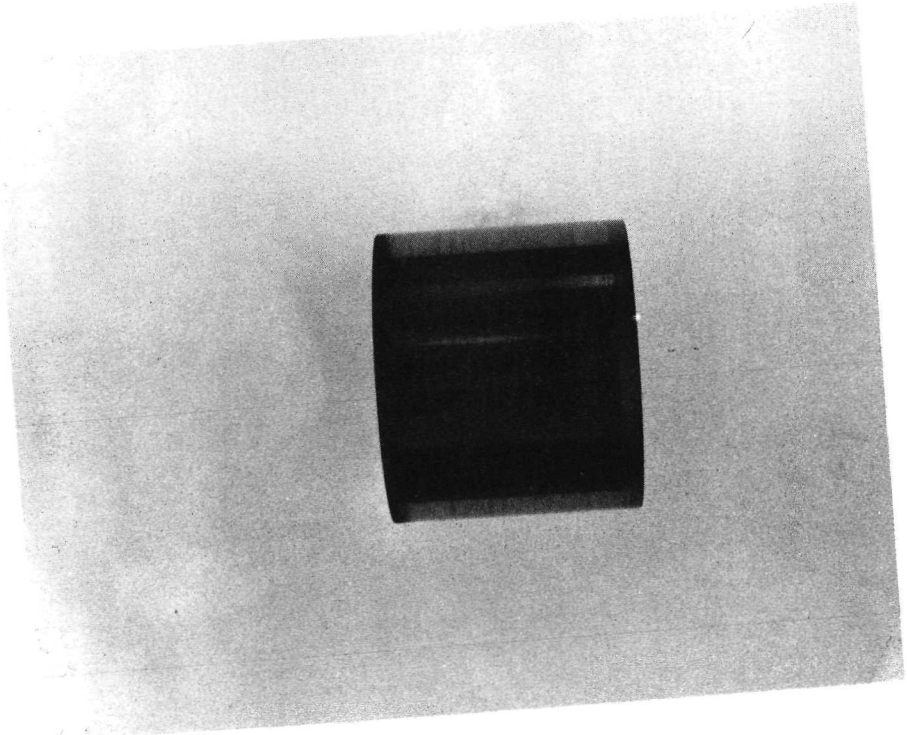

Sleeve After Testing

Plate 22 21B Sputtered MoS_2

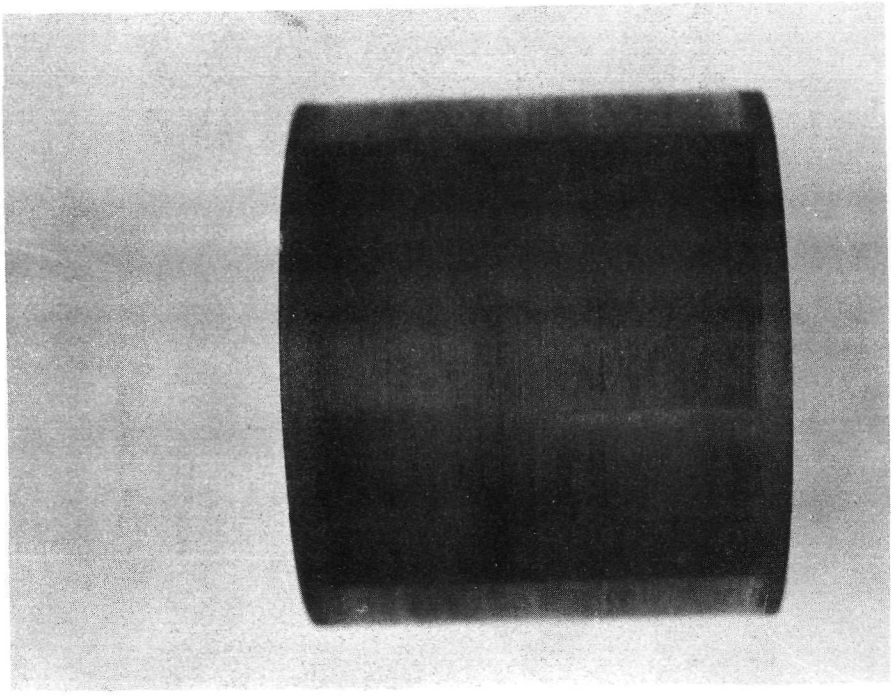

Sleeve After Testing

Plate 23 22B Polyimide MoS_2

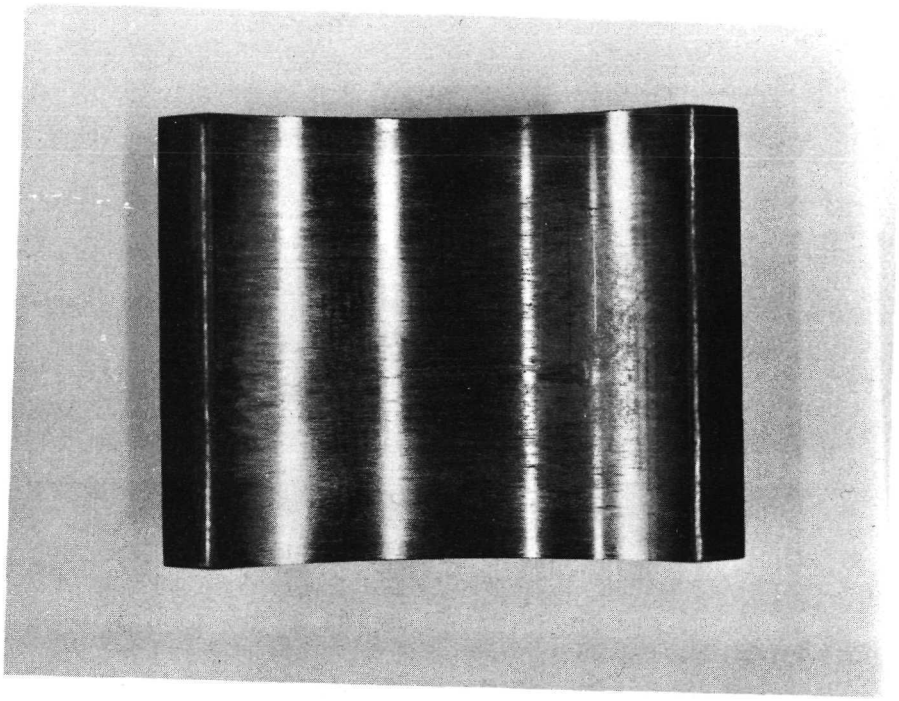

Pad After Testing

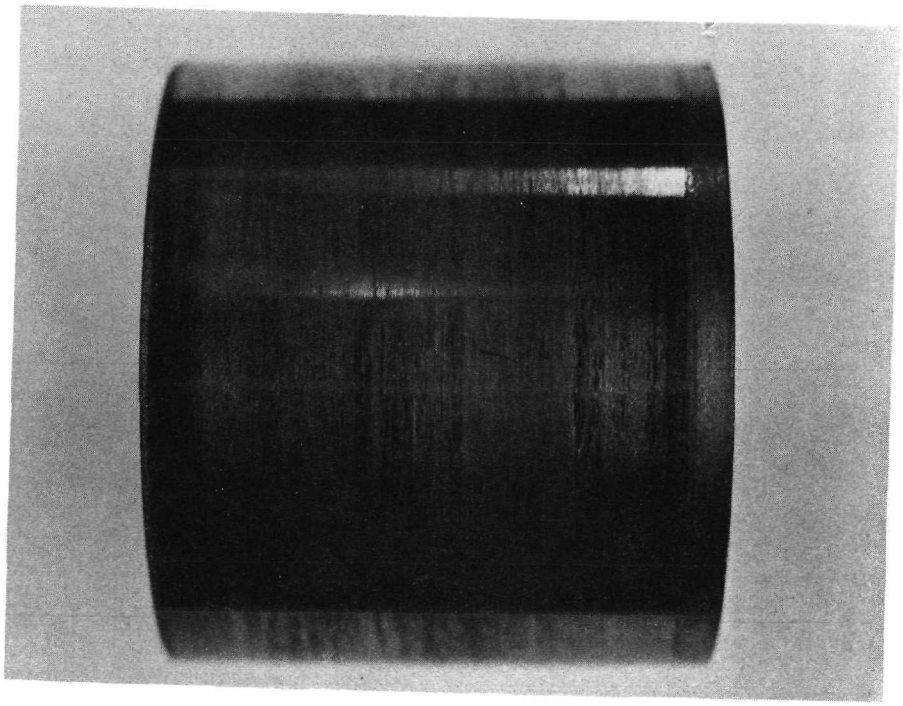

Sleeve After Testing

Plate 24 23B Metal Matrix MoS_2

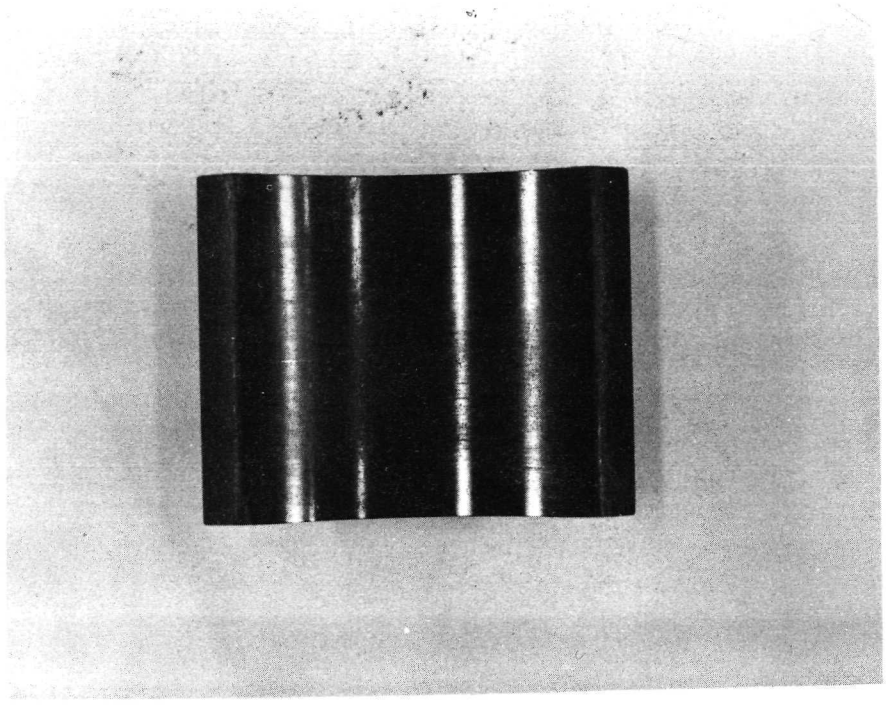

Pad After Testing

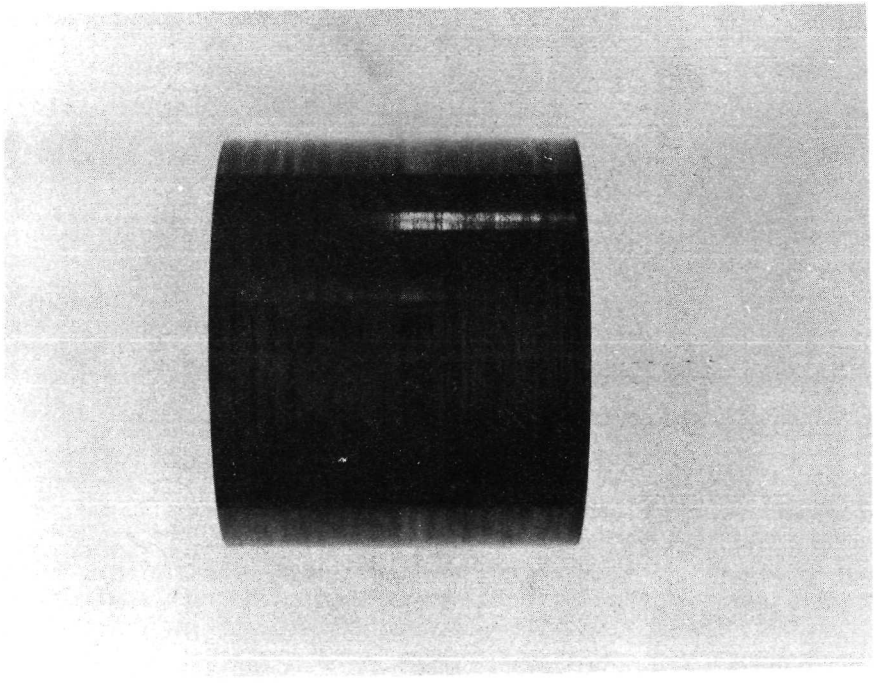

Sleeve After Testing

Plate 25 24B Burnished CF

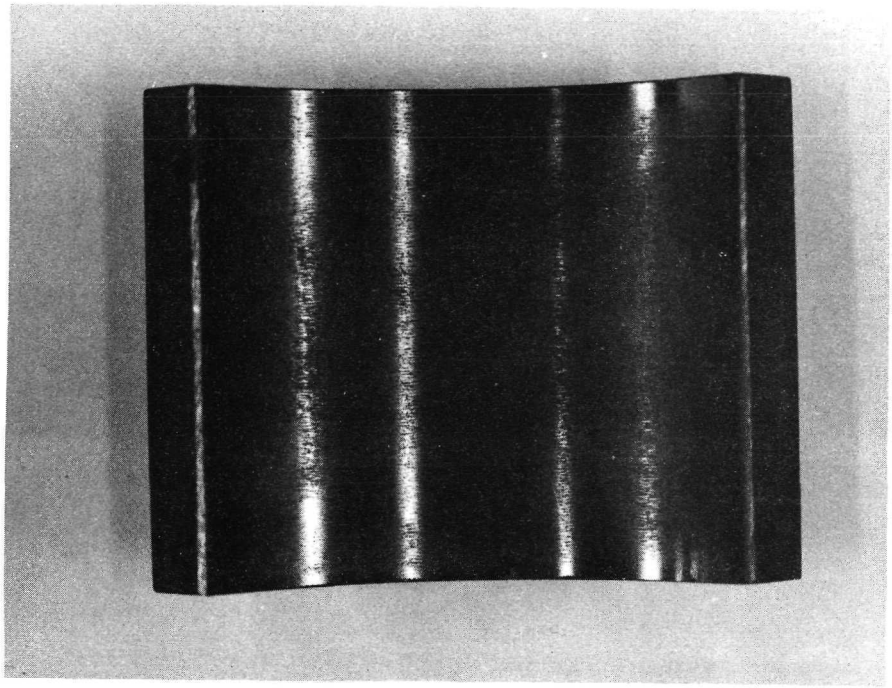

Pad After Testing

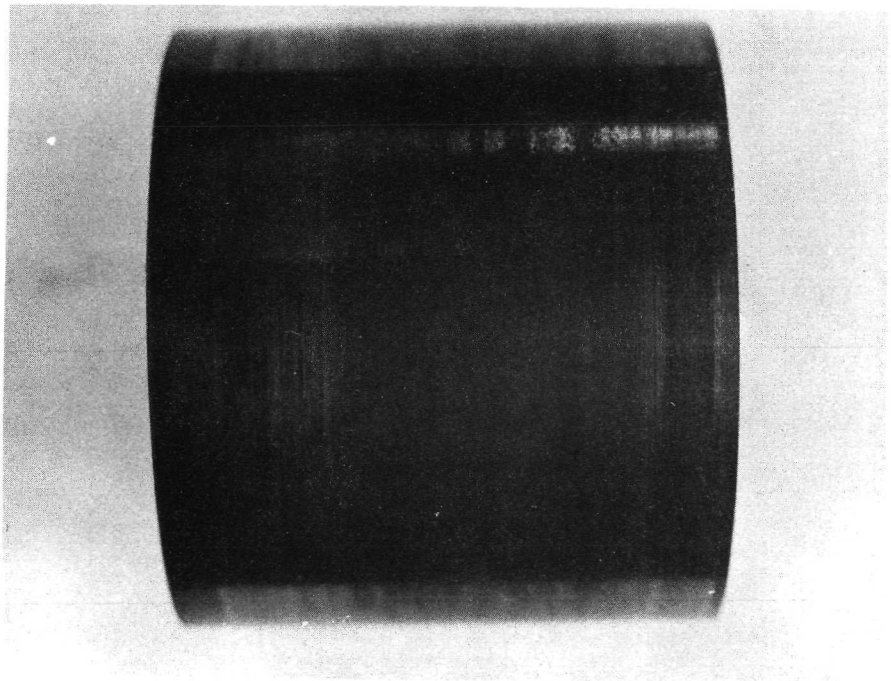

Sleeve After Testing

Plate 26 25B Polyimide CF

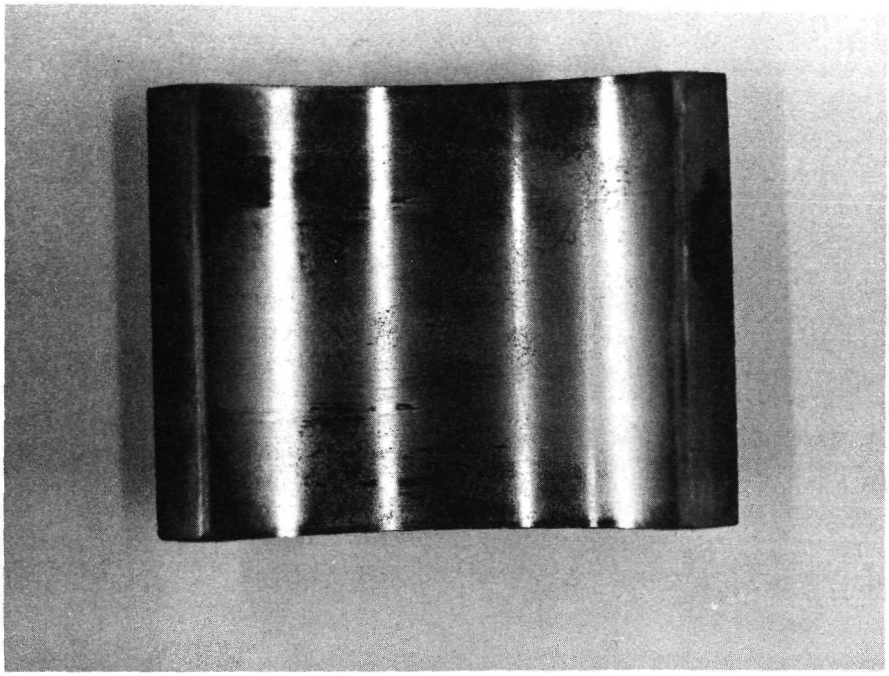

Pad After Testing

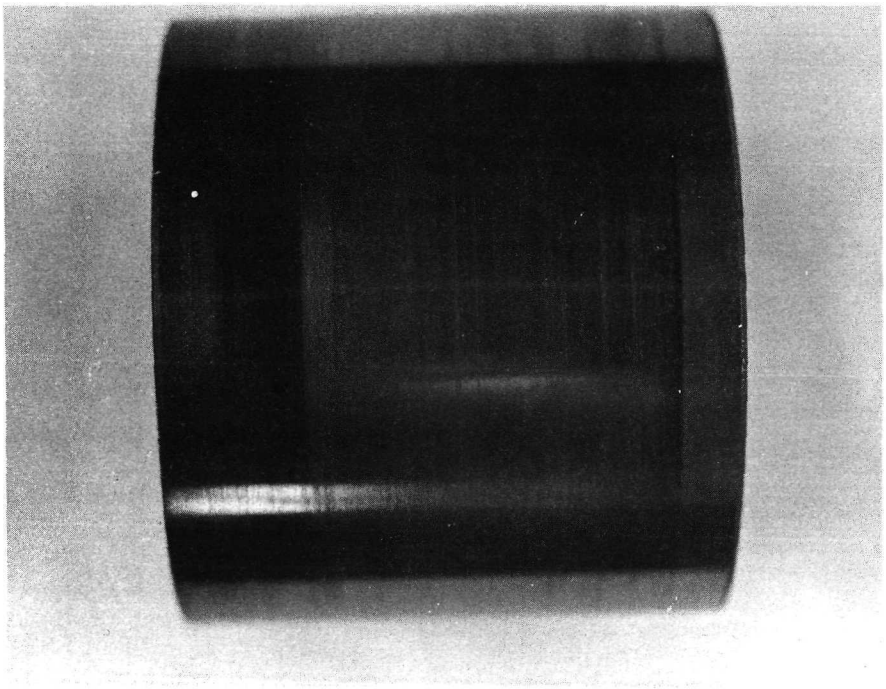

Sleeve After Testing

Plate 27 10C Burnished MoS_2

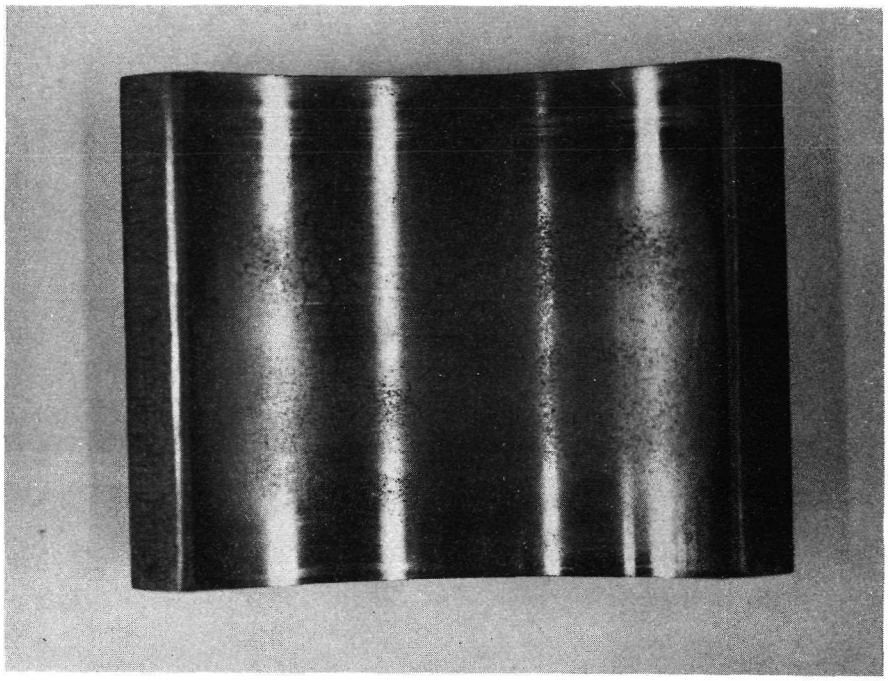

Pad After Testing

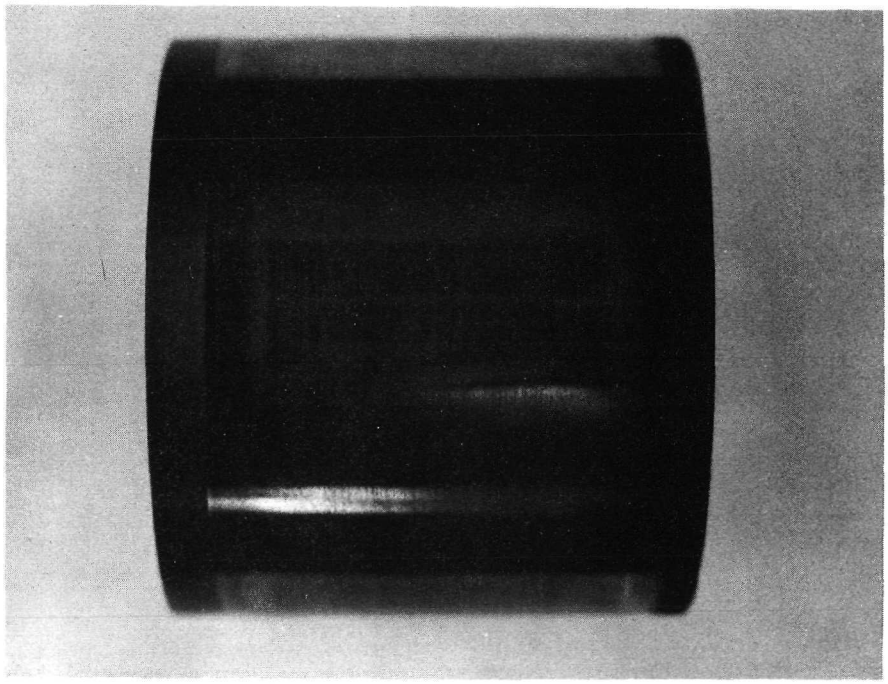

Sleeve After Testing

Plate 28 11C Sputtered MoS_2

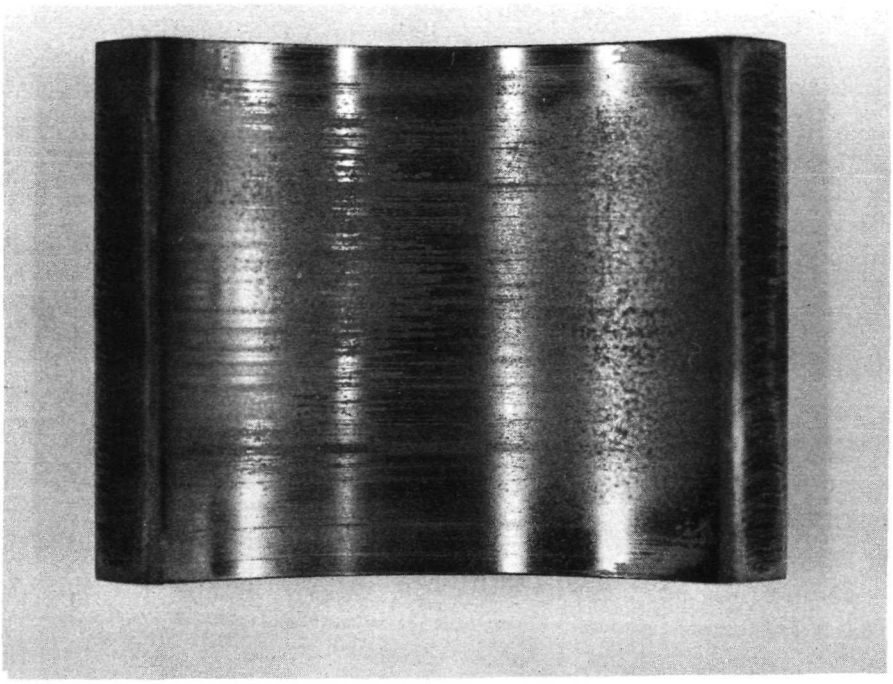

Pad After Testing

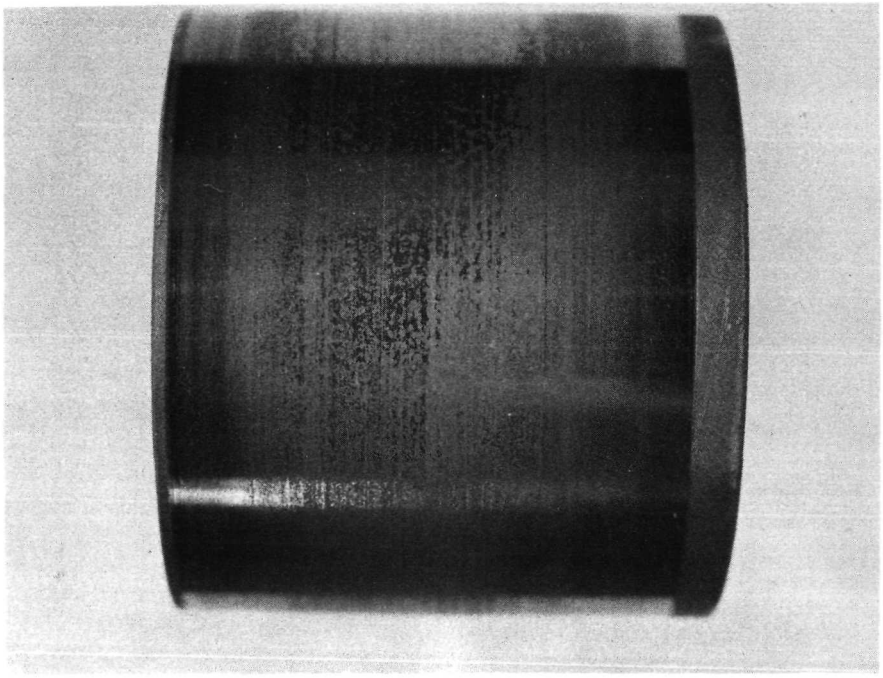

Sleeve After Testing

Plate 29 12C Polyimide MoS_2

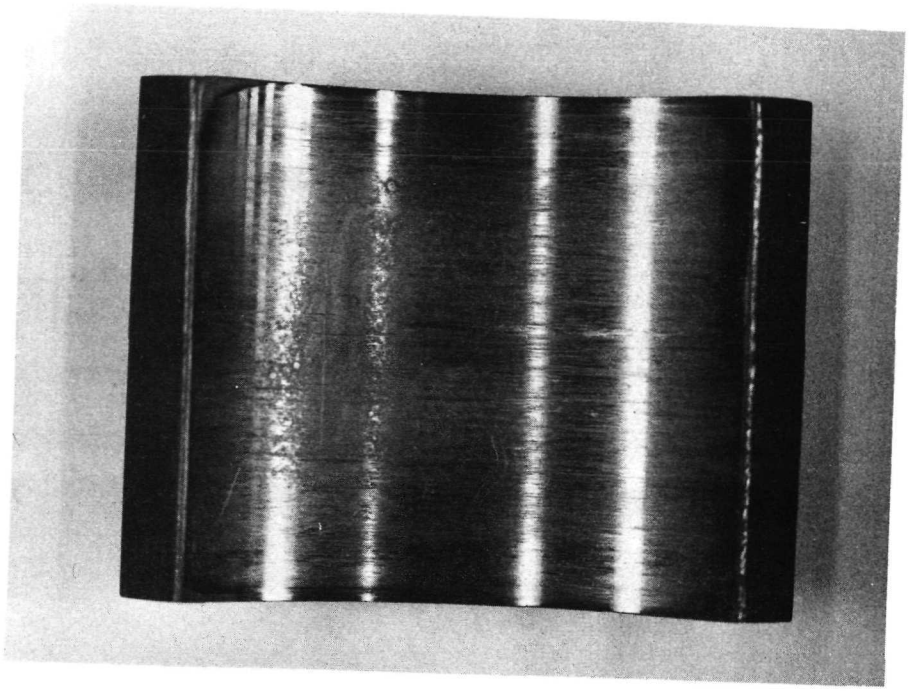

Pad After Testing

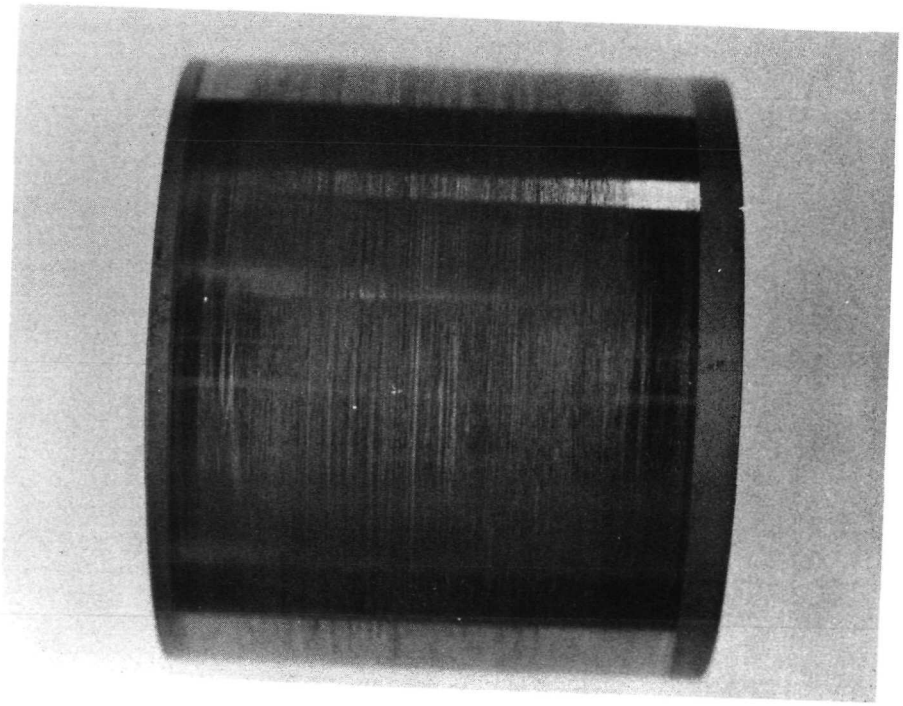

Sleeve After Testing

Plate 30 13C Metal Matrix MoS_2

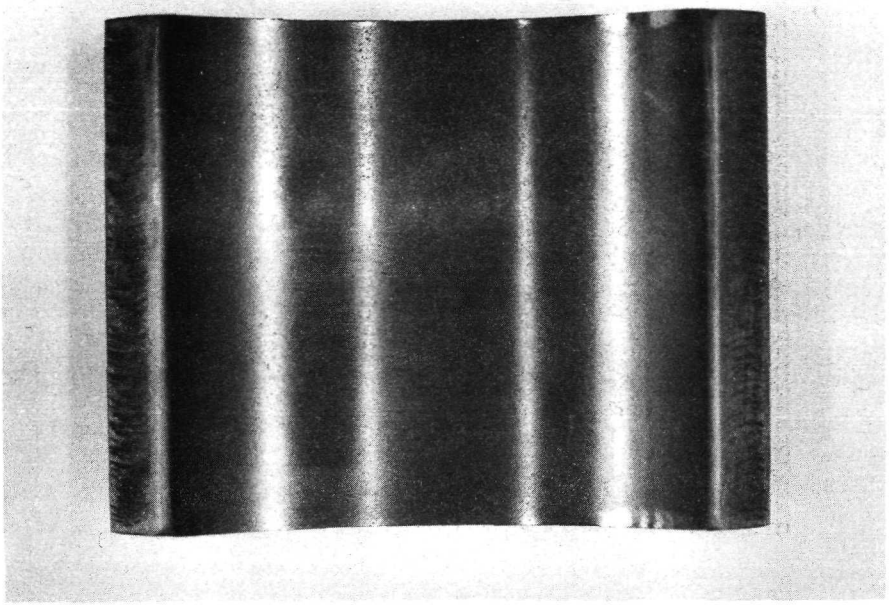

Pad After Testing

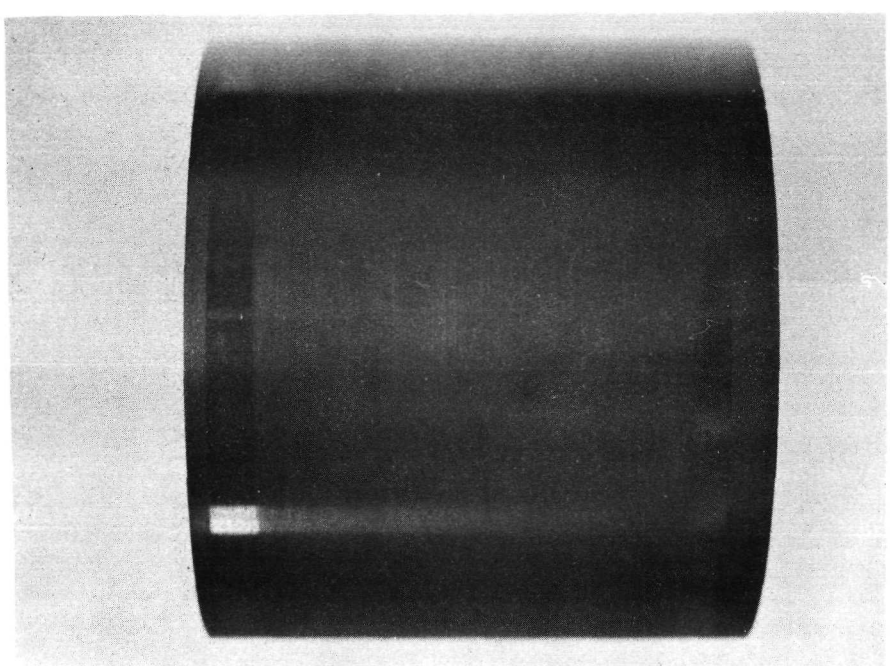

Sleeve After Testing

Plate 31 14C Burnished CF

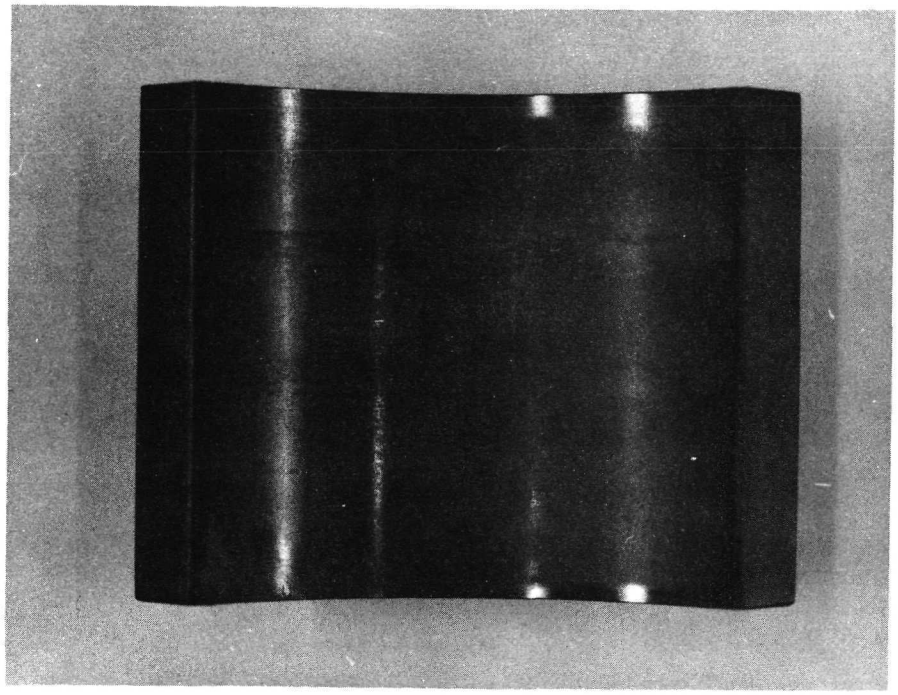

Pad After Testing

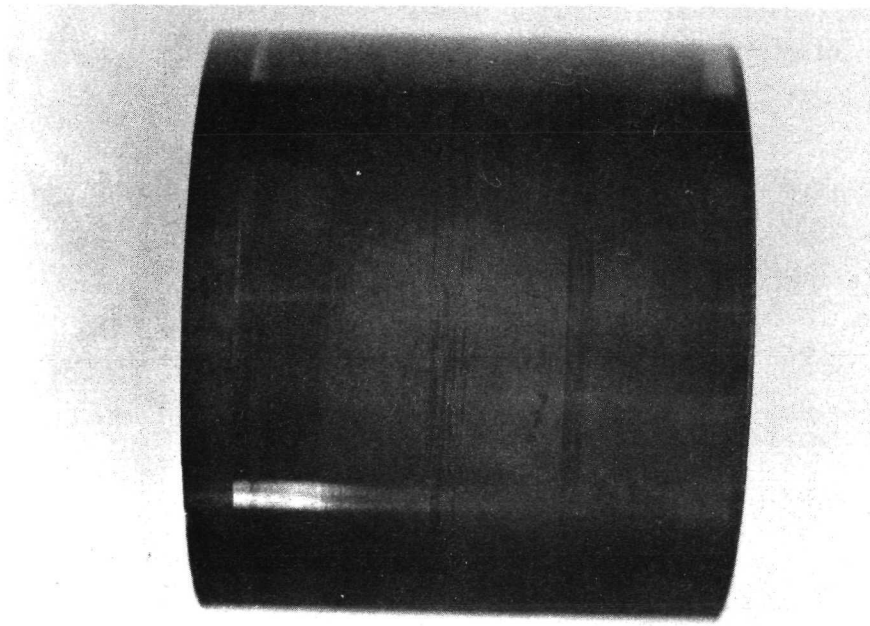

Sleeve After Testing

Plate 32 15C Polyimide CF

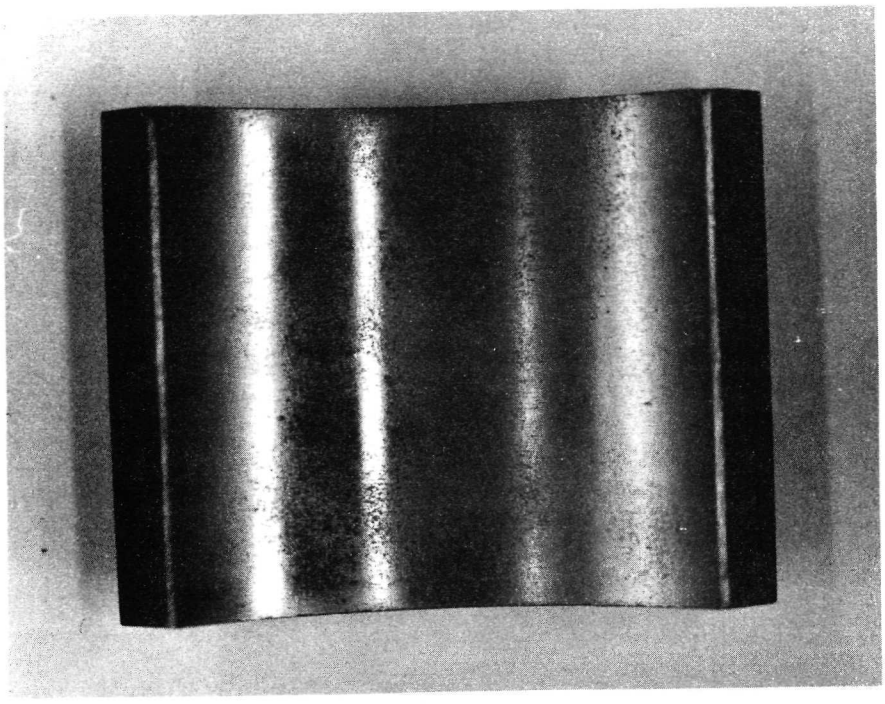

Pad After Testing

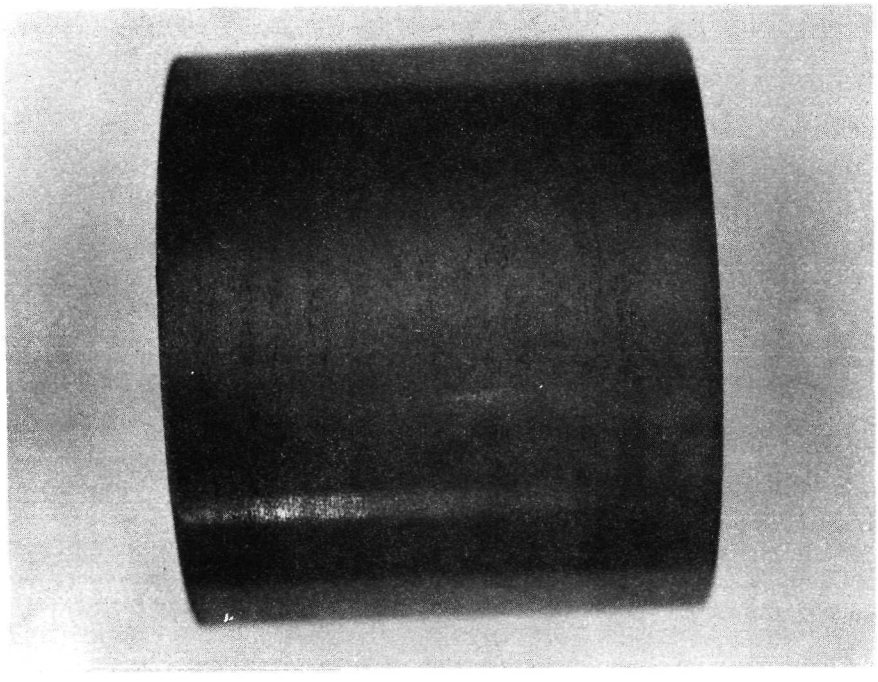

Sleeve After Testing

Plate 33 20C Burnished MoS_2

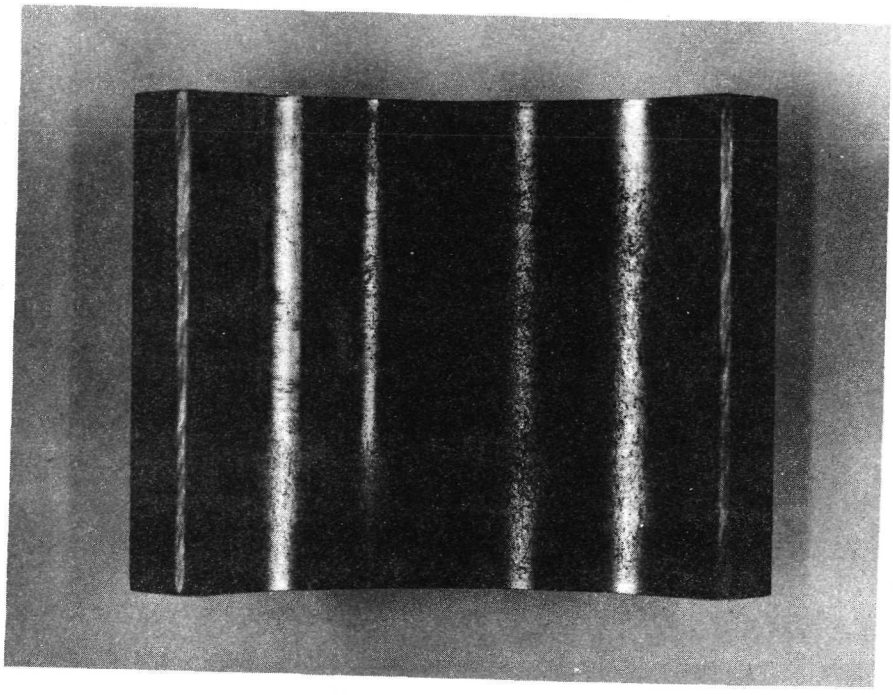

Pad After Testing

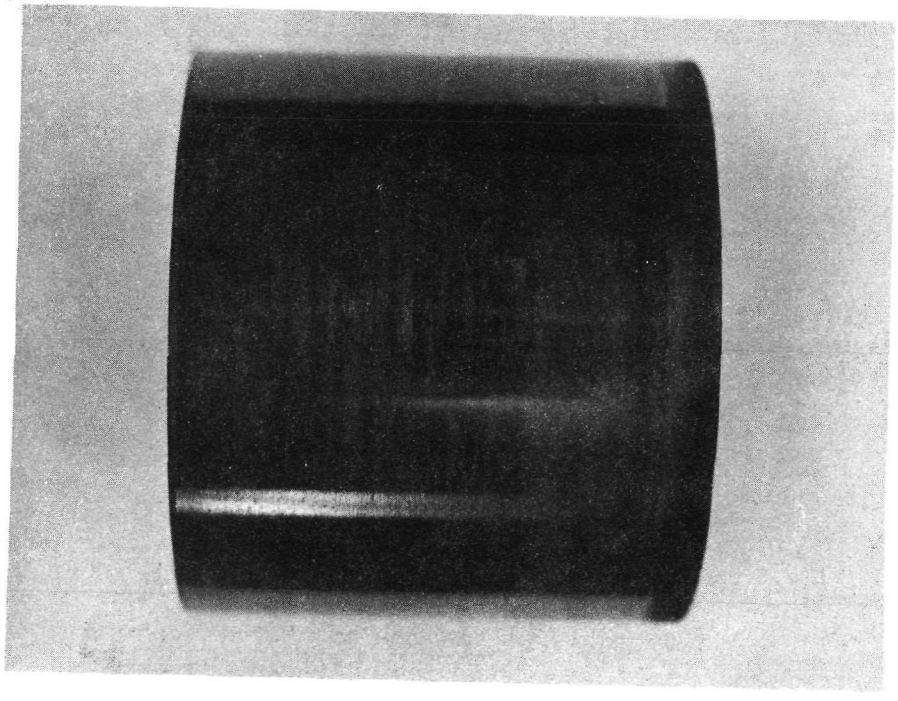

Sleeve After Testing

Plate 34 21C Sputtered MoS_2

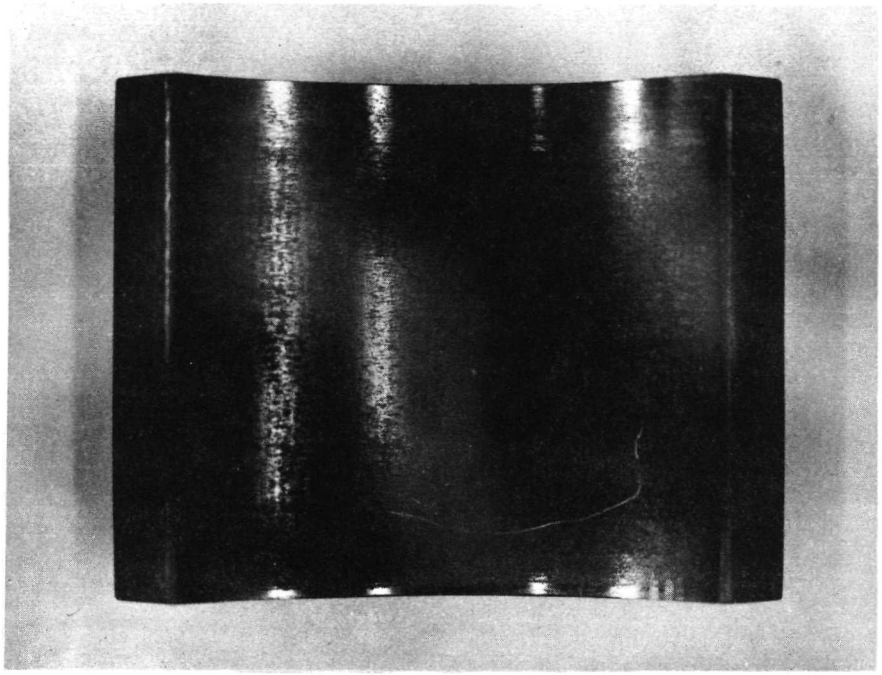

Pad After Testing

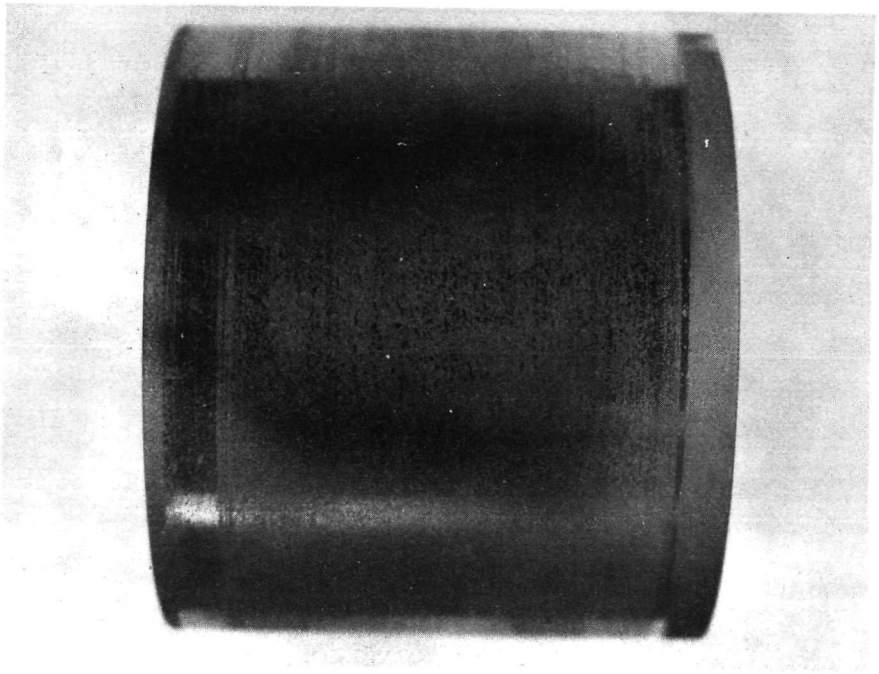

Sleeve After Testing

Plate 35 22C Polyimide MoS_2

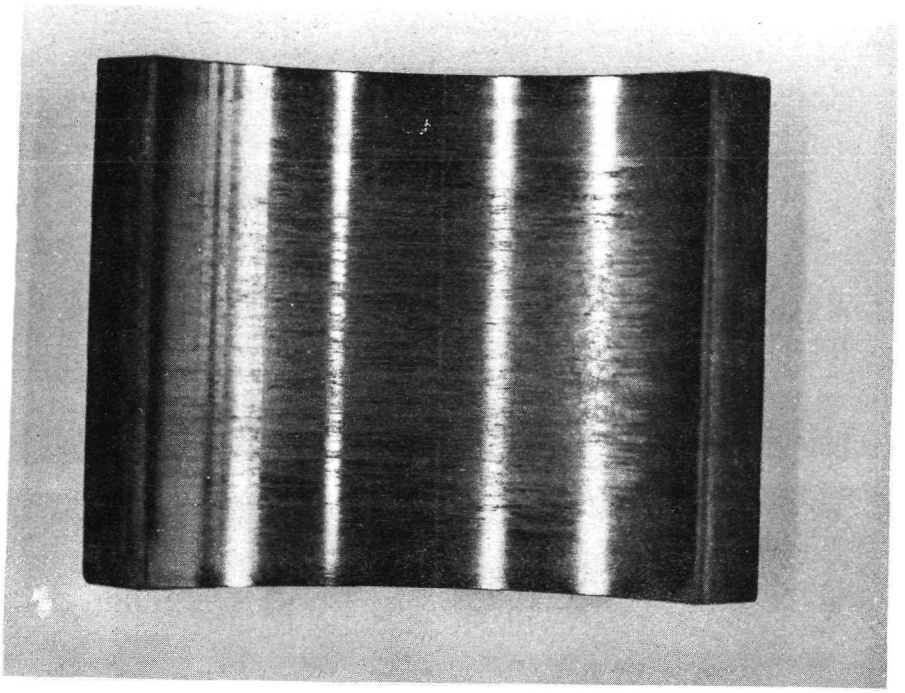

Pad After Testing

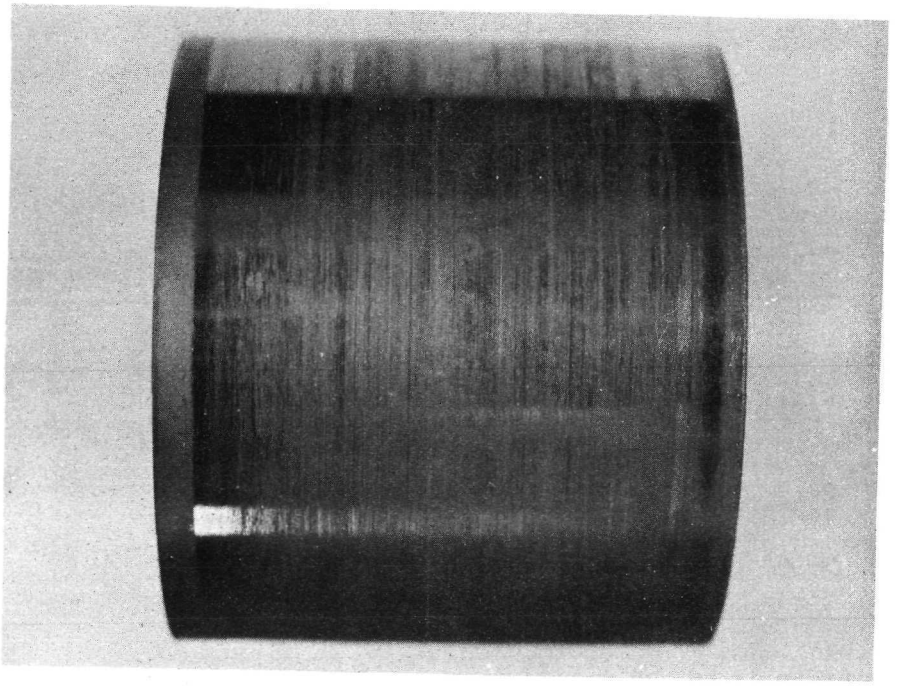

Sleeve After Testing

Plate 36 23C Metal Matrix MoS_2

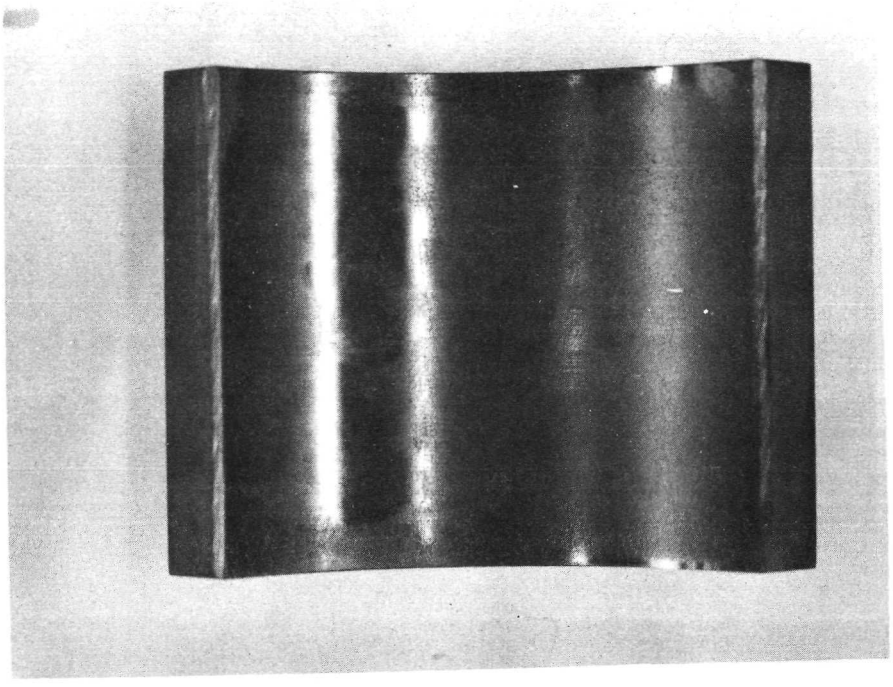

Pad After Testing

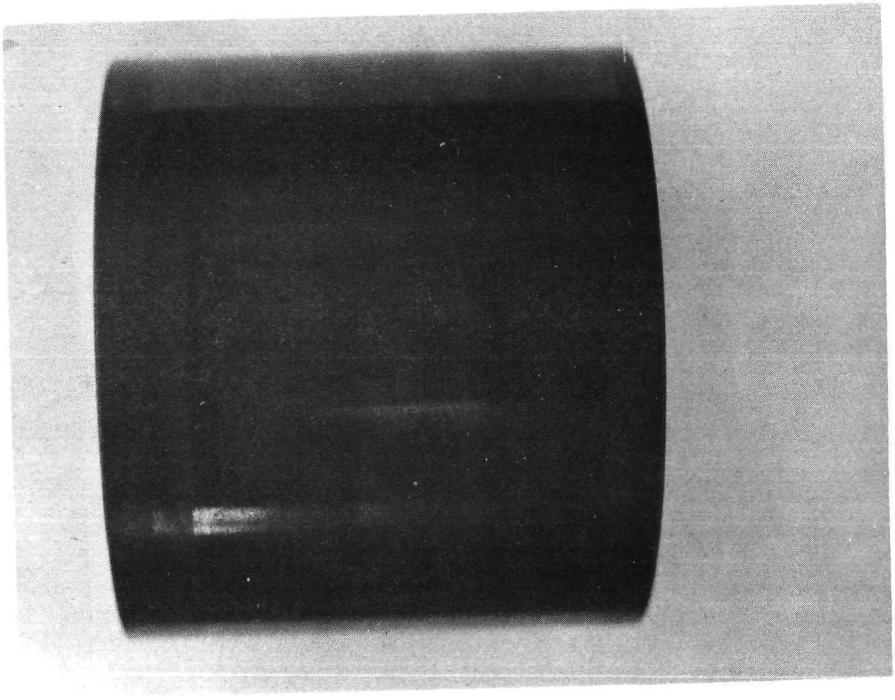

Sleeve After Testing

Plate 37 24C Burnished CF

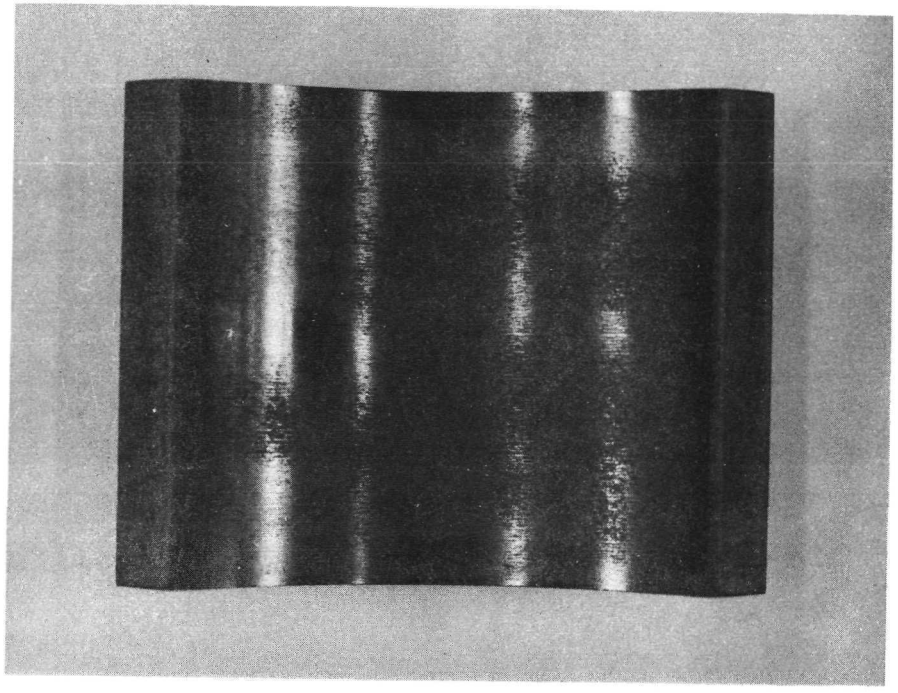

Pad After Testing

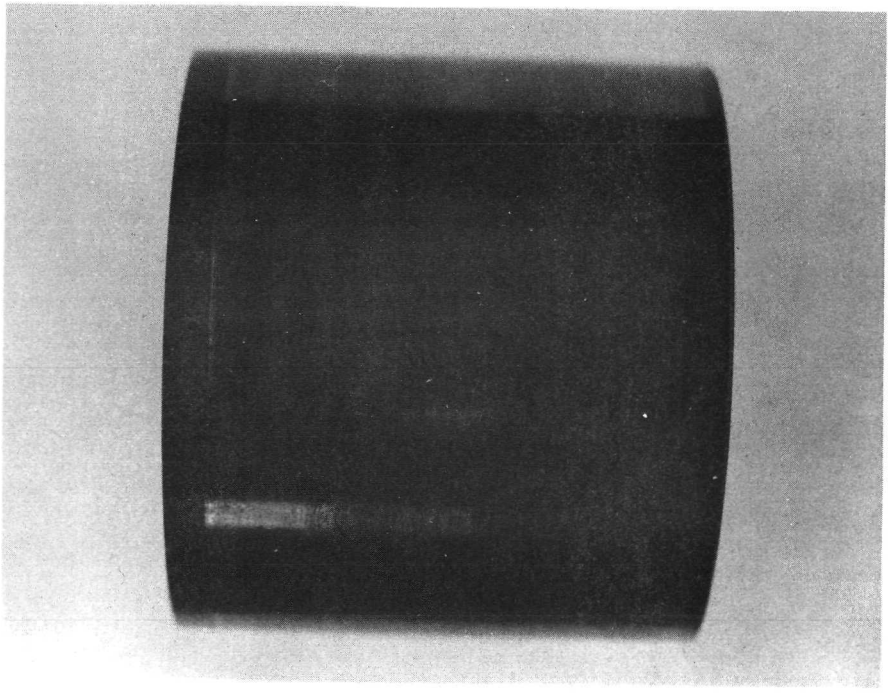

Sleeve After Testing

Plate 38 25C Polyimide CF

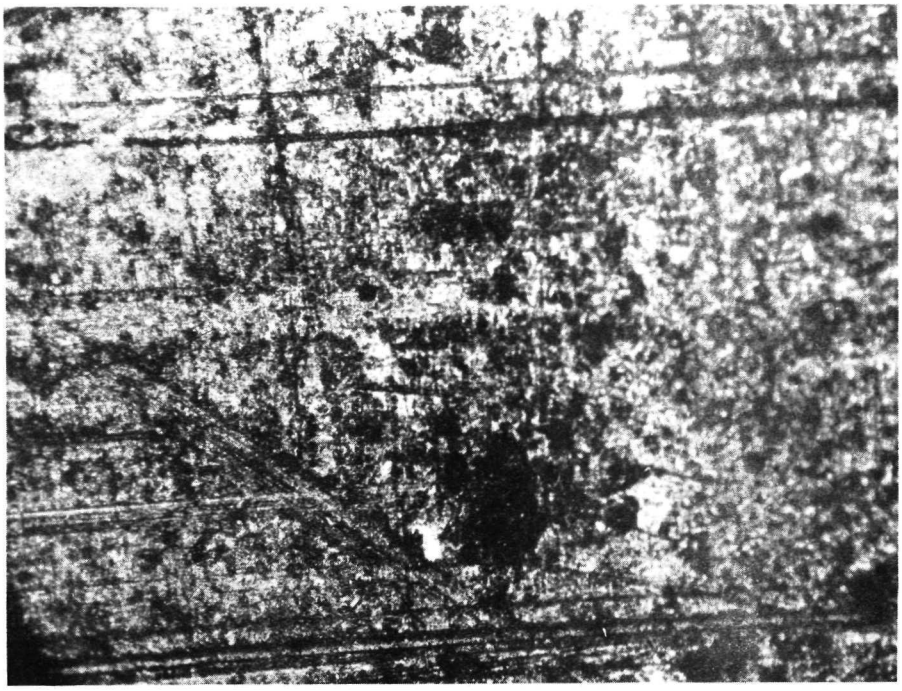

Pad After Testing

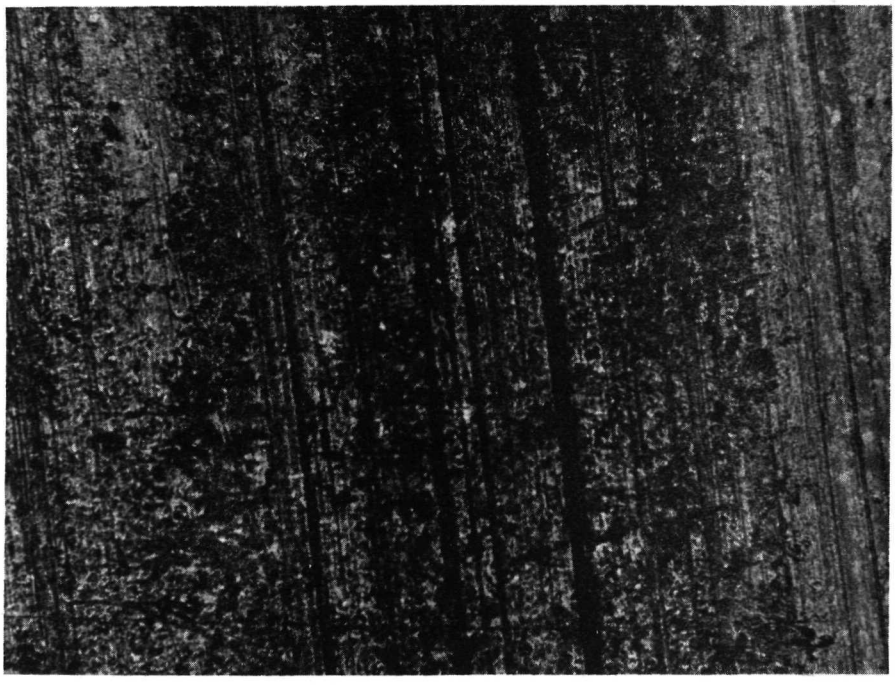

Sleeve After Testing

Plate 39 13A Metal Matrix MoS_2

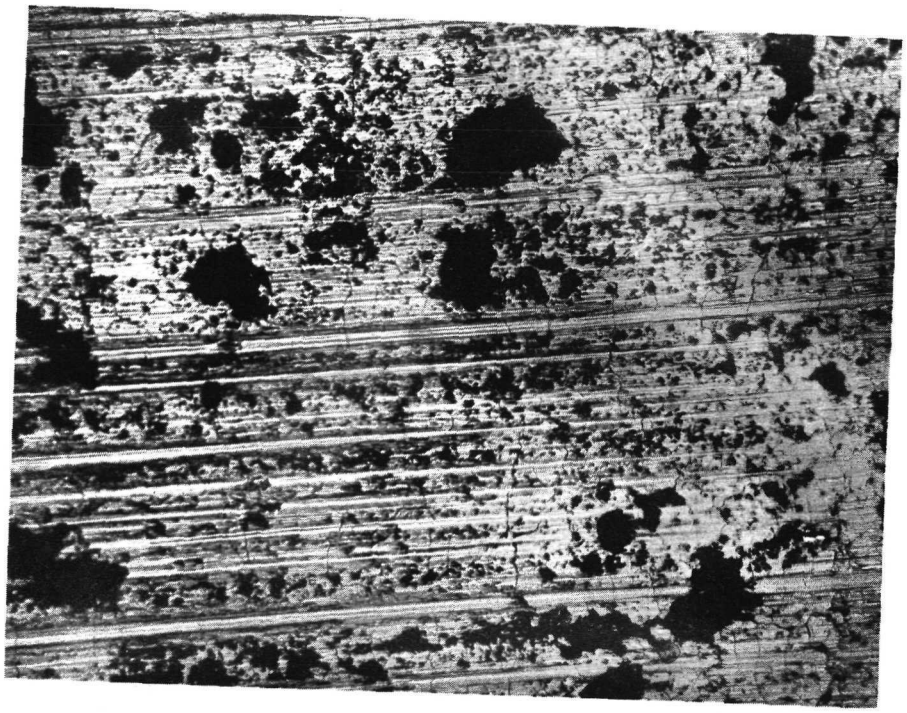

Pad After Testing

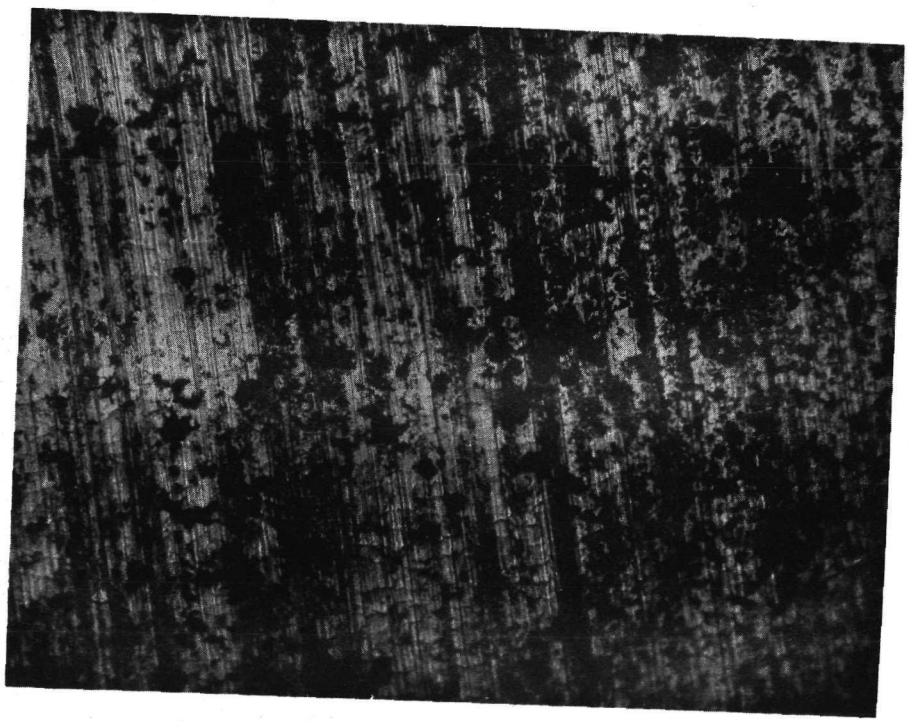

Sleeve After Testing

Plate 40 10B Burnished MoS_2

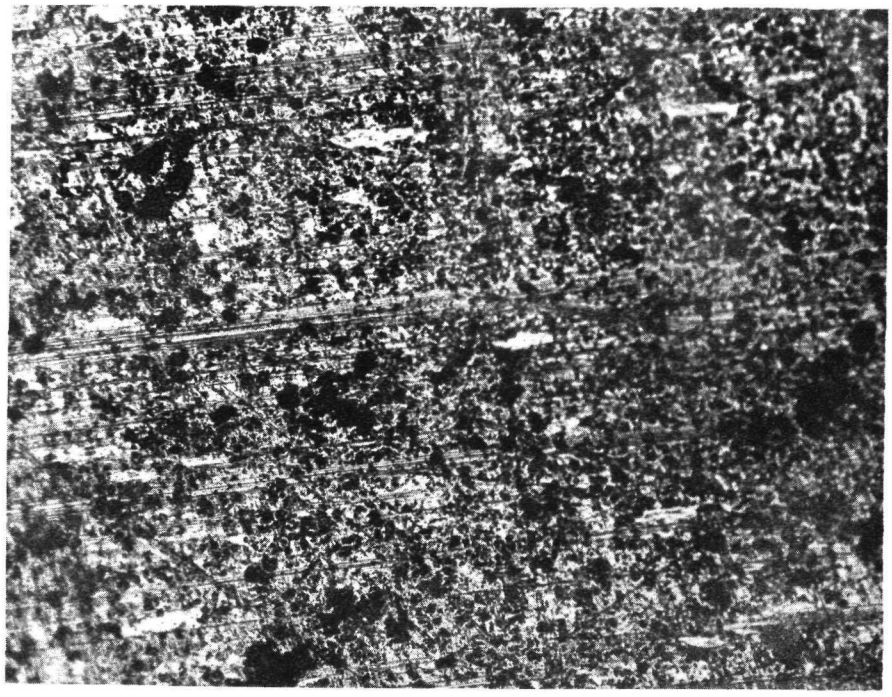

Pad After Testing

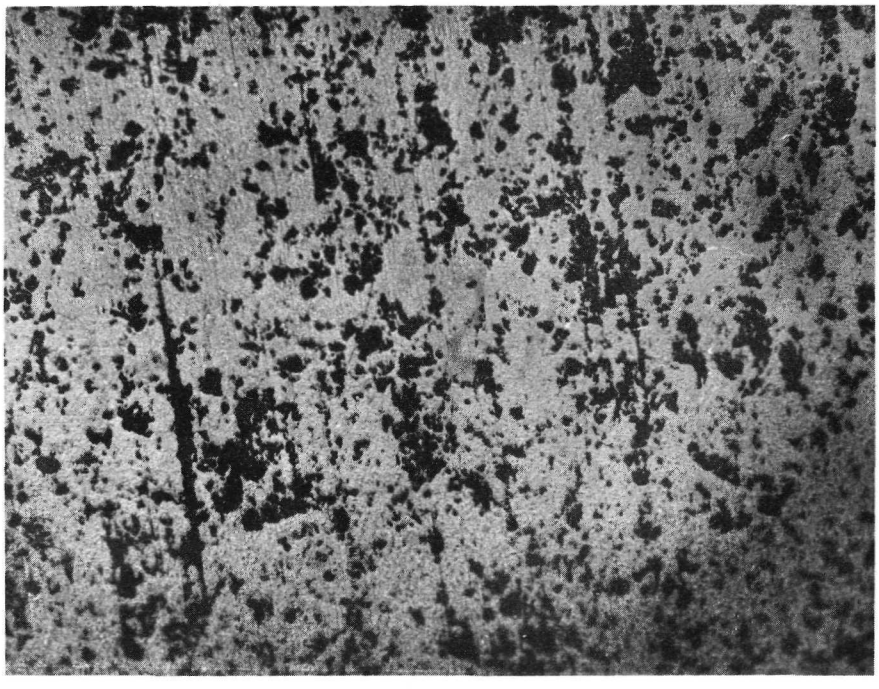

Sleeve After Testing

Plate 41 11B Sputtered MoS_2

Pad After Testing

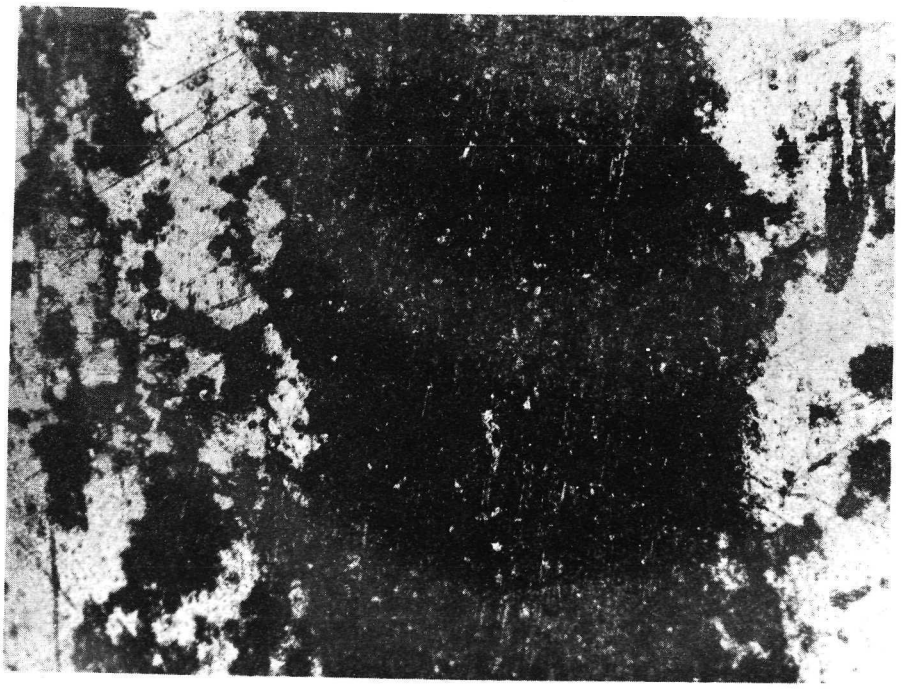

Sleeve After Testing

Plate 42 12B Polyimide MoS_2

Pad After Testing

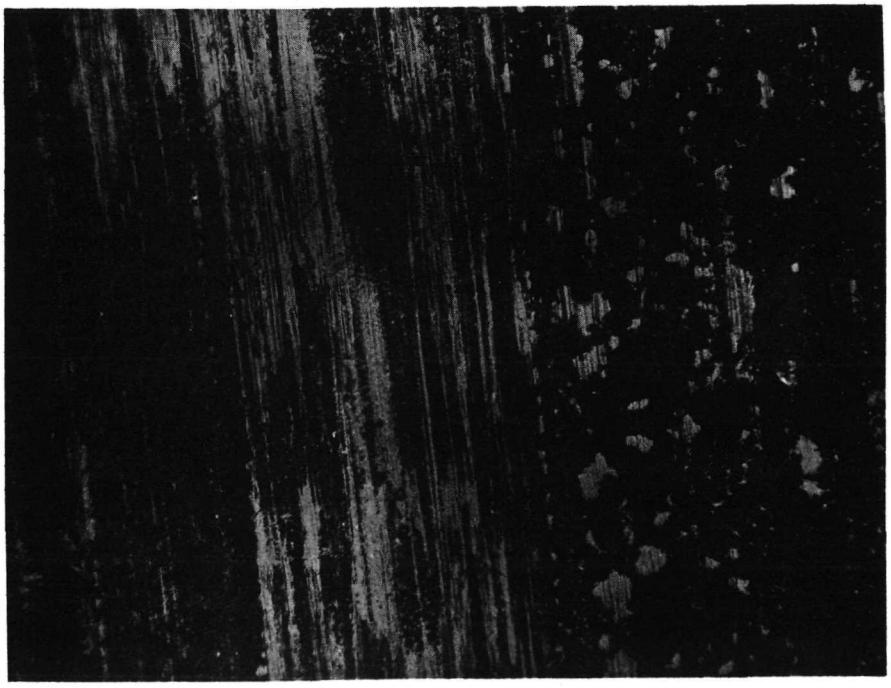

Sleeve After Testing

Plate 43 13B Metal Matrix MoS_2

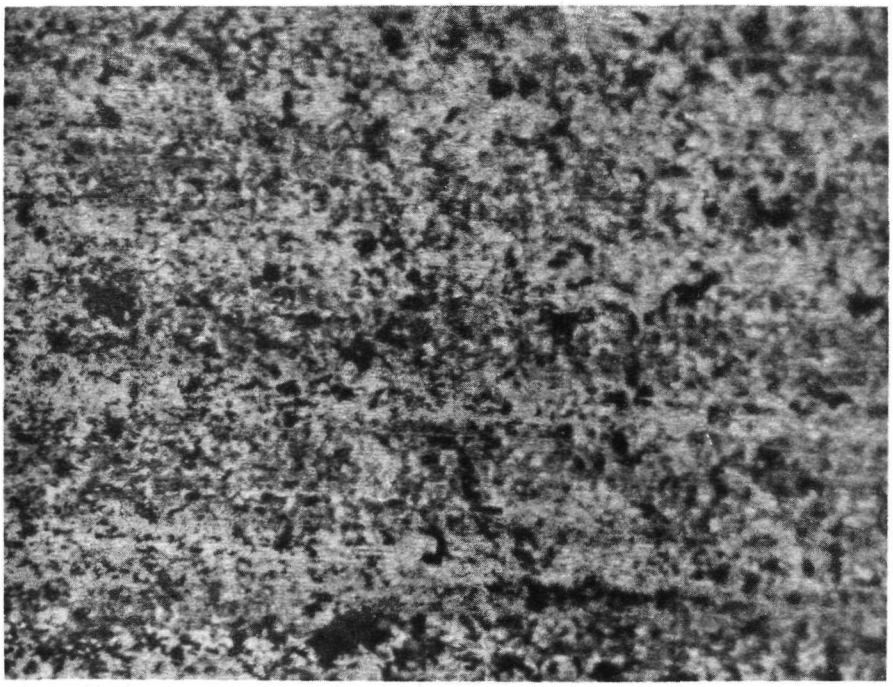

Pad After Testing

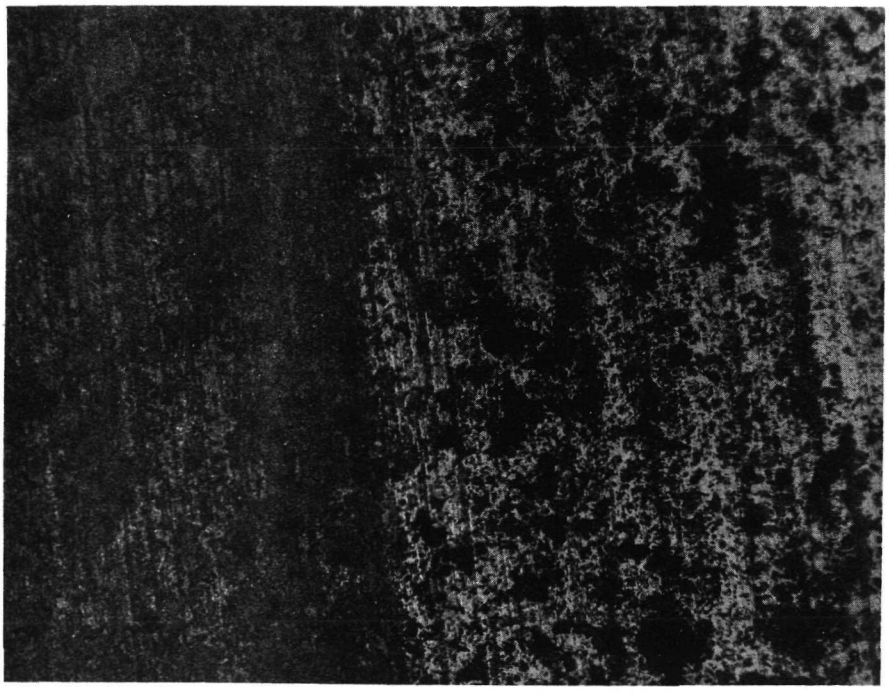

Sleeve After Testing

Plate 44 14B Burnished CF

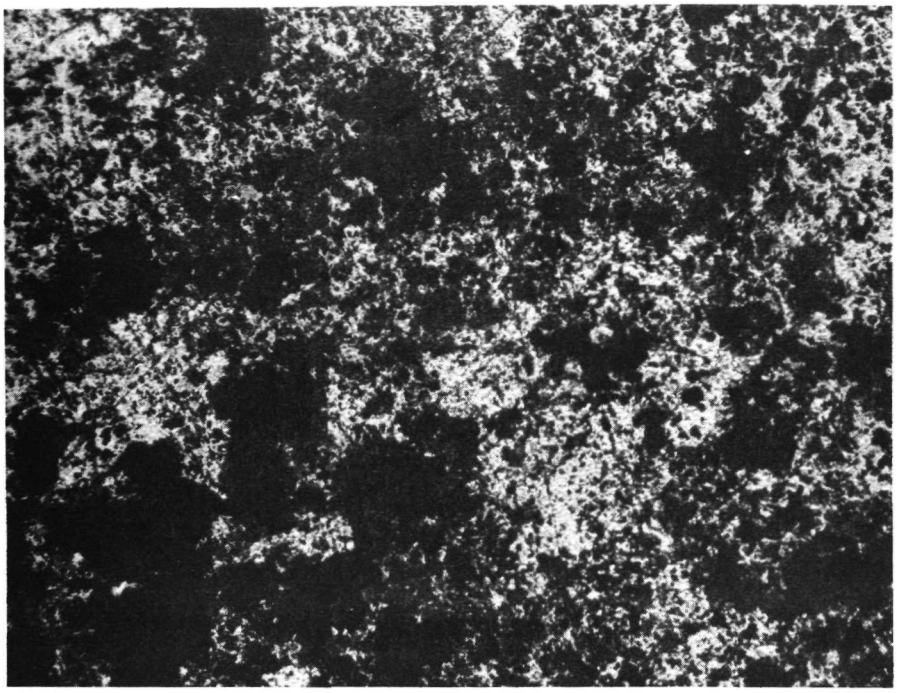

Pad After Testing

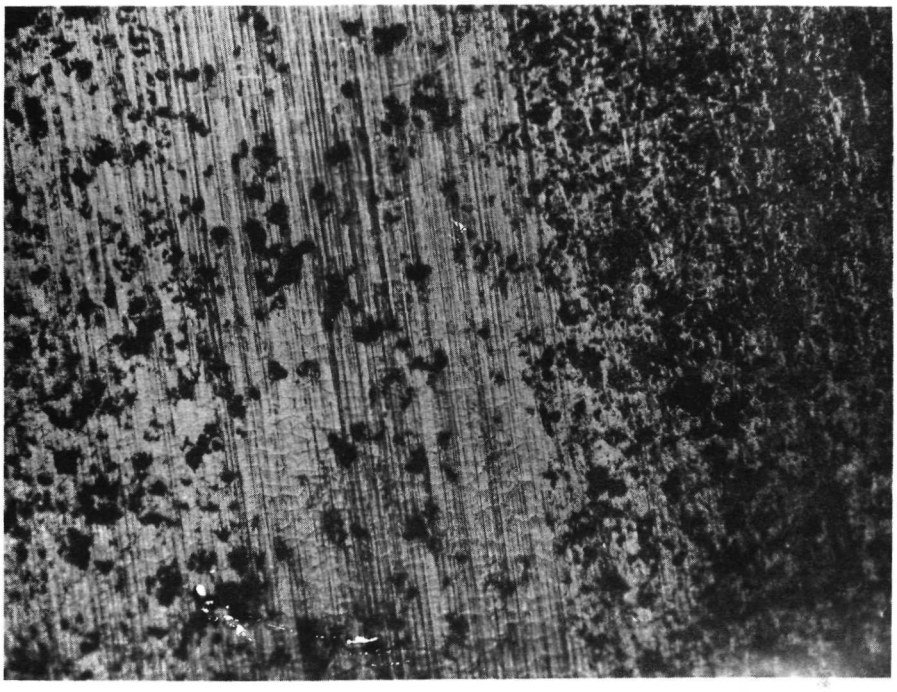

Sleeve After Testing

Plate 45 15B Polyimide CF

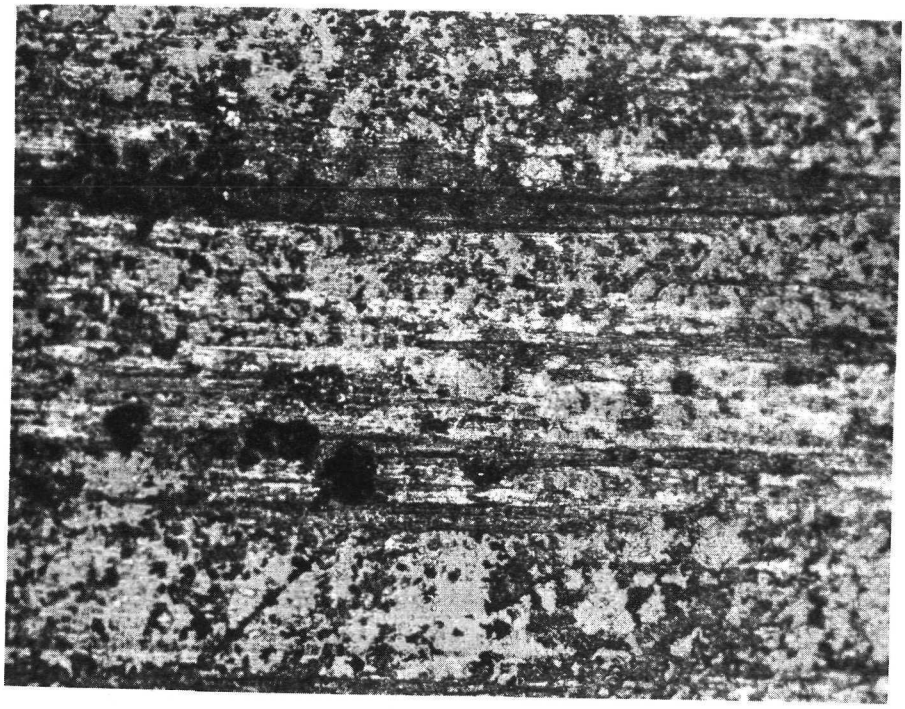

Pad After Testing

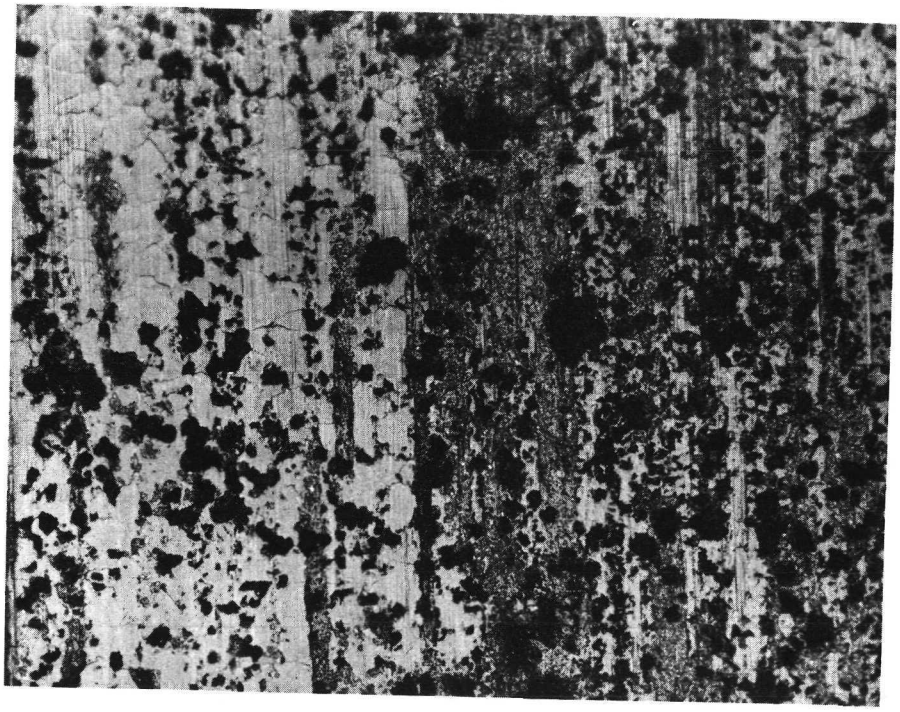

Sleeve After Testing

Plate 46 20B Burnished MoS_2

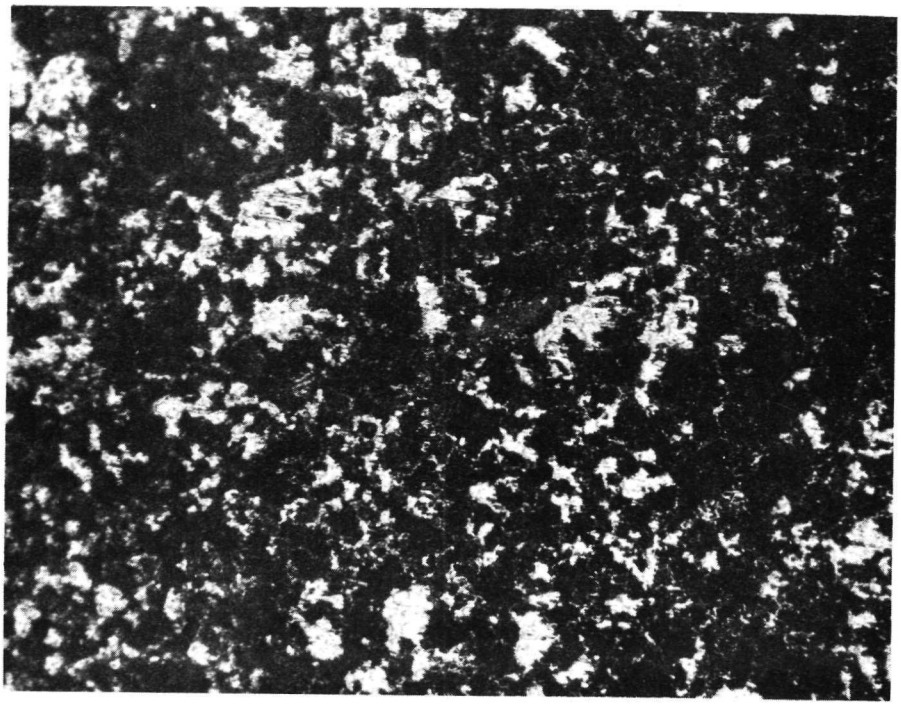

Pad After Testing

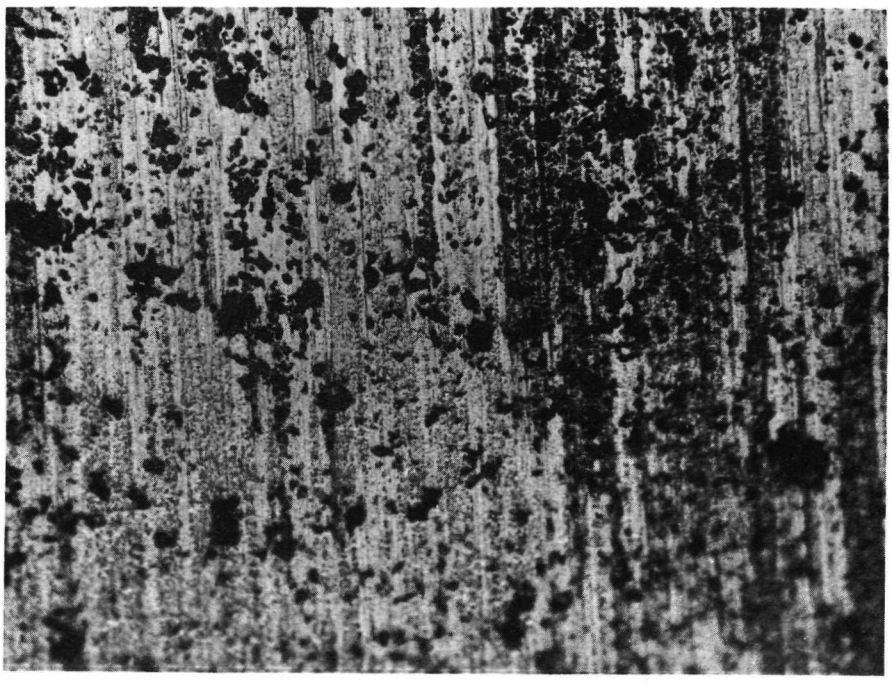

Sleeve After Testing

Plate 47 21B Sputtered MoS_2

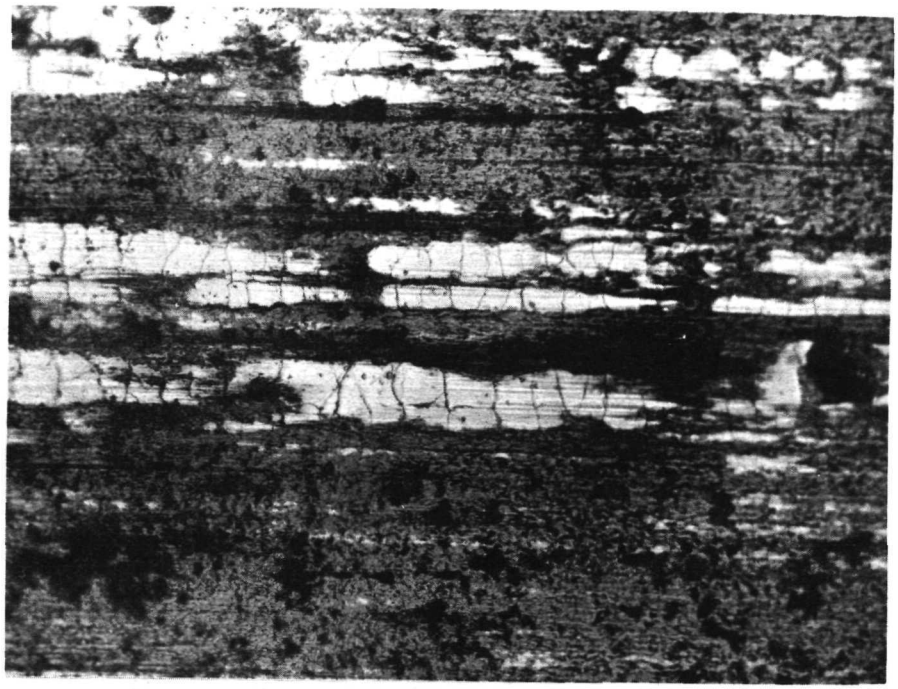

Pad After Testing

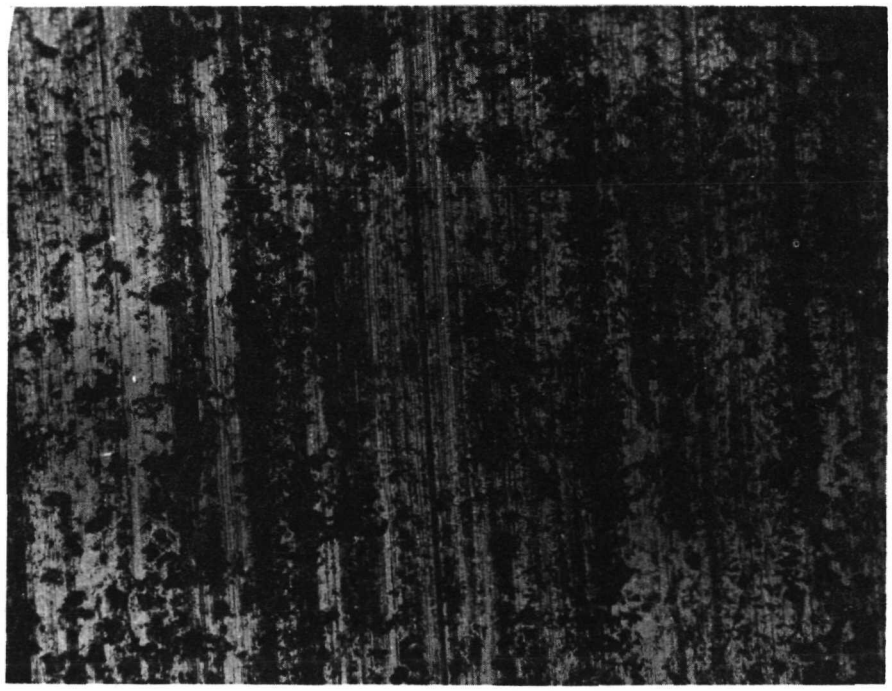

Sleeve After Testing

Plate 48 22B Polyimide MoS_2

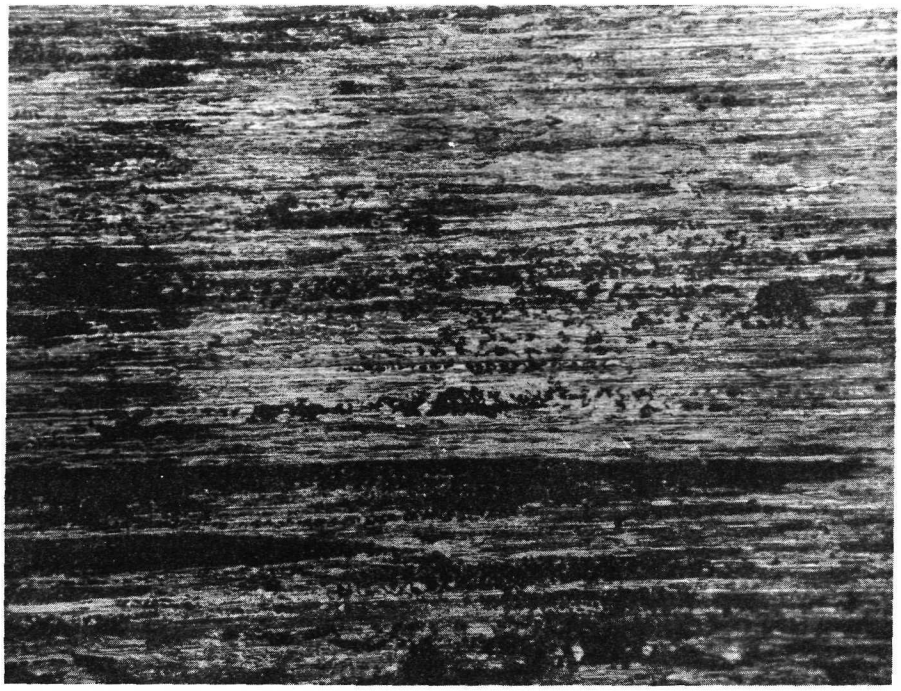

Pad After Testing

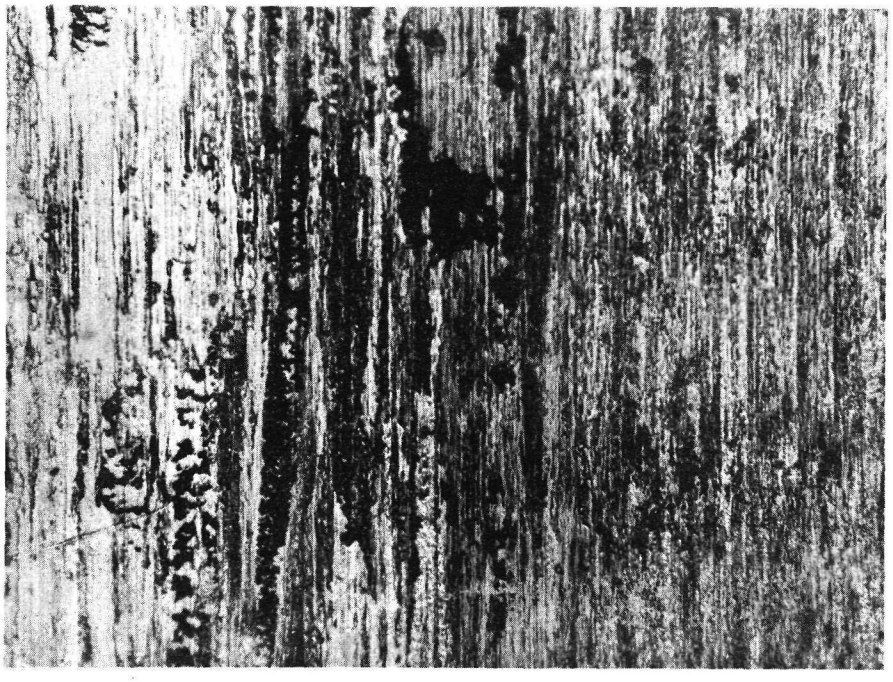

Sleeve After Testing

Plate 49 23B Metal Matrix MoS_2

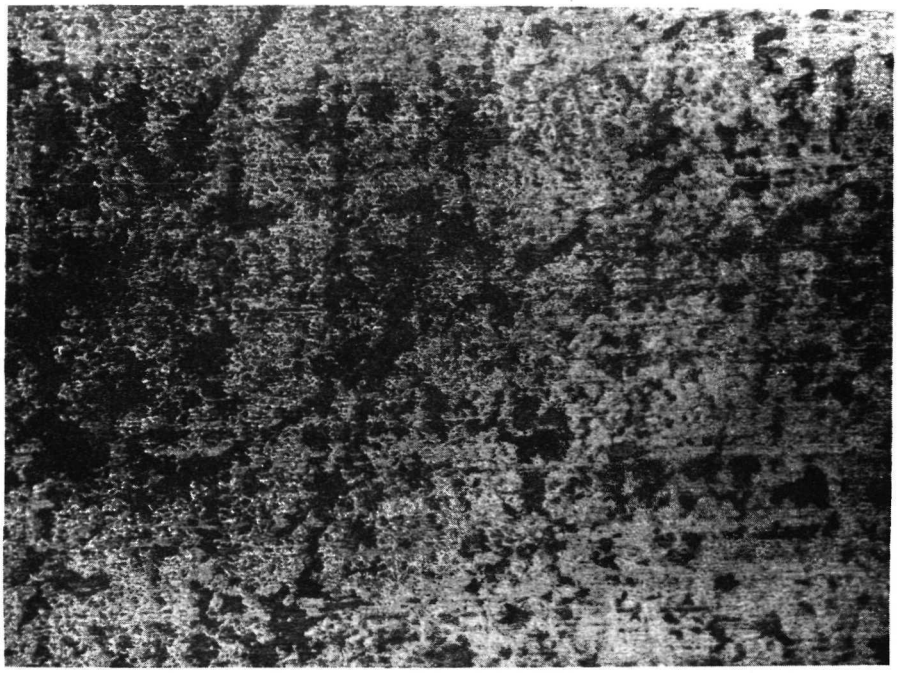

Pad After Testing

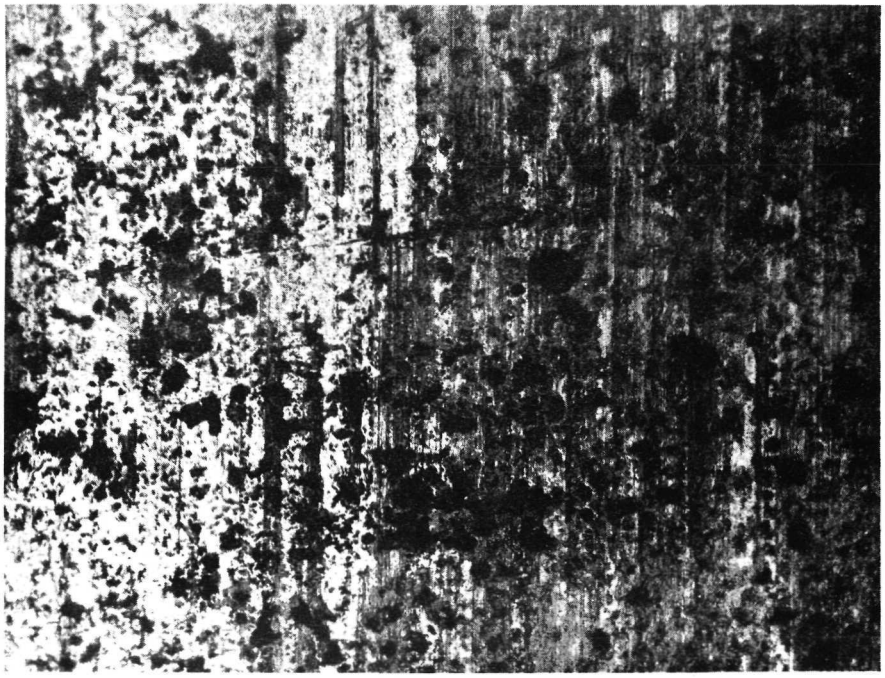

Sleeve After Testing

Plate 50 24B Burnished CF

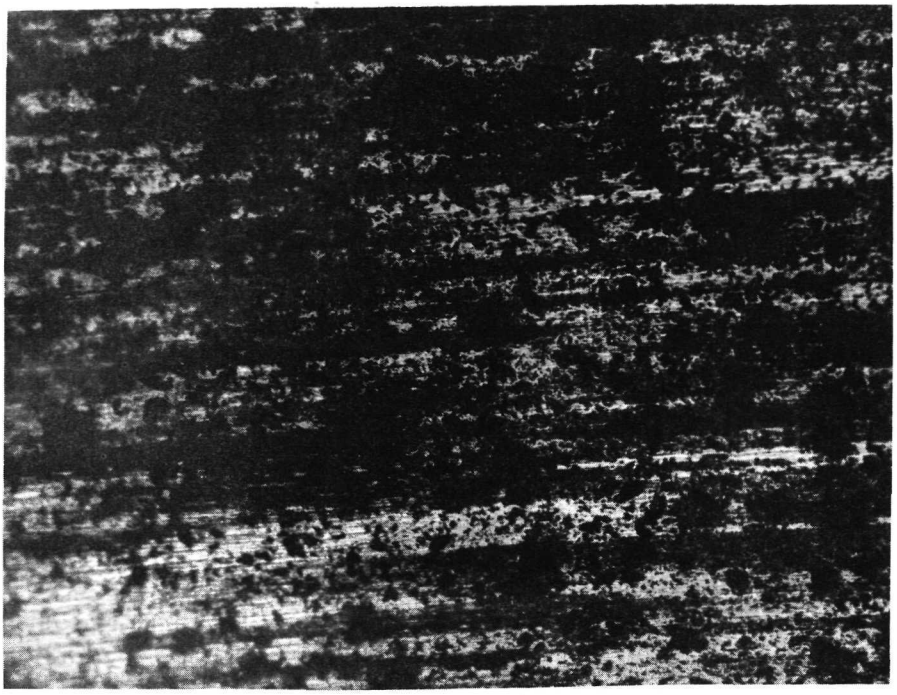

Pad After Testing

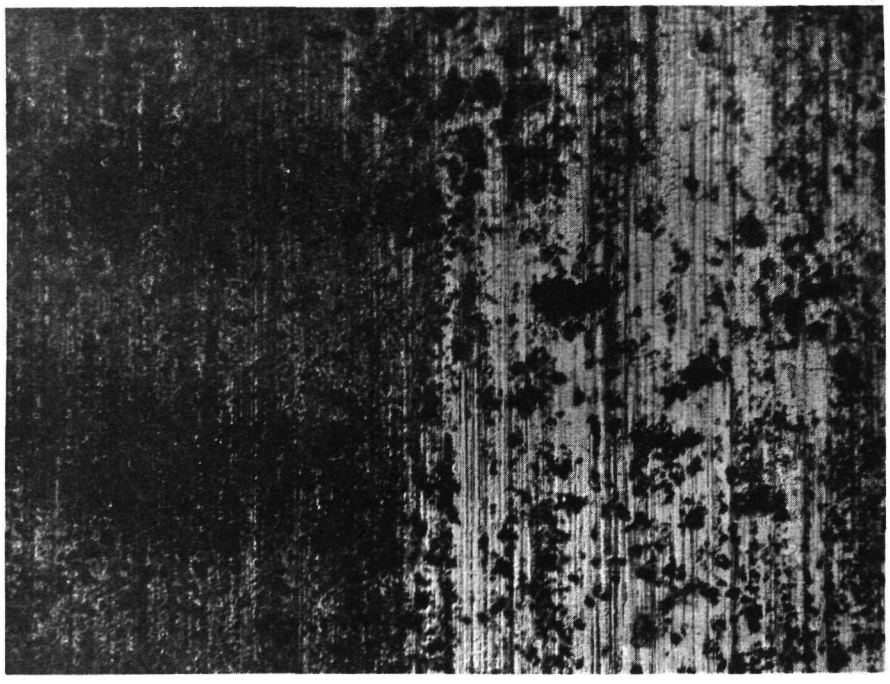

Sleeve After Testing

Plate 51 25B Polyimide CF

Pad After Testing

Sleeve After Testing

Plate 52 10C Burnished MoS_2

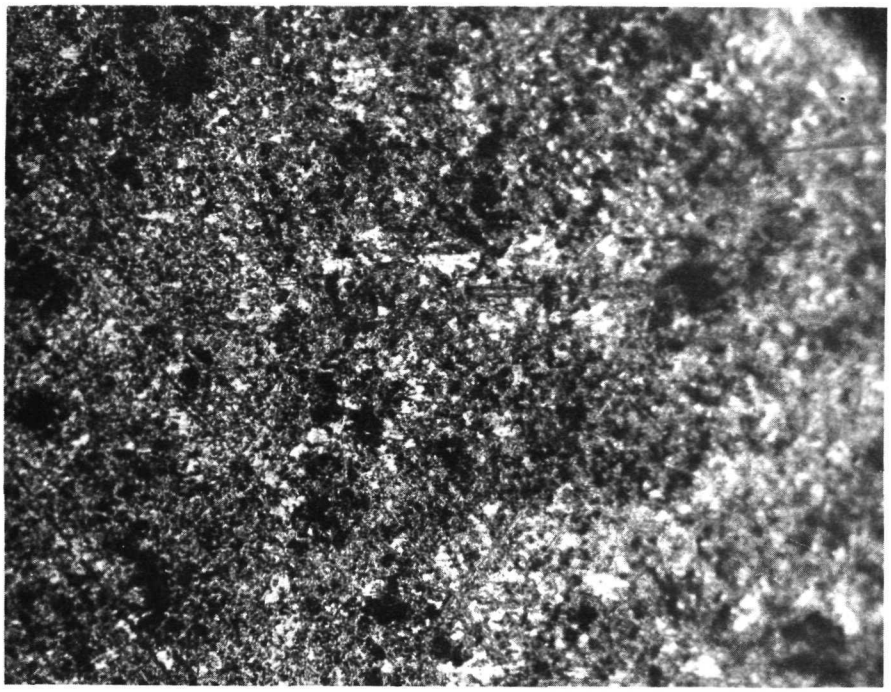

Pad After Testing

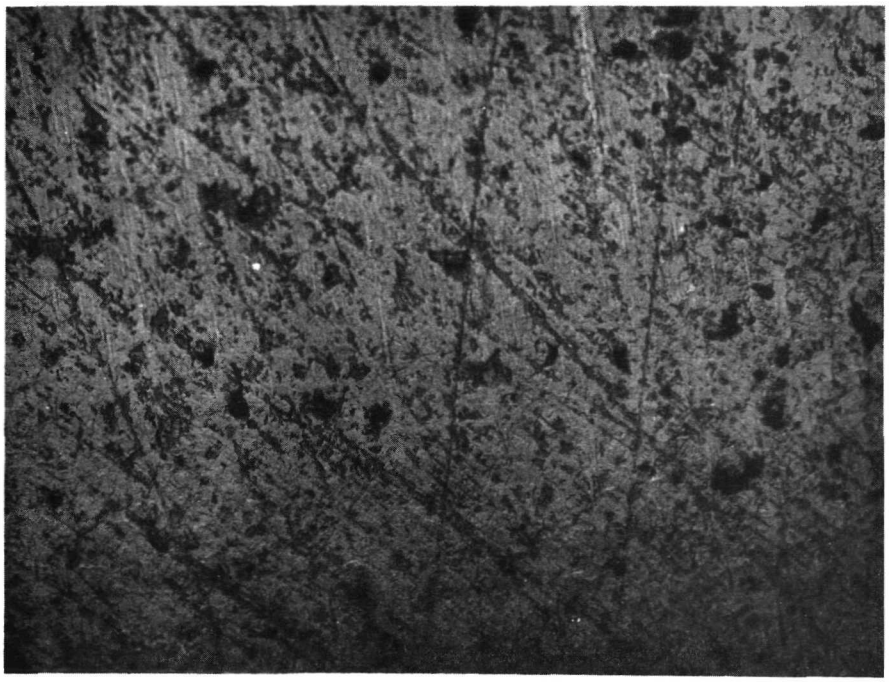

Sleeve After Testing

Plate 53 11C Sputtered MoS_2

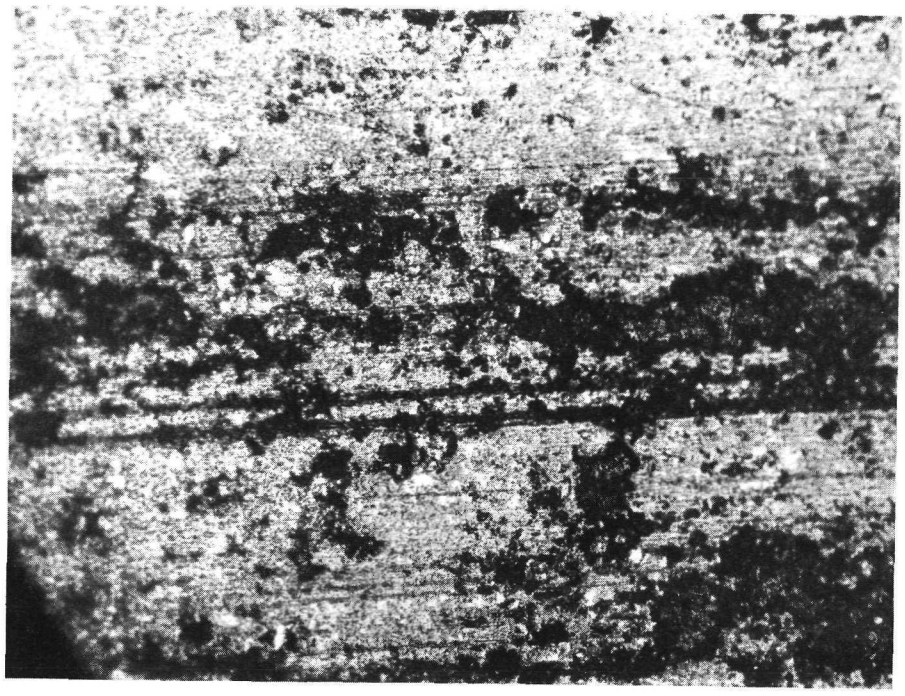

Pad After Testing

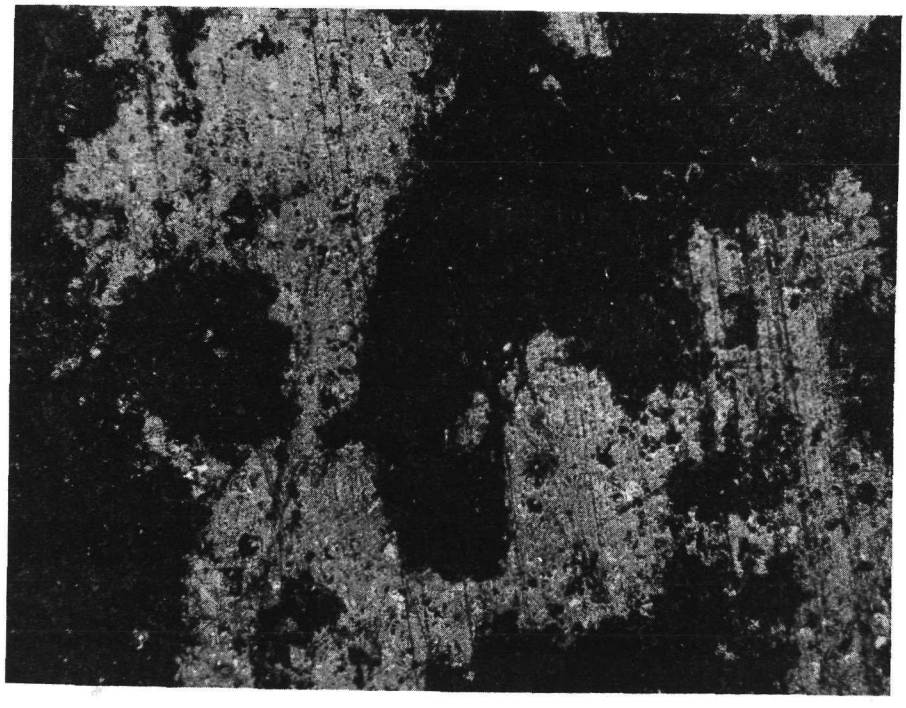

Sleeve After Testing

Plate 54 12C Polyimide MoS_2

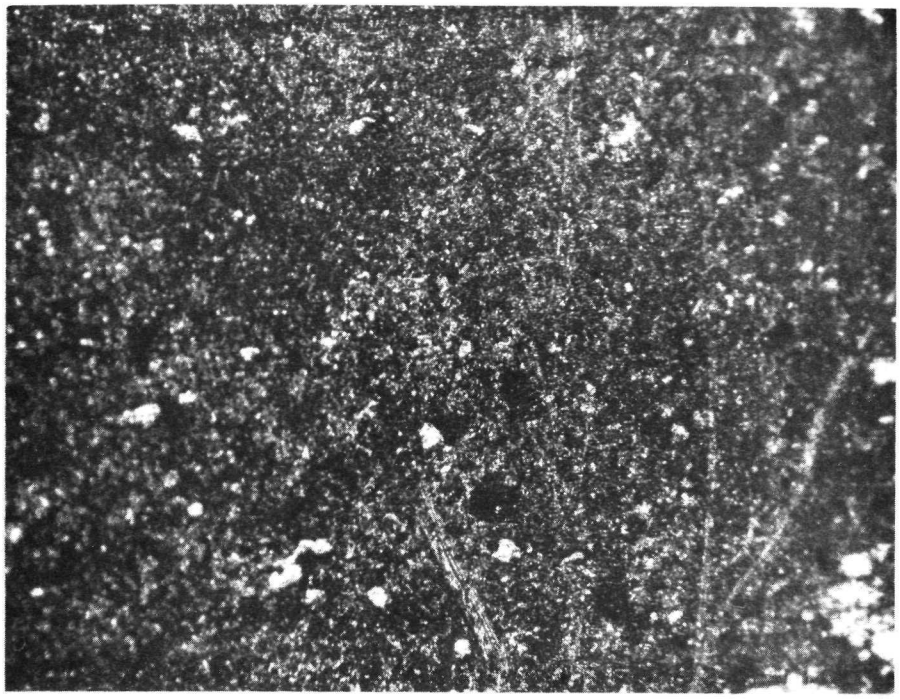

Pad After Testing

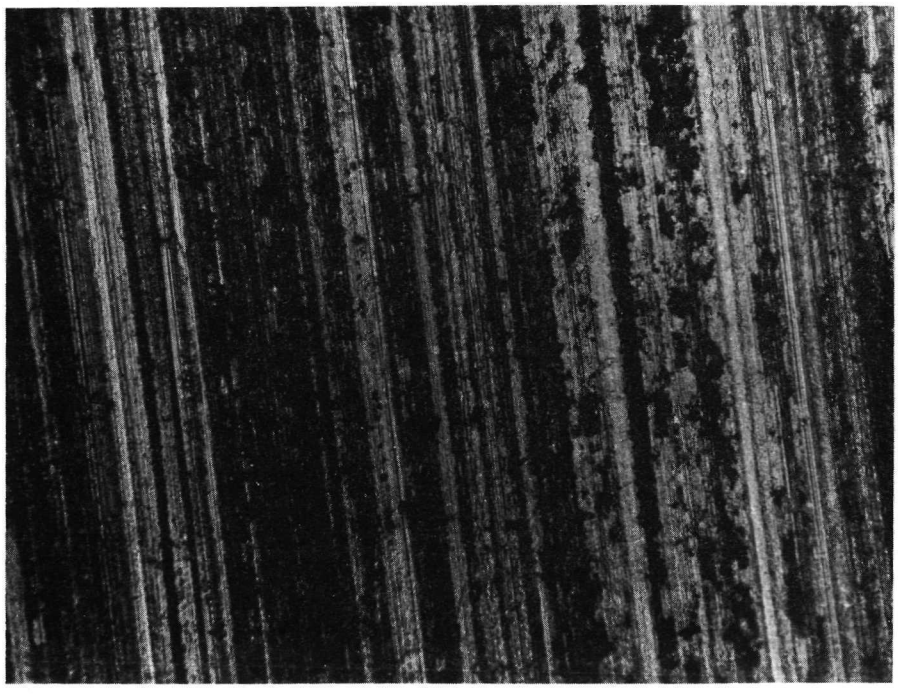

Sleeve After Testing

Plate 55 13C Metal Matrix MoS_2

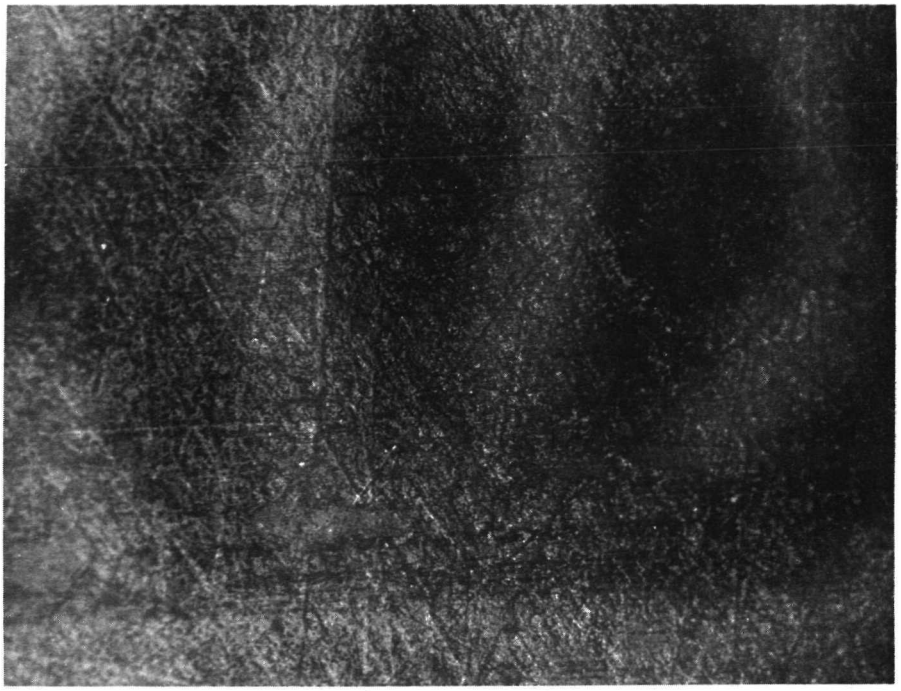

Pad After Testing

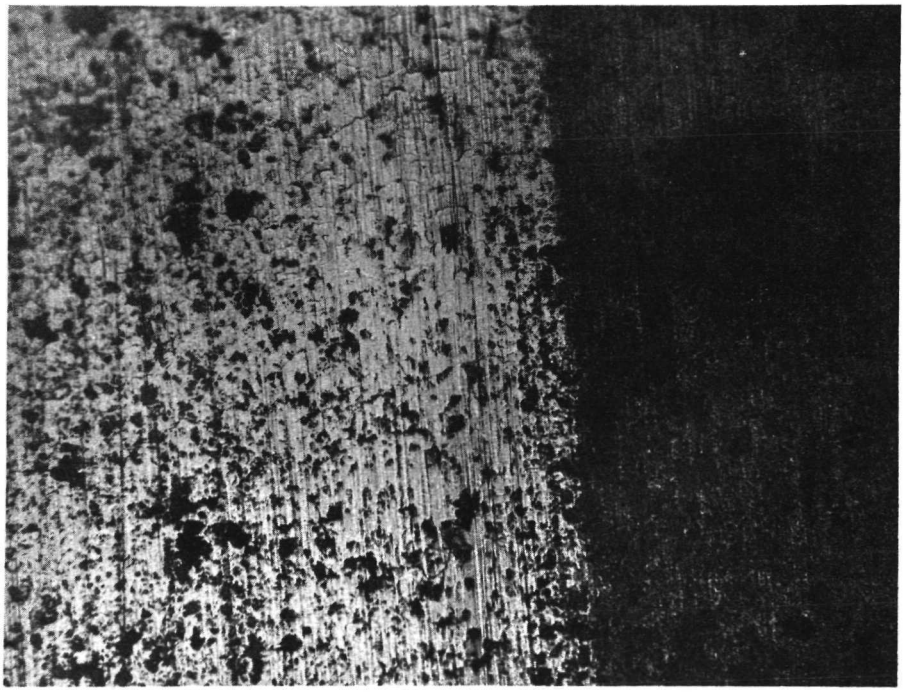

Sleeve After Testing

Plate 56 14C Burnished CF

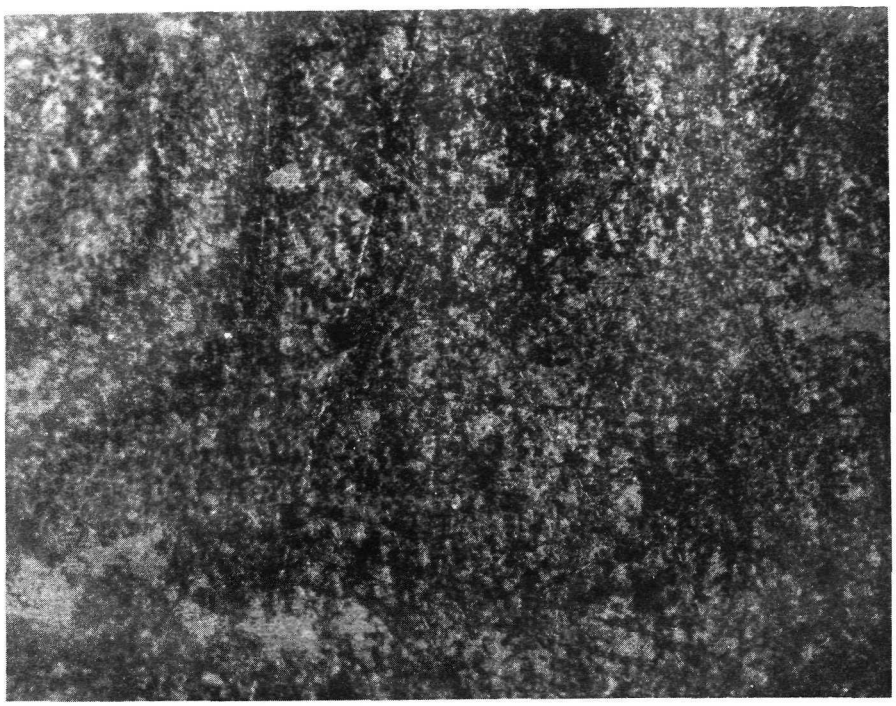

Pad After Testing

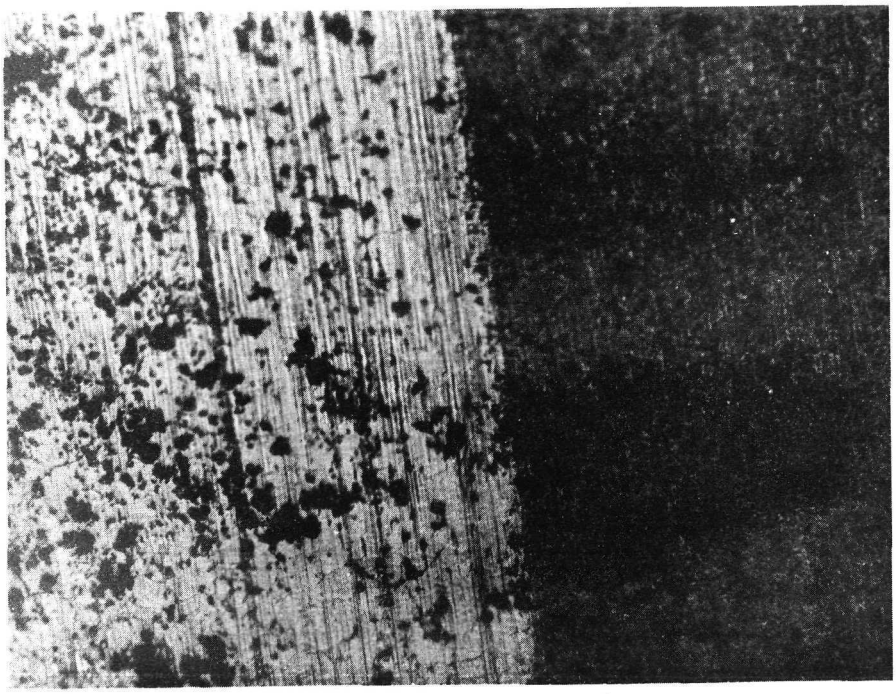

Sleeve After Testing

Plate 57 15C Polyimide CF

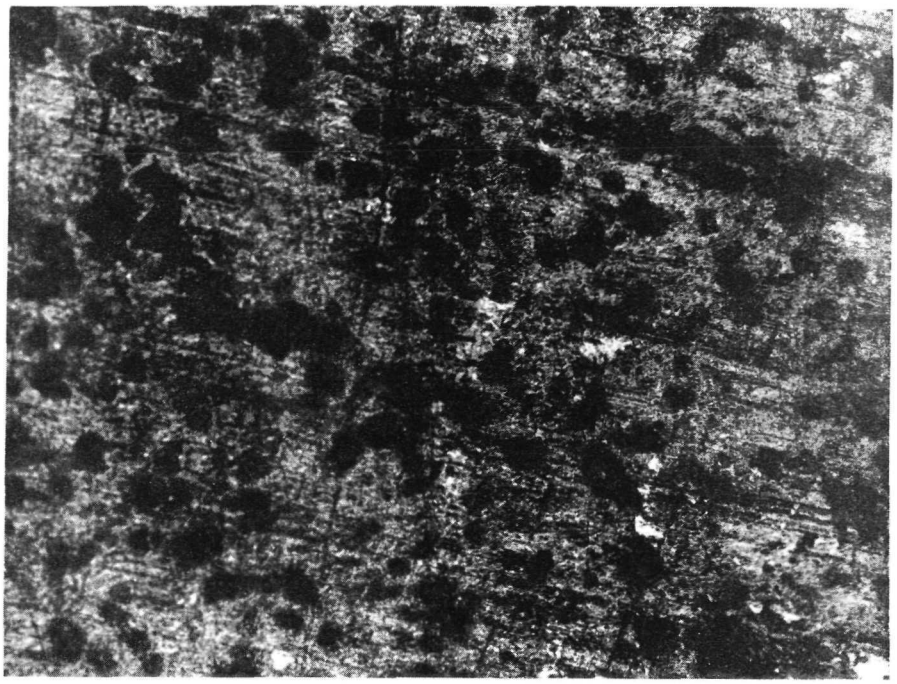

Pad After Testing

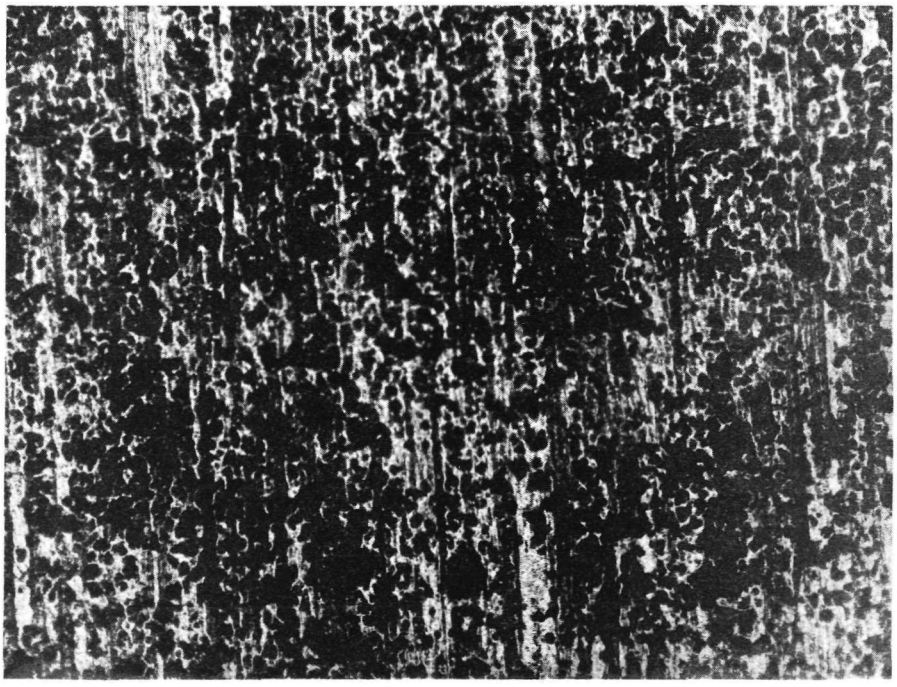

Sleeve After Testing

Plate 58 20C Burnished MoS_2

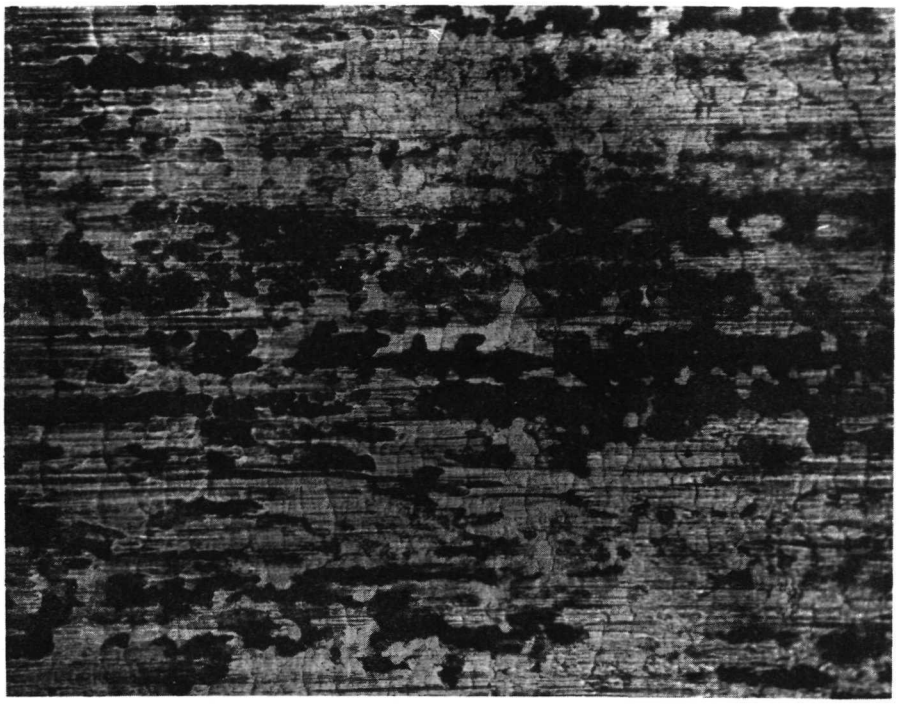

Pad After Testing

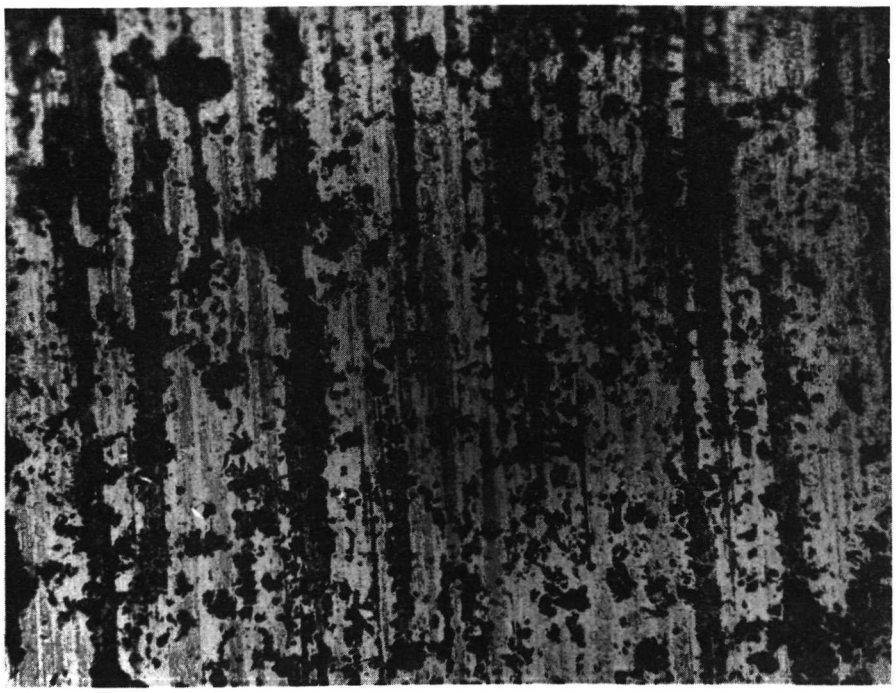

Sleeve After Testing

Plate 59 21C Sputtered MoS_2

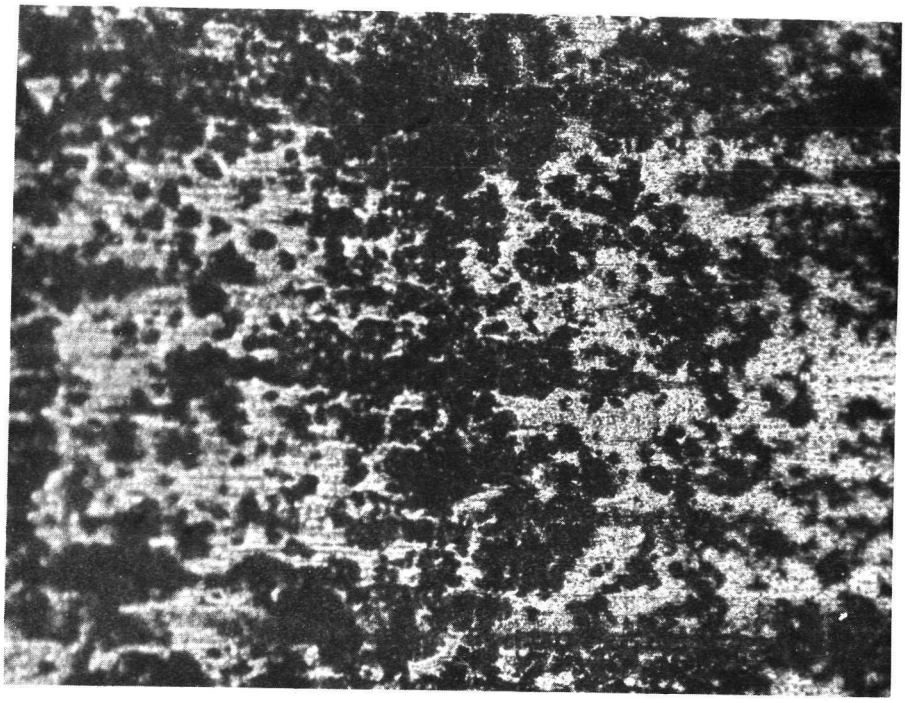

Pad After Testing

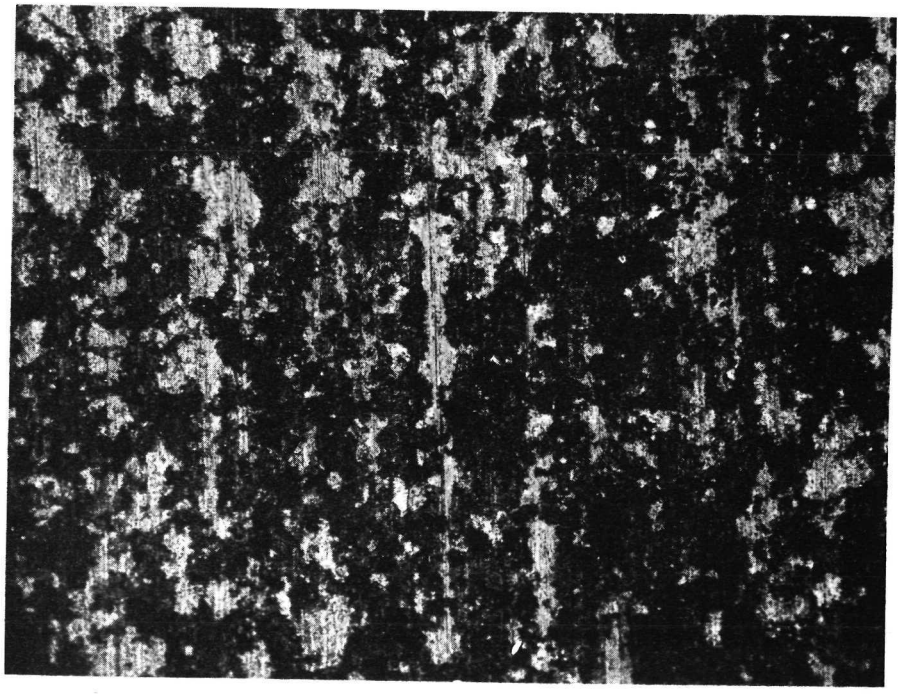

Sleeve After Testing

Plate 60 22C Polyimide MoS_2

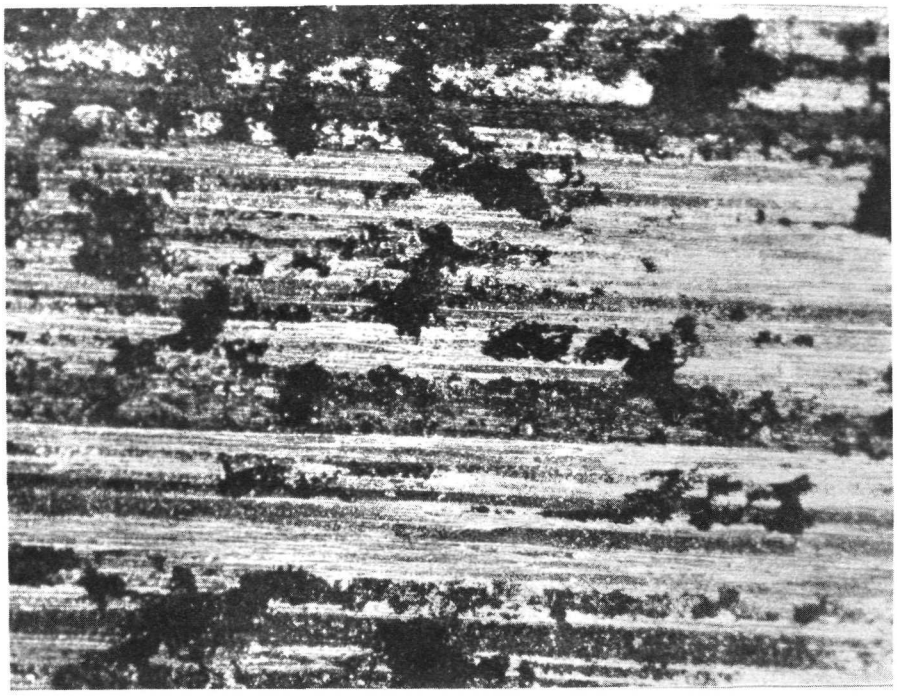

Pad After Testing

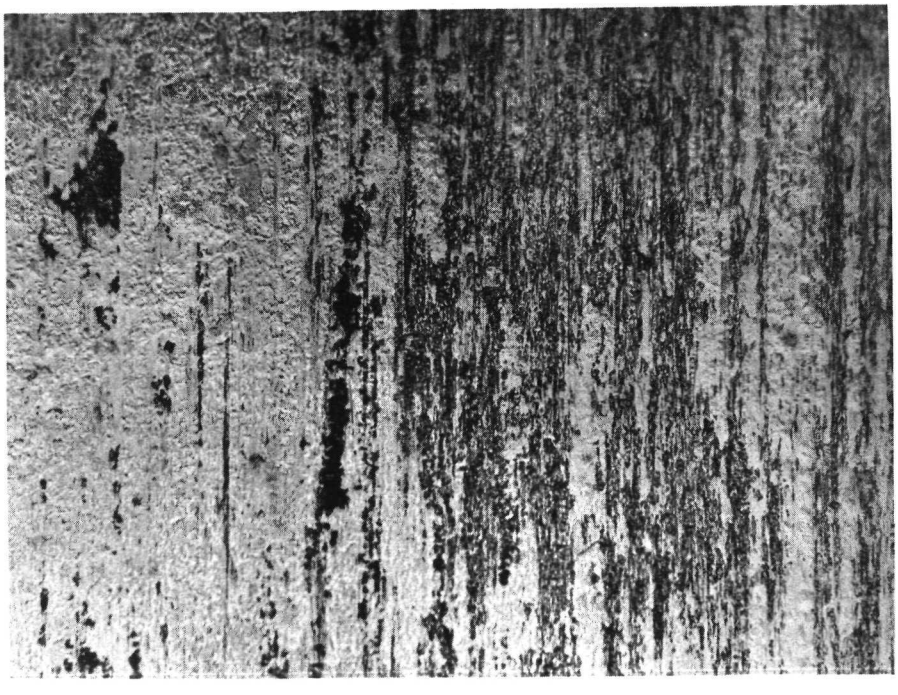

Sleeve After Testing

Plate 61 23C Metal Matrix MoS_2

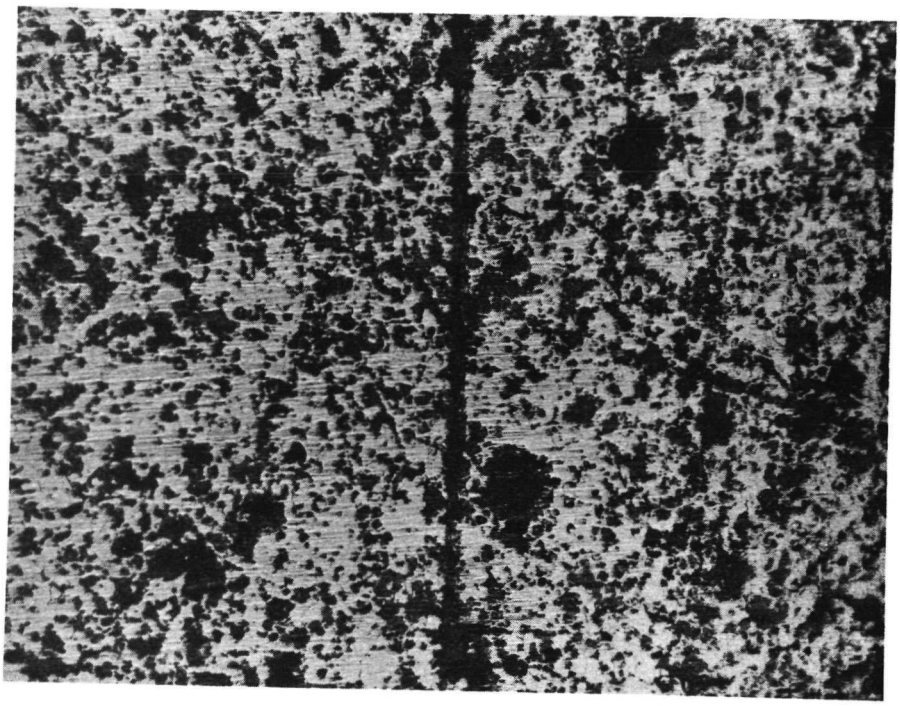

Pad After Testing

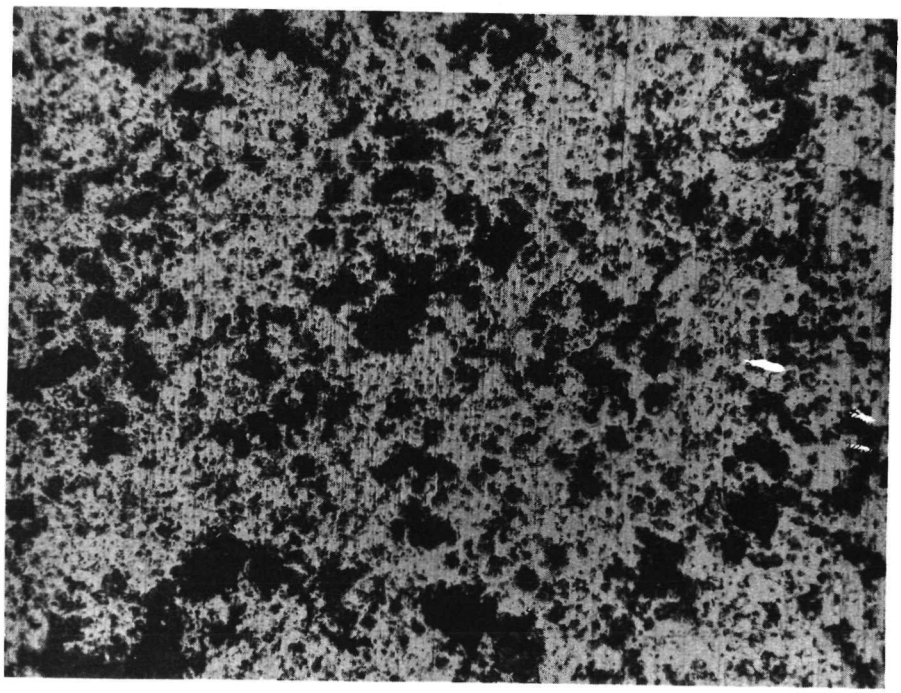

Sleeve After Testing

Plate 62 24C Burnished CF

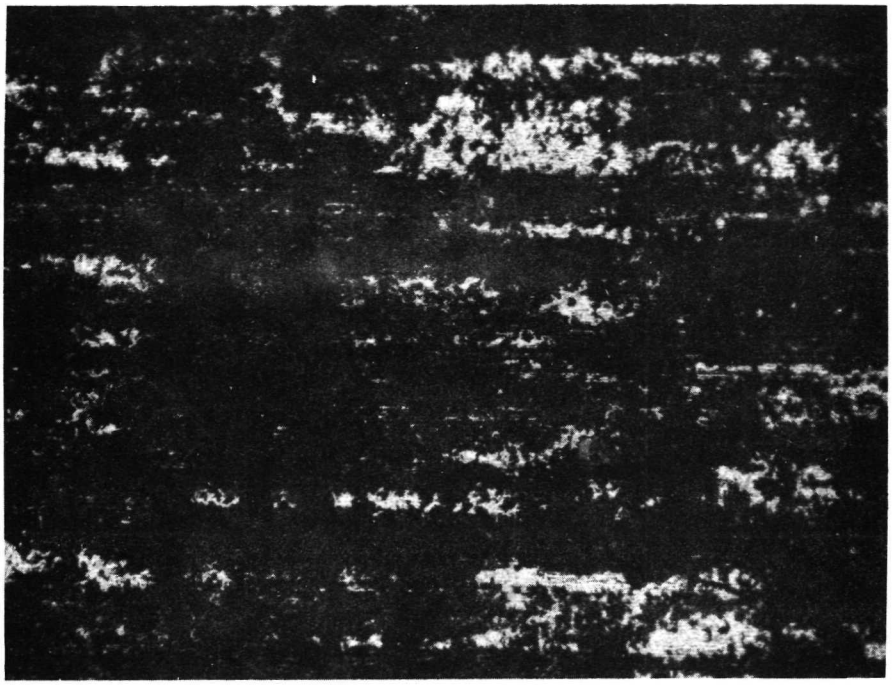

Pad After Testing

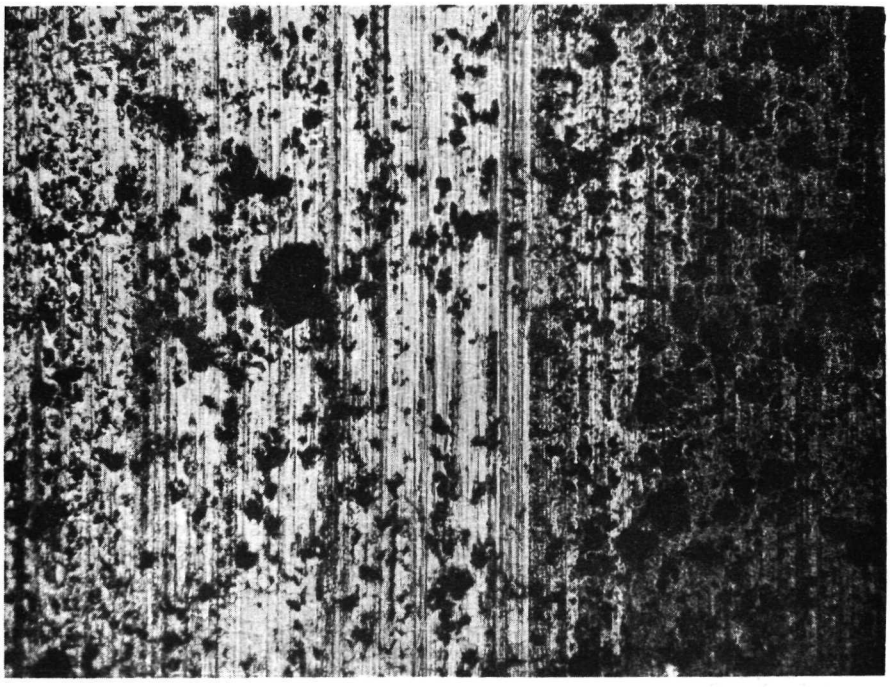

Sleeve After Testing

Plate 63 25C Polyimide CF

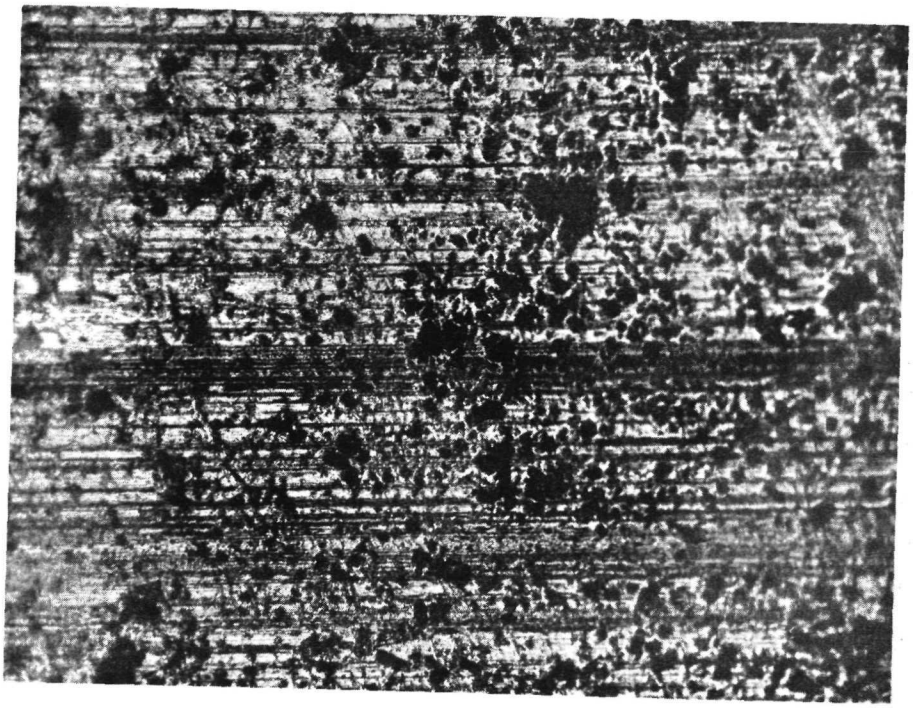

Pad After Testing

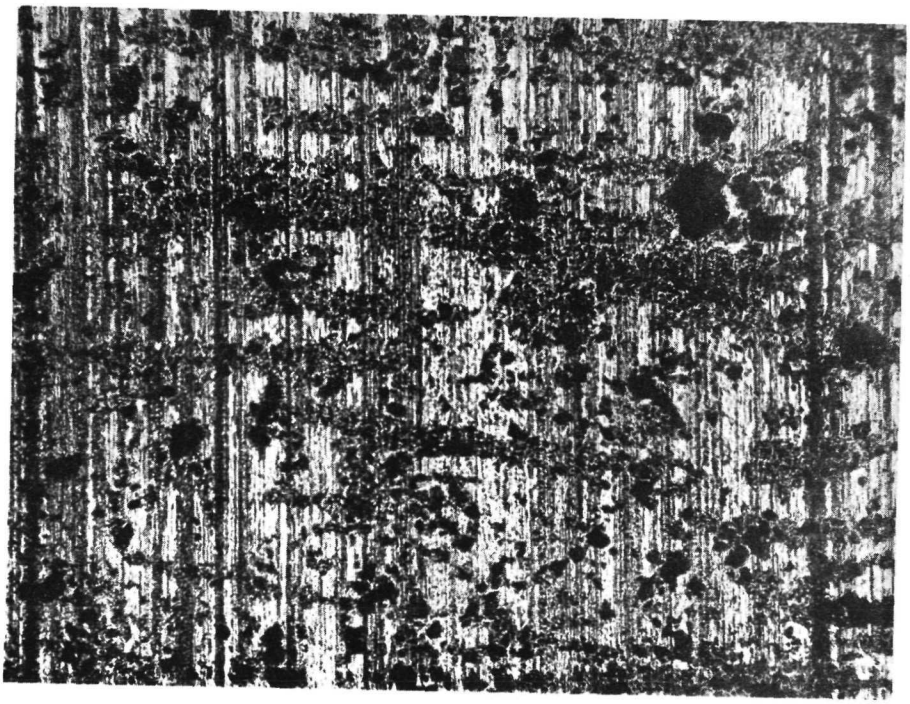

Sleeve After Testing

Plate 64 42 Sputtered MoS_2

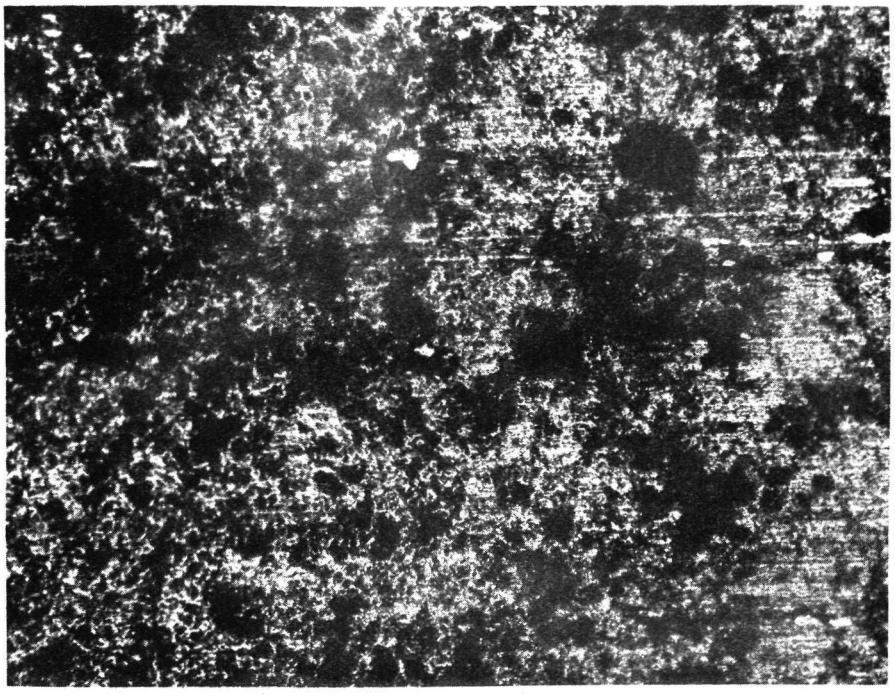

Pad After Testing

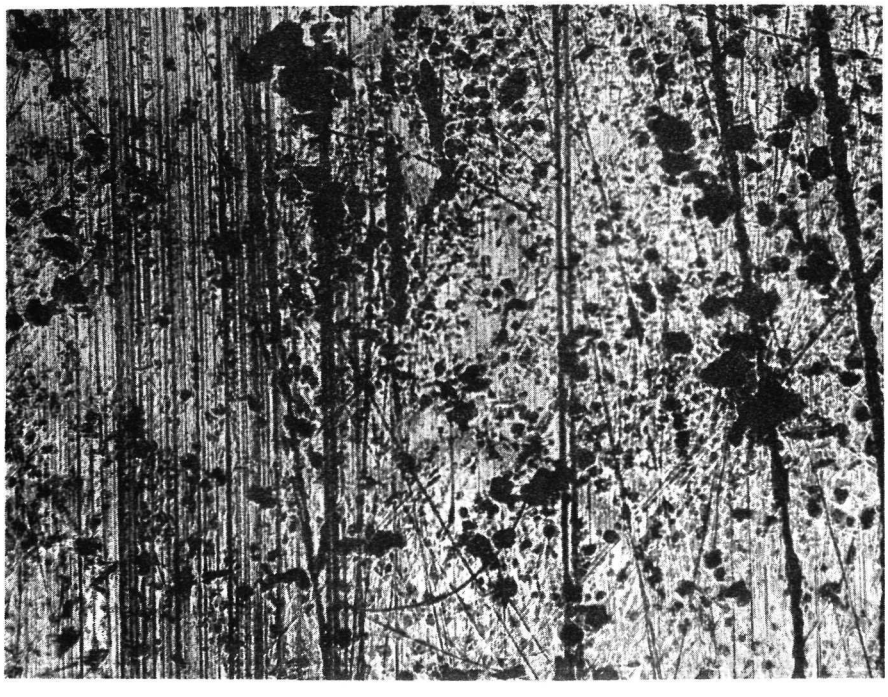

Sleeve After Testing

Plate 65 44 Sputtered MoS_2

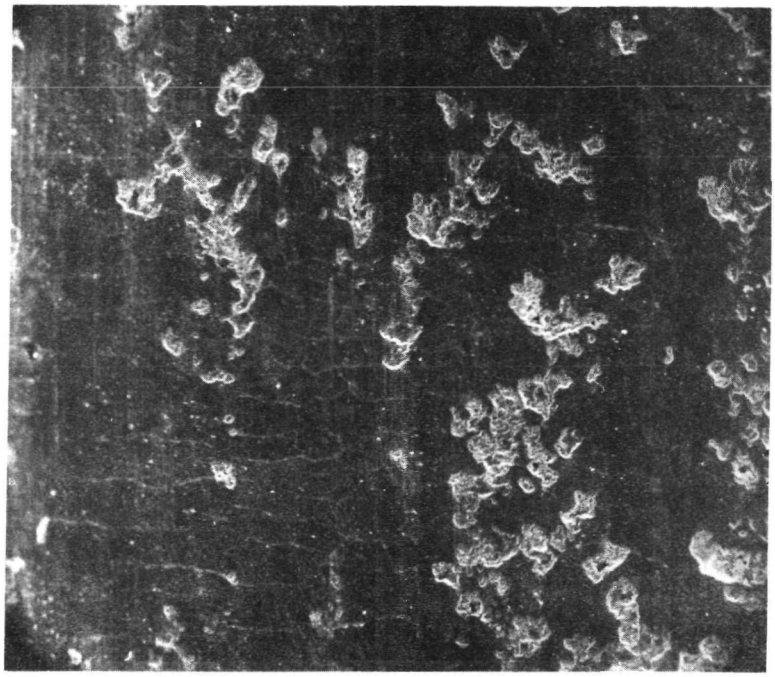

Pad After Testing – 100X

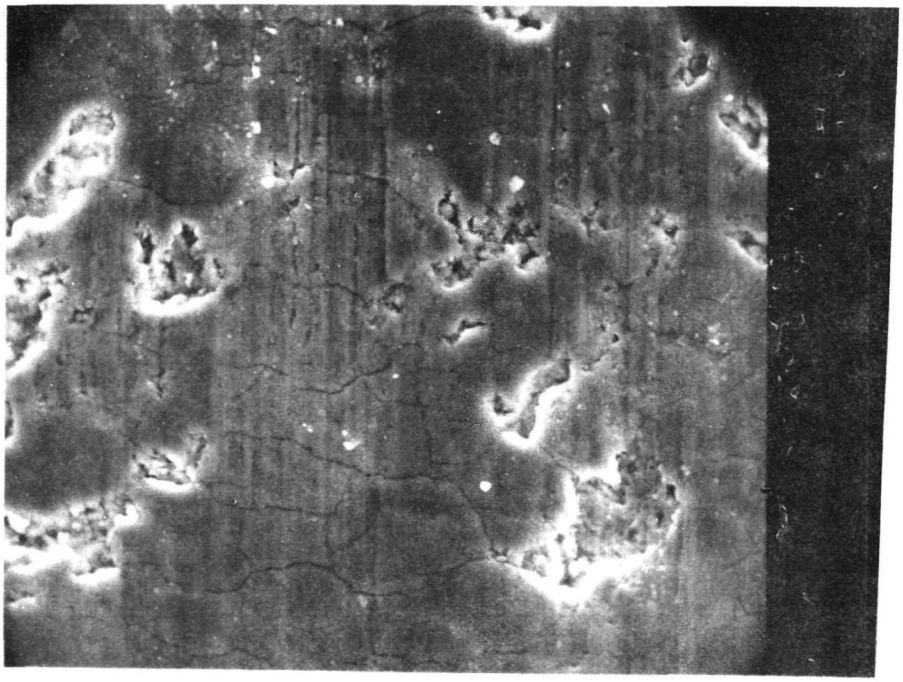

Pad After Testing – 1000X

Plate 66 32 Reference

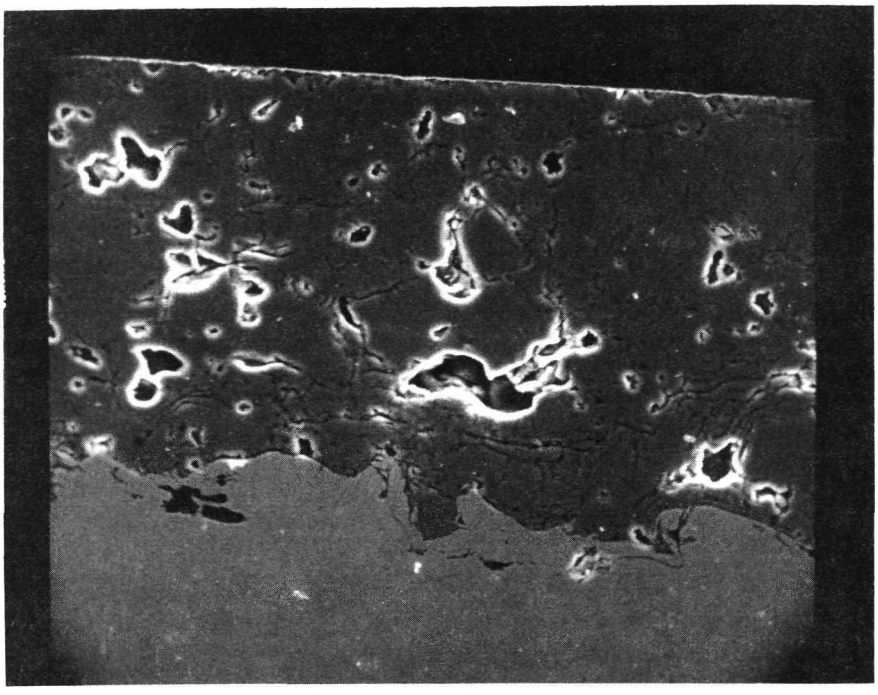

Pad After Testing — 500X

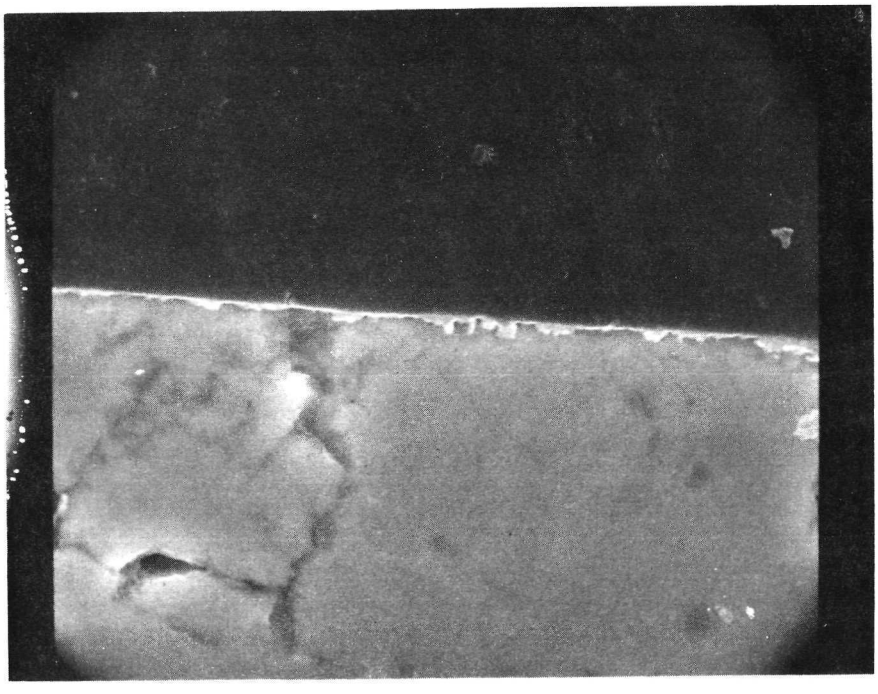

Pad After Testing — 3000X

Plate 67 11A Sputtered MoS_2

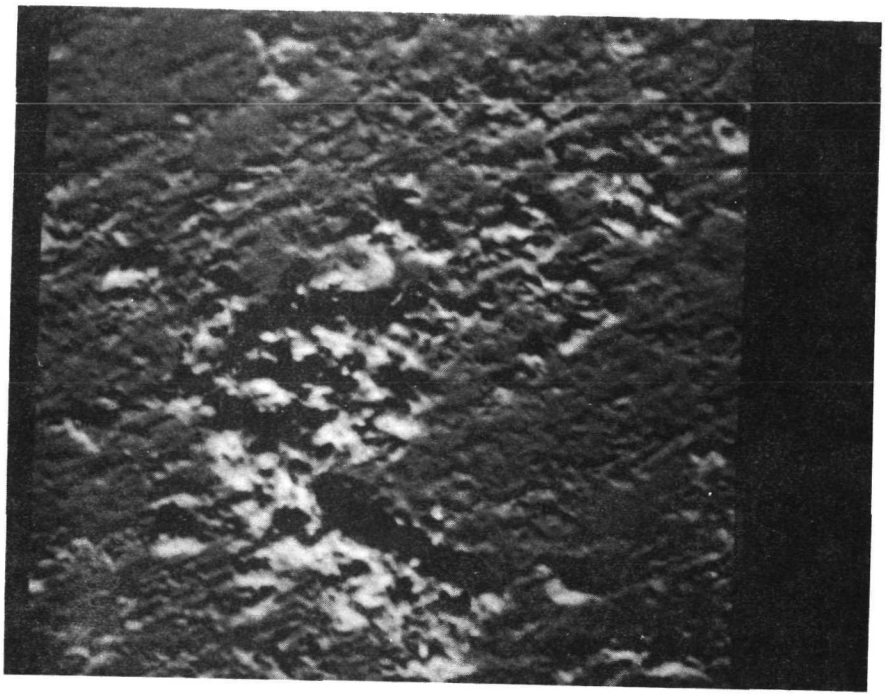

Pad After Testing — 300X X-Ray Topography

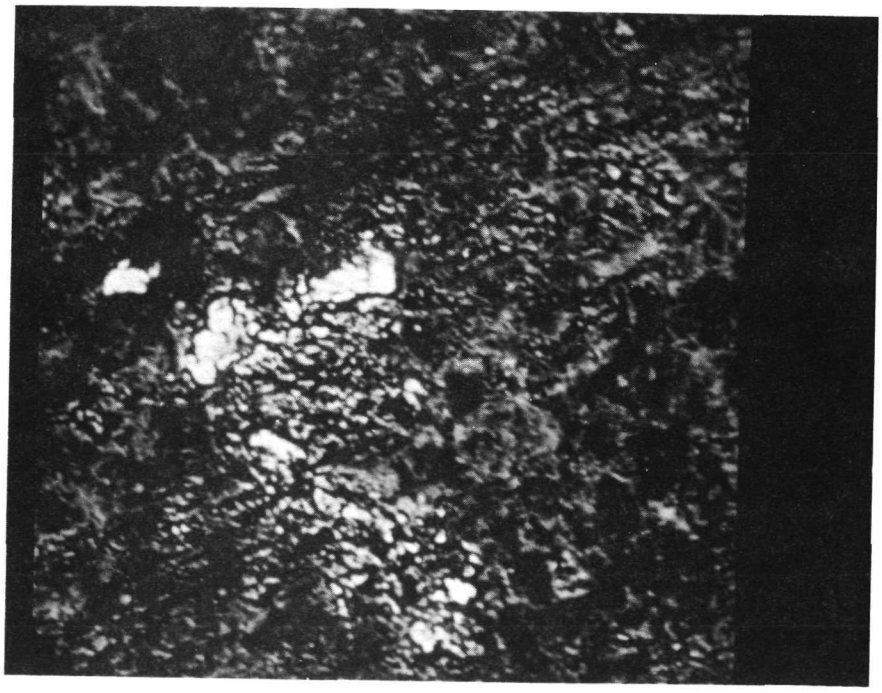

Pad After Testing — 300X X-Ray Composition

Plate 68 11A Sputtered MoS_2

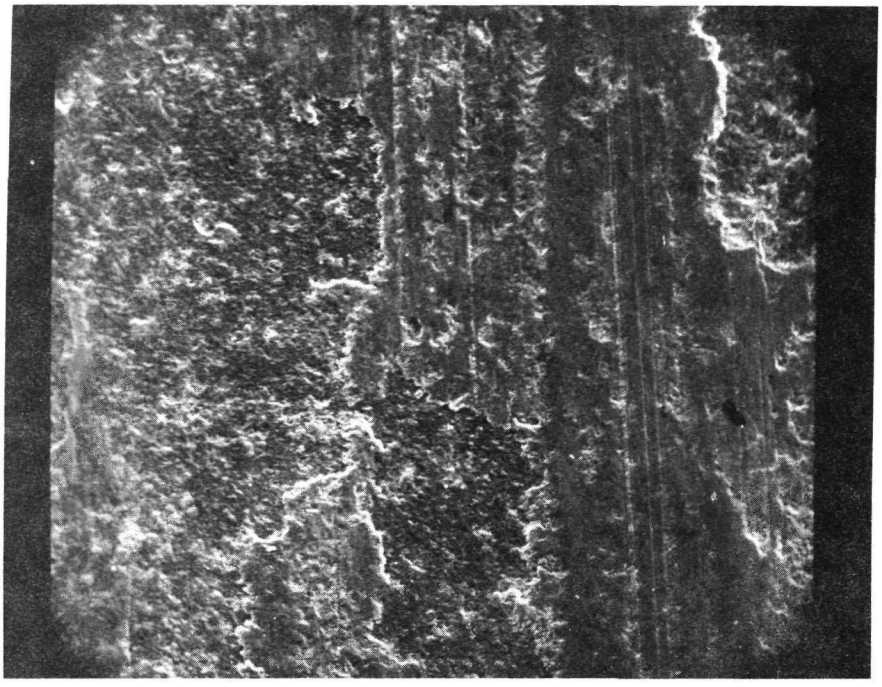

Pad After Testing – 100X

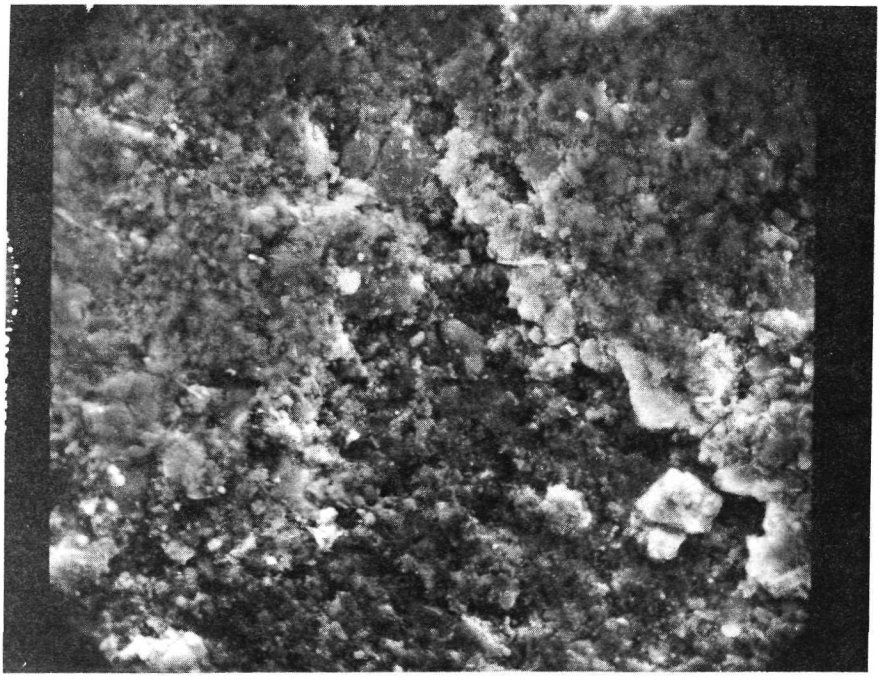

Pad After Testing – 1000X

Plate 69 13A Metal Matrix MoS_2

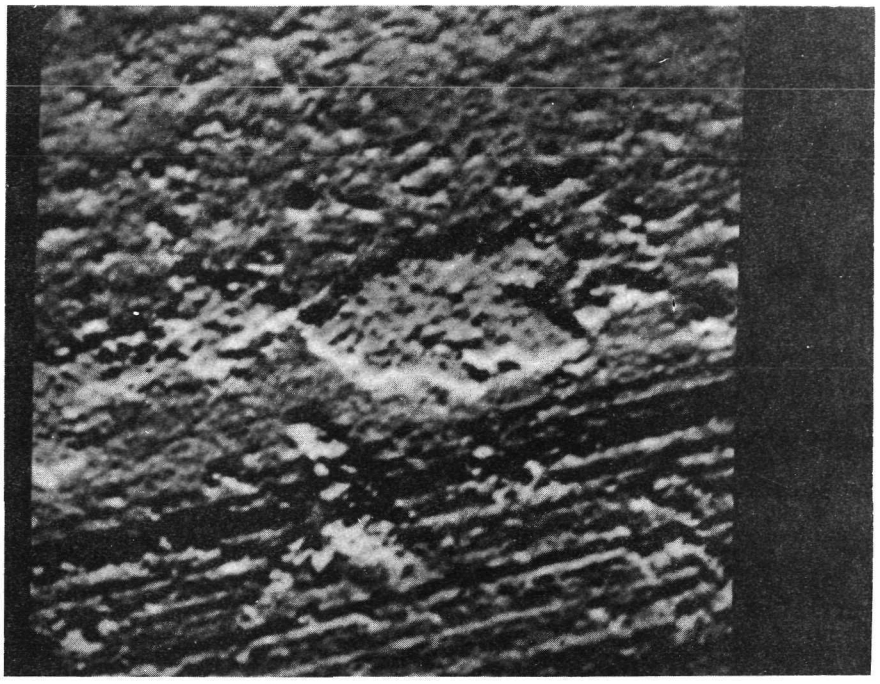

Pad After Testing — 300X X-Ray Topography

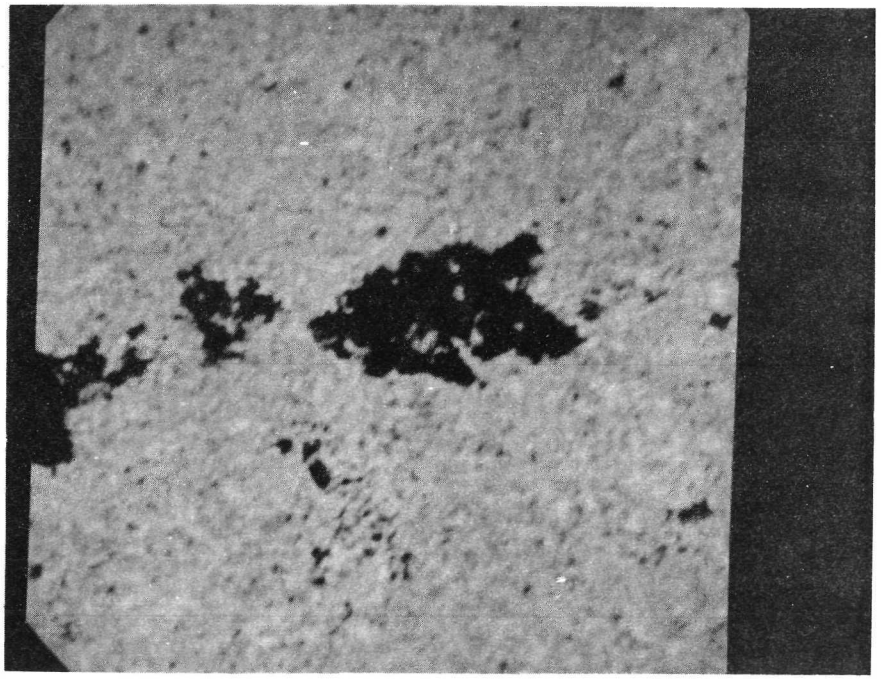

Pad After Testing — 300X X-Ray Composition

Plate 70 13A Metal Matrix MoS_2

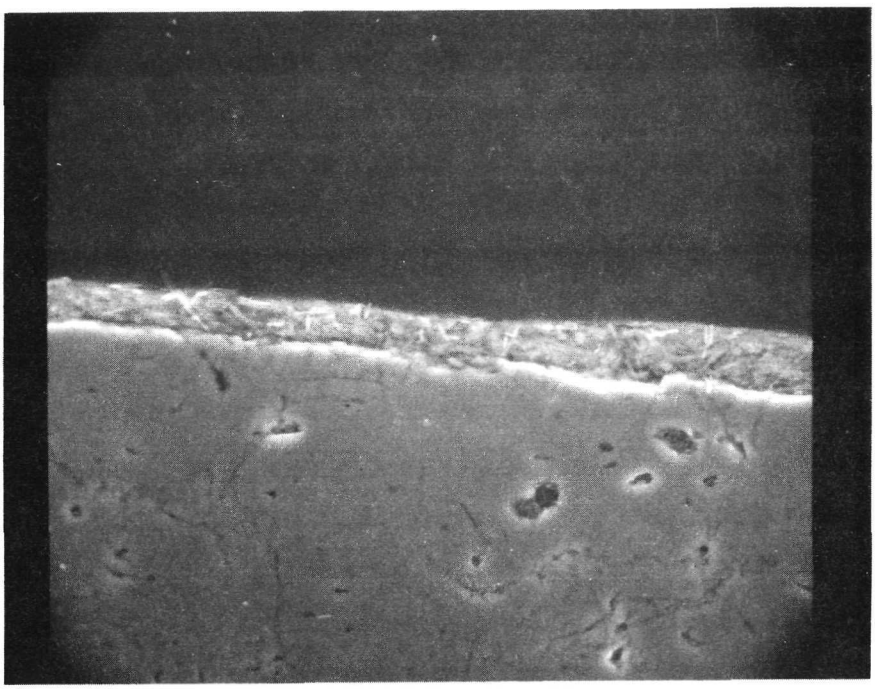

Pad After Testing — 1000X

Plate 71 13A Metal Matrix MoS_2

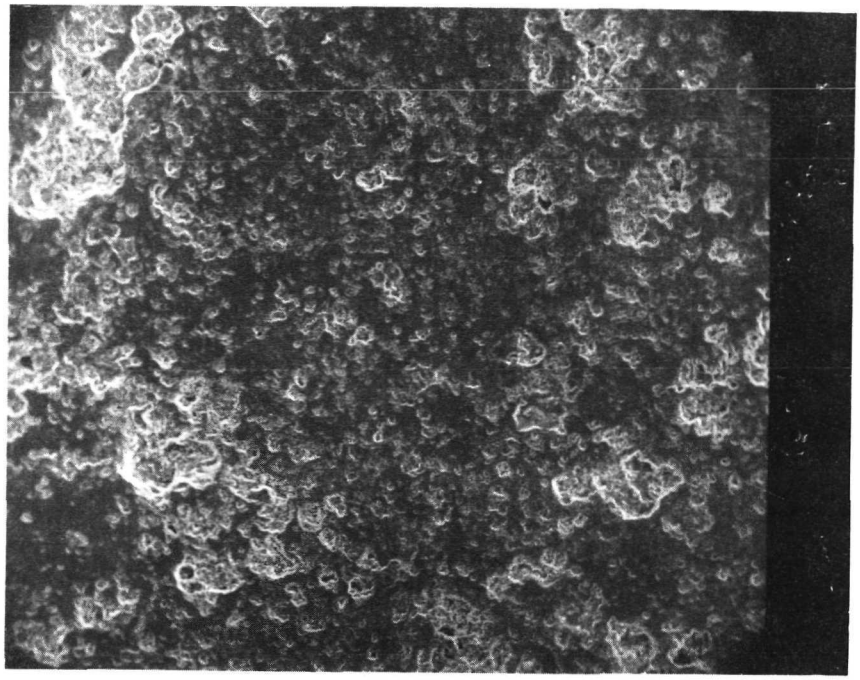

Pad After Testing – 100X

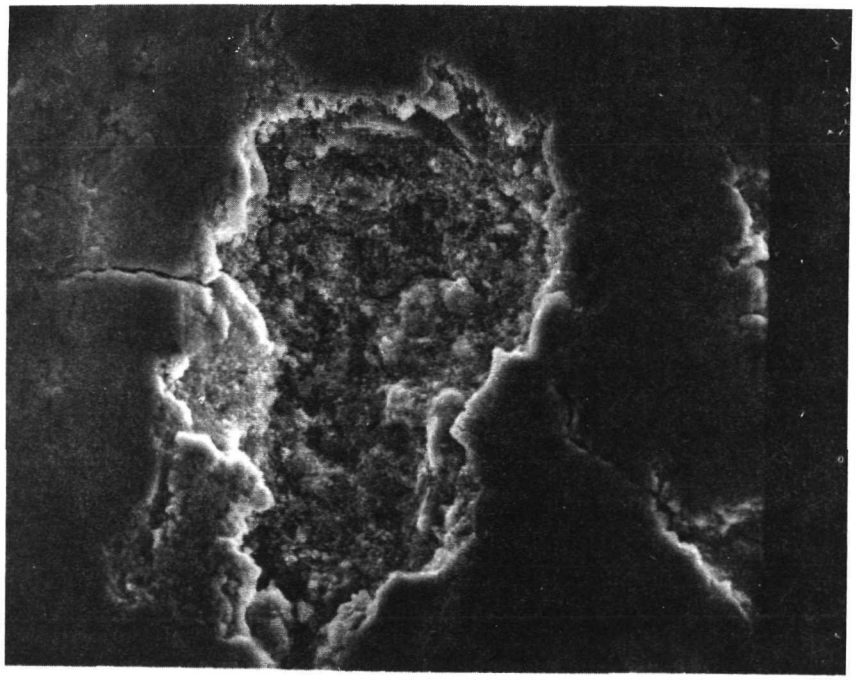

Pad After Testing – 1000X

Plate 72 10B Burnished MoS_2

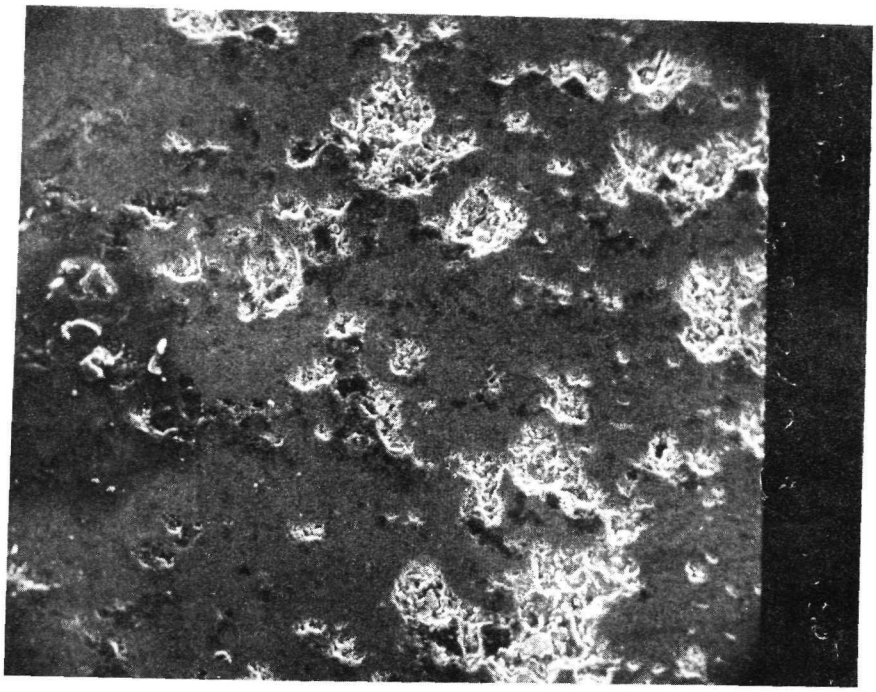

Pad After Testing – 100X

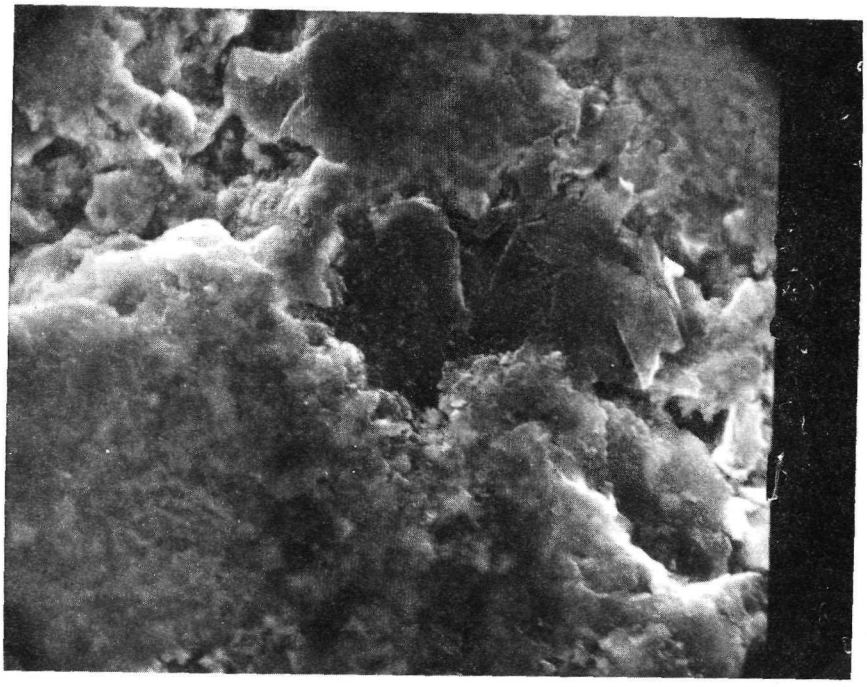

Pad After Testing – 1000X

Plate 73 12B Polyimide MoS_2

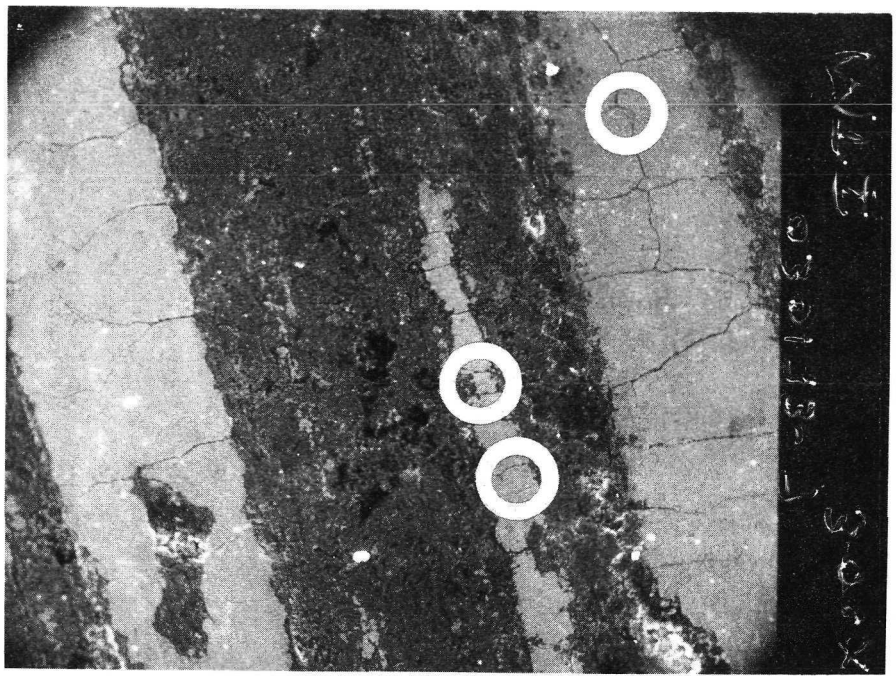

Pad After Testing – 300X

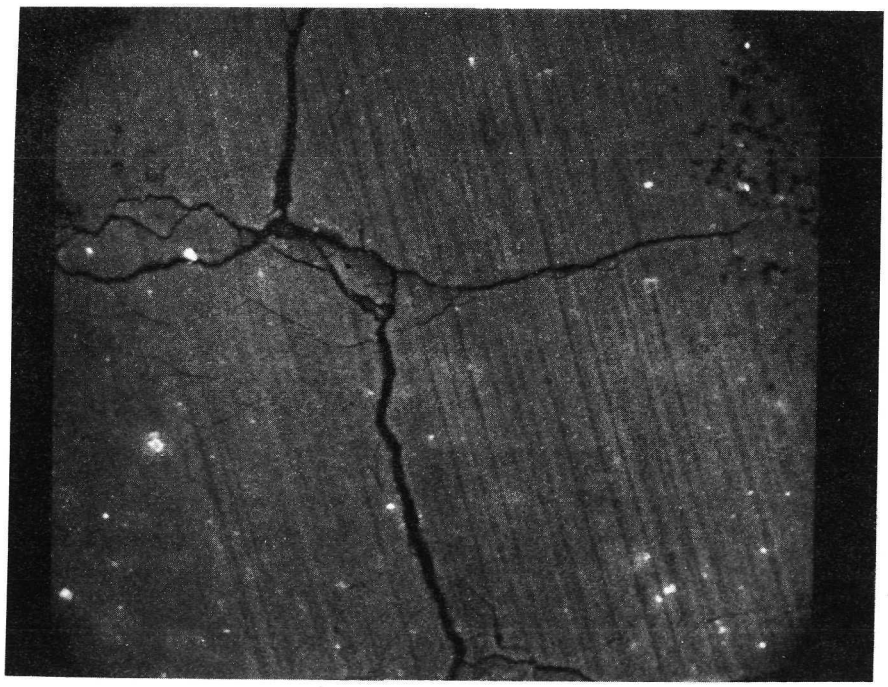

Pad After Testing – 2000X Circle A

Plate 74 22B Polyimide MoS_2

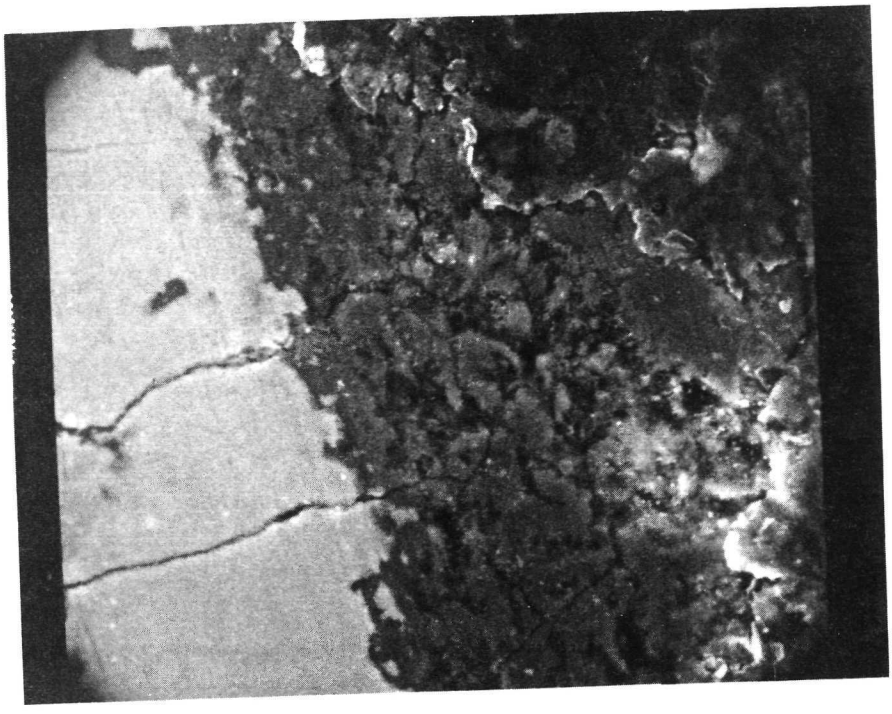

Pad After Testing — 2000X Circle B

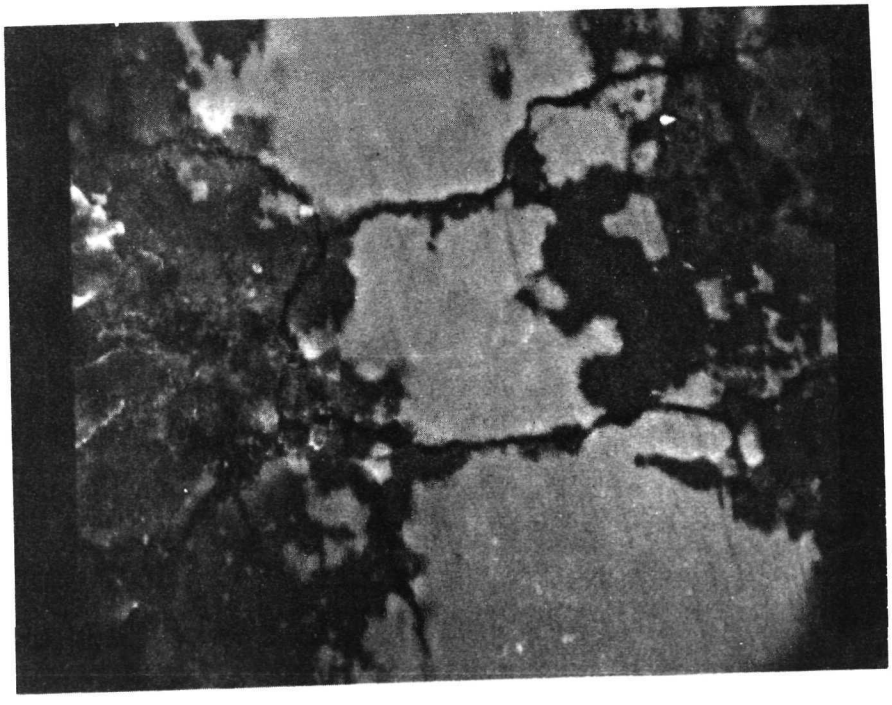

Pad After Testing — 3000X Circle C

Plate 75 22B Polyimide MoS_2

Pad After Testing – 100X
Electron Back Scatter Composition

Plate 76 22B Polyimide MoS_2

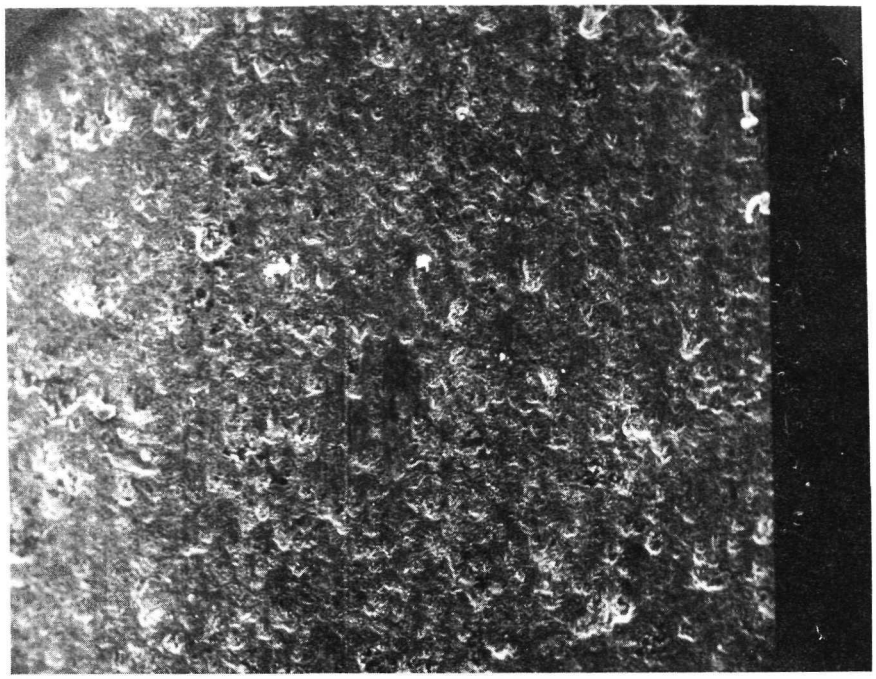

Pad After Testing – 100X

Pad After Testing – 1000X

Plate 77 25B Polyimide CF

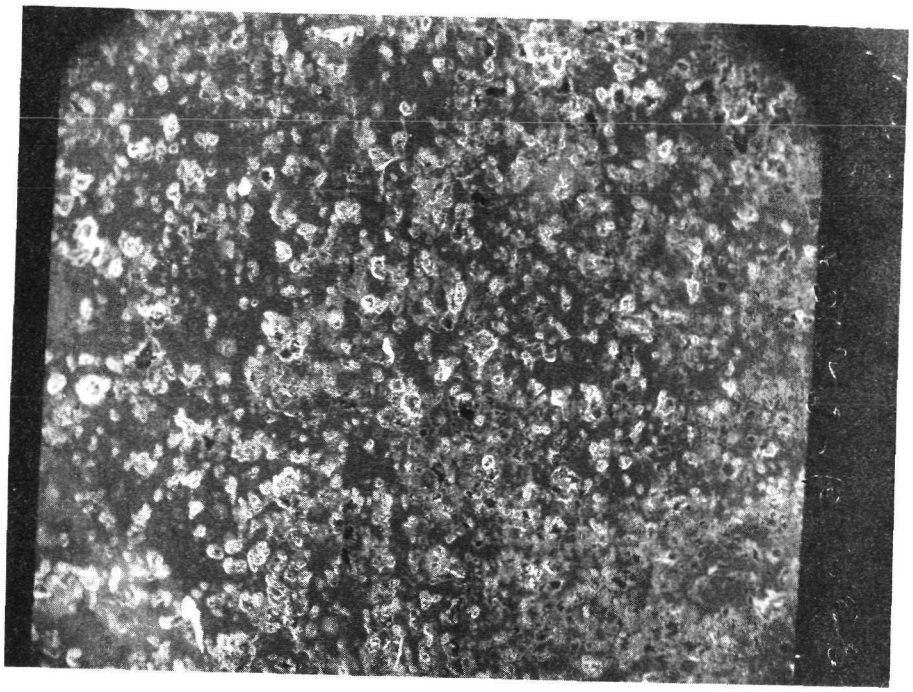

Pad After Testing – 100X

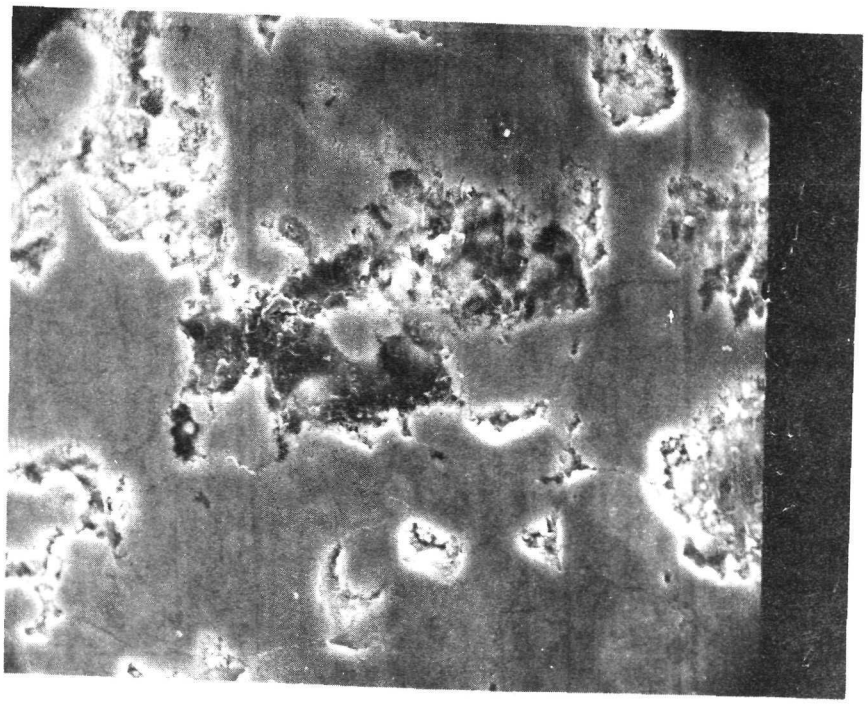

Pad After Testing – 1000X

Plate 78 24C Burnished CF

☆ U.S. GOVERNMENT PRINTING OFFICE: 1974—739-161/134

NATIONAL AERONAUTICS AND SPACE ADMINISTRATION
WASHINGTON, D.C. 20546

OFFICIAL BUSINESS
PENALTY FOR PRIVATE USE $300

SPECIAL FOURTH-CLASS RATE BOOK

POSTAGE AND FEES PAID
NATIONAL AERONAUTICS AND SPACE ADMINISTRATION
451

U.S.MAIL

POSTMASTER: If Undeliverable (Section 158 Postal Manual) Do Not Return

"The aeronautical and space activities of the United States shall be conducted so as to contribute . . . to the expansion of human knowledge of phenomena in the atmosphere and space. The Administration shall provide for the widest practicable and appropriate dissemination of information concerning its activities and the results thereof."

—NATIONAL AERONAUTICS AND SPACE ACT OF 1958

NASA SCIENTIFIC AND TECHNICAL PUBLICATIONS

TECHNICAL REPORTS: Scientific and technical information considered important, complete, and a lasting contribution to existing knowledge.

TECHNICAL NOTES: Information less broad in scope but nevertheless of importance as a contribution to existing knowledge.

TECHNICAL MEMORANDUMS: Information receiving limited distribution because of preliminary data, security classification, or other reasons. Also includes conference proceedings with either limited or unlimited distribution.

CONTRACTOR REPORTS: Scientific and technical information generated under a NASA contract or grant and considered an important contribution to existing knowledge.

TECHNICAL TRANSLATIONS: Information published in a foreign language considered to merit NASA distribution in English.

SPECIAL PUBLICATIONS: Information derived from or of value to NASA activities. Publications include final reports of major projects, monographs, data compilations, handbooks, sourcebooks, and special bibliographies.

TECHNOLOGY UTILIZATION PUBLICATIONS: Information on technology used by NASA that may be of particular interest in commercial and other non-aerospace applications. Publications include Tech Briefs, Technology Utilization Reports and Technology Surveys.

Details on the availability of these publications may be obtained from:

SCIENTIFIC AND TECHNICAL INFORMATION OFFICE

NATIONAL AERONAUTICS AND SPACE ADMINISTRATION

Washington, D.C. 20546